Enhanced Potentiation of Anticancer Drugs using Magnetic Fluid Hyperthermia (MFH): *In vitro* and *in vivo* studies

by

Merlis P. Alvarez - Berríos

A dissertation submitted in partial fulfillment of the requirements for the degree of

DOCTOR OF PHILOSOPHY
In
CHEMICAL ENGINEERING
UNIVERSITY OF PUERTO RICO
MAYAGÜEZ CAMPUS
2014

Approved by:

_____	_____
Dr. Madeline Torres-Lugo President, Graduate Committee	Date
_____	_____
Dr. Carlos Rinaldi-Ramos Co-President, Graduate Committee	Date
_____	_____
Dr. Patricia Ortiz-Bermudez Member, Graduate Committee	Date
_____	_____
Dr. Aldo Acevedo-Rullán Member, Graduate Committee Chairperson of the Department	Date
_____	_____
Dr. Dorial Castellanos Graduate School Representative	Date

This dissertation contains portions that were published by the author in the *International Journal of Nanomedicine*.

Abstract

Clinical studies have demonstrated the effectiveness of combined hyperthermia and anticancer drug treatments. Challenges related to effective heat transfer have limited its clinical application. The use of magnetic fluids to induce hyperthermia is an attractive alternative to other forms of hyperthermia. It is based on the heat released by magnetic nanoparticles subjected to magnetic field. Recent studies have shown that magnetic fluid hyperthermia (MFH) enhances the therapeutic effects of chemotherapeutic agents. Knowledge regarding the underlying cellular and molecular mechanisms by which such phenomena occur requires more in depth understanding, and it is the focus of this work. It is hypothesized that by inducing hyperthermia via magnetic nanoparticles (MFH) significant cellular effects will be induced that will result in enhanced cytotoxicity of anticancer drugs, which currently possess limited clinical applications. For this purpose, *in vitro* therapeutic enhancement of bortezomib (BZ) and cisplatin (cDDP) using heat dissipated by magnetic nanoparticles was evaluated. Potential mechanisms to explain our observations of potentiation of these anti-cancer drugs by MFH were also elucidated. Finally, the *in vivo* therapeutic effects of cisplatin combined with MFH were assessed. Our results conclusively demonstrate that MFH produced marked cellular effects such as membrane fluidity, protein damage and microtubule instability, which were responsible for the *in vitro* enhanced potentiation between MFH and BZ or cDDP. *In vivo* studies showed therapeutic enhancement of cisplatin when combined with MFH. These results are significant because this approach could become a potentially effective anticancer therapy platform even in those cell lines that show intrinsic resistance to the drug.

Resumen

Estudios clínicos han demostrado que hipertermia mejora la efectividad de drogas anti cáncer. Sin embargo, retos relacionados a la transferencia de calor ha limitado su aplicación a nivel clínico. El uso de fluidos magnéticos para inducir hipertermia (MFH) es una alternativa atractiva cuando es comparado con otras formas de hipertermia. Este tratamiento está basado en la liberación de calor de nanoparticulas magnéticas en presencia de un campo magnético. Estudios recientes han demostrado que hipertermia usando fluido magnético mejora el efecto terapéutico de agentes quimioterapéuticos. Sin embargo, los mecanismos celulares y moleculares por los cuales se produce este fenómeno requieren un conocimiento mas profundo, el cual es el enfoque de este trabajo. La hipótesis planteada es que al inducir hipertermia con nanopartículas magnéticas (MFH) inducirá efectos celulares importantes los cuales producirán una mayor citotoxicidad de drogas anti cáncer que han mostrado efectos clínicos limitados. Con el fin de probar esta hipótesis el efecto terapéutico de bortezomib (BZ) y cisplatin (cDDP) en combinación con MFH fue evaluado. Potenciales mecanismos para explicar nuestras previas observaciones sobre la potenciación terapéutica de estas drogas utilizando el calor disipado por nanopartículas magnéticas fueron elucidados. Finalmente, estudios preliminares *in vivo* fueron realizados con el fin de evaluar los efectos terapéuticos de cisplatino en combinación con MFH en modelos de animales. Nuestros resultados demuestran de forma concluyente que MFH produce marcados efectos celulares tales como fluidez membranal, daño de proteínas e inestabilidad de los microtúbulos, los cuales son responsables de la potenciación observada entre BZ o cDDP y MFH. Estudios *in vivo* mostraron que MFH aumentó la efectividad terapéutica de cisplatino. Este tratamiento podría convertirse en una plataforma potencialmente eficaz para el tratamiento de cáncer, incluso en aquellas líneas celulares que muestran resistencia intrínseca a dichas drogas.

List of Publications and Conferences

Publications

- **Alvarez-Berrios MP**, Castillo A, Rinaldi C, Torres-Lugo M. Enhanced proteotoxic stress is responsible for hyperthermic potentiation of the proteasome inhibitor bortezomib using magnetic nanoparticles. Submitted.Nanomedicine. 2014.
- **Alvarez-Berrios MP**, Castillo A, Rinaldi C, Torres-Lugo M. Magnetic fluid hyperthermia enhances cytotoxicity of bortezomib in sensitive and resistant cancer cell lines. Int J Nanomedicine. 2013;9:145-153.
- **Alvarez-Berrios MP**, Castillo A, Mendez J, Soto O, Rinaldi C, Torres-Lugo M. Hyperthermic potentiation of cisplatin by magnetic nanoparticle heaters is correlated with an increase in cell membrane fluidity. Int J Nanomedicine. 2013;8:1003-1013

Oral Presentations

- **Alvarez-Berrios MP**, Castillo A, Rinaldi C, Torres-Lugo M. "Proteotoxic Stress Induced By Magnetic Fluid Hyperthermia (MFH) Enhances Bortezomib Cytotoxicity", AichE Annual Meeting, San Francisco, CA, November 2013.
- **Alvarez-Berrios MP**, Castillo A, Soto O, Mendez J, Rinaldi C, Torres-Lugo M "Synergistic potentiation of cisplatin with magnetic fluid hyperthermia is correlated with an increase in cell membrane fluidity", Emerging Researchers National Conference in STEM, Washington, DC, February 2013.

To God,
to my parents Maria Berrios and Leovigildo Alvarez
and to my beloved husband Jorge Fuentes

Acknowledgments

First of all, I wish to thank God for giving me the wisdom and patience to accomplish each goal in my life. I am very grateful to my parents Maria Berrios and Leovigildo Alvarez for their support, care and love. I thank God for putting on my path my beloved husband Jorge Fuentes who has been my unconditional support and voice of wisdom in my life.

I want to express my gratitude to my advisor Dr. Madeline Torres for her guidance and support. I appreciate all the scientific discussions that we had which has helped me become a better researcher. I also wish to acknowledge to my co-advisor Dr. Carlos Rinaldi for his assistance, mentoring, and advice. I would like to thank to my graduate committee members Dr. Patricia Ortiz and Dr. Aldo Acevedo for their comments and corrections of this thesis.

I also wish to thank all my CBEN lab mates for the unique and wonderful experiences we shared, which have allowed me to grow in different areas of my life. I want to give special thanks to my undergraduate student Amalchi Castillo for his support, dedication and commitment to the development of the experiments of this work and to Karem Court, Cristina Castro and Dr. Edna Mora for their support in the execution of the *in vivo* experiments.

Finally, I offer acknowledgements to the funding agencies that have allowed this work possible: U.S. National Science Foundation (NSF) under Award No HRD-0833112 (CREST program), the PR Institute for Functional Nanomaterials under the NSF Award No EPS-1002410 and the US National Institutes of Health under Award No U54 CA 96300/U54 CA 96297

Table of Contents

List of tables

List of Figures

Chapter 1

Introduction

1.1. Background and Rationale

In the past decades, alternative cancer treatments have been explored.[1-5] Hyperthermia, the increase of physiological temperature to 41- 46°C, has gained great interest as new treatment to treat cancer. It has been used for many years for the treatment of various diseases.[6, 7] The use of heat to treat cancer was visualized by Diedir in 1725 who established that patients with bacterial infections, especially those patients with syphilis, demonstrated lower incidence of cancer and tumor remission than those who did not have recurrent bacterial infections.[8] Busch and Coley also observed tumor remission in human patients by fever induction using *streptococcus pyogenes*.[8,9, 10]

Today clinical hyperthermia for cancer treatment focuses in local, regional, and total body hyperthermia.[6, 11-15] Local hyperthermia is used to induce heat in small areas with the purpose of increasing tumor temperature without affecting surrounding tissues. Local hyperthermia can be induced using surface applicators (RF, microwave, or ultrasound) and microwave techniques (small antennas microwave, hot water tubes and laser fibers). Surface applicators reach therapeutic depth of few centimeters, which limits their use to other types of tumors. On the other hand, microwave techniques can reach high temperatures with a controlled temperature distribution; however, this is an invasive method that can not be repeated several

times to patients.[6, 7]

Regional hyperthermia is used for deep-seated tumors. This type of hyperthermia is more complicated than local hyperthermia, because it is difficult to maintain the heat application in the tumor without causing damage to adjacent tissues. External applicators around the body or organ and perfusion techniques are used to perform this type of hyperthermia. However, it produces various side effects such as tachycardia and malaise.[7, 16-18]

Finally, whole body hyperthermia (WBH) is mostly used for cancer that has metastasized to other tissues or organs. For this technique thermal conduction using thermal chamber, immersion in hot liquids etc are commonly used. The challenge with this type of hyperthermia is to prevent that the body temperature exceeds the maximum temperature (42 ^{o}C) permissible by brain and liver. Additionally, WBH has a great impact on tissue metabolism, blood flow, organ function, and tissue repair.[6, 7, 19, 20]

Recently hyperthermia has been studied to improve the cytotoxicity of anticancer drugs, including those with restricted use in clinical setting, such as bortezomib (BZ) and cisplatin (cDDP).[7, 21, 22] Bortezomib is a proteasome inhibitor which has been tested to treat some types of cancer including breast, colon, ovarian, lung, as well as certain hematological neoplasms. However, it has not been effective for some of these types of cancer. [23 24-28] The platinum based drug cisplatin has been widely used to treat different cancer such as testicular, ovarian, bladder, head and neck, and non-small cell lung cancer.[29] But, severe side effects and drug resistance developed for some types of cancer have limited its use.[29, 30] Nevertheless, combining cisplatin or bortezomib with conventional hyperthermia has shown positive results.[31,32]

Recent studies have shown that hyperthermia using water bath (HWH) sensitized breast cancer cells to BZ, showing enhanced cell death when they were combined.[26] On the other hand, *in vitro* and *in vivo* results have evidenced that hyperthermia improves the therapeutic effect of cisplatin.[33-36] For example, Wang *et. al*. demonstrated that hyperthermia at 43°C enhanced the efficacy of cisplatin in MCF-7 and MDAMB-453 cells.[37] Zakris *et al*. showed that regional abdominal hyperthermia potentiated the *in vivo* therapeutic effect of cisplatin in ovarian tumors.[33] This thermopotentiation was also observed when patients with cervical carcinoma were treated with locoregional hyperthermia in combination with cisplatin.[36] However, these hyperthermic treatments induced side effects to patients and animals such as nausea, vomiting, subcutaneous fatty necrosis and skin burns.[33, 36]

Considering all the disadvantages provided by current clinical hyperthermic treatments, the employment of magnetic fluid to induce local hyperthermia has gained significant interest.[38-40] It consists of magnetic nanoparticles (2-20 nm in diameter) dispersed in a liquid carrier. [22, 41, 42] Magnetic nanoparticles must be biocompatible and colloidally stable to prevent toxicity, agglomeration and precipitation.[22] For that reason, they are synthesized with a nontoxic inorganic magnetic core which is coated with an organic sell that provides colloidally stability. A variety of materials can be used as an inorganic core; however, iron oxide based nanoparticles are preferred because they are not toxic to biological systems. [41]Although various organic shells such as PEG and chitosan have been used to coat magnetic nanoparticles, dextran has been widely used to cover nanoparticles due to its polarity and high biocompatibility.[22, 40, 41, 43]

Magnetic nanoparticles provide properties that make them attractive for biomedical applications such as hyperthermia.[22, 40] They can accumulate in the tumor by direct injection, passively through the tumors due to EPR effect provided by tumor vasculature or by engineering

them with ligands that recognize specific receptors on the cell.[22, 44] In addition, they have the capacity to dissipate the magnetic field energy in the form of heat by physical rotation or internal dipole reorientation in an alternating magnetic field.[41, 42, 45] This phenomenon can be used to directly destroy cells or it can be used to improve the therapeutic outcome of many chemotherapeutic agents including those that have shown clinical limitations.[46-50]

Several studies have confirmed that MFH is a promissing method to treat cancer.[51 , 7, 13, 14] *In vitro* tests demonstrated that MFH significantly reduces Caco-2 cell viability in a higher extent that an external heating under the same thermal dose.[48] Creixell *et al*. proved that magnetic nanoparticles conjugated to the protein epidermal growth factor (EGF) caused significant (99%) reductions in cell viability without a macroscopically perceptible temperature rise in breast cancer cells.[49] Recently, an *in vivo* study used EGFR-targeted superparagmagnetic iron oxide nanoparticles for targeting non-small cell lung cancer in a mouse orthotopic model. Results showed that when a magnetic field was applied, significant inhibition of tumor was observed. [52]

Balivada *et al*. revealed that application of MFH after intratumoral or intravenous injection of bimagnetic nanoparticles (Fe/Fe_3O_4) produced significant anti-tumor effect on murine B16-F10 melanoma model**.** [57] Studies also have reported that hyperthermia using iron oxide nanoparticles inhibited breast tumor growth and produced destruction of the head and neck cancer tumor model.[53, 54, 55, 56]

These results have encouraged scientists to explore MFH as an adjuvant to improve the therapeutic effect of other antineoplastic modalities such as chemotherapy. For example, Brusentsov *et al.* demonstrated that combination treatments of a dextran-ferrite magnetic fluid with melphalan or cyclophosphamide increased the animal's life span by 180 % and 290 % respectively.[58] Thermochemosensitization using magnetic nanoparticles was also observed in an

in vivo model of leukemia for overcoming multidrug resistance. Results indicated that MFH in combination with 5-bromotetrandrine (5-BrTet) and daunorubicin induced a noticeable reduction of tumors.[59] Recently, Ito *et al.* proved the *In vitro* and *in vivo* effectiveness of geldanamycin in combination with MFH in a B16 melanoma model. [60]

The thermopotentiation of cisplatin using MFH has also been investigated. Babincová *et al.* evaluated the effectiveness of magnetic nanoparticles functionalized with cisplatin at short time. Authors demonstrated the synergistic effect of cisplatin when combined with MFH in BP6 rat sarcoma cells.[61] Lee *et al.* evaluated also at short term the effects of treatment sequence on Caco-2 cell line, indicanding that the combined treatment (cisplatin and MFH) produces the highest cytotoxicity.[47] This enhanced potentiation was also observed *in vivo* by Petryk *et al*. using 110 nm hydroxyethyl starch-coated magnetic nanoparticles. Results indicated that the combinated treatment was 1.7 times more effective than hyperthermia alone and 1.4 times more effective than cisplatin alone.[62] However, the mechanisms involved in this enhanced cytotocixity have not been elucidated.

The use of magnetic nanoparticles to induce local hyperthermia is a promising therapeutic approach to enhance the cytotoxicity of chemotherapeutics even when drug resistance has been developed. This novel treatment provides attractive advantages over conventional hyperthermia methods which make it a better platform for an effective anticancer treatment with fewer side effects and less harmful treatment.

1.2. Justification

Cancer has proved to be our toughest rival in the clinics today. It is characterized by uncontrolled growth of cells, which can invade other tissues. For more than fifty years, cancer has been the second greatest cause of death in the United States.[63] In 2014 235,030 new cases of

invasive breast cancer, 96,830 cases of colon and 21,980 new cases of ovarian cancer are expected.[64] Although, the five year relative survival rate for all cancers diagnosed between 2001 and 2007 is 67%, up from 49% in 1975-1977; approximately 585,720 Americans are expected to die of cancer in 2014.[64]

Cancer is known to exhibit rapid and sometimes undetected recurrences making it difficult to treat and eliminate effectively. Based on the fact that the development of cancer is essentially due to genetic mutations, which promote uncontrolled cell division causing death, ideal chemotherapeutic agents for this disease would have to be specific for the type of cancerous cell and the mutations they express.[65, 66] Those types of anticancer drugs attack cells that divide rapidly. However, they produce deleterious side effects such as diarrhea, vomit, effects on normal cells in the body such as hair cells and some types of cancer develop resistance to these chemotherapeutic treatments.[67, 68]

These reasons have motivated scientists to develop improved and less harmful forms of treatment, maximizing clinical benefits using novel agents and/or forms of treatment. Surgical interventions, radiotherapy, immunotherapy, and hyperthermia are used in combination with chemotherapy to enhance treatment efficacy.[1, 69-71]

Hyperthermia in conjunction with antineoplastic modalities has provided substantial evidence of its enhanced efficacy.[7, 72, 73] Nonetheless, current clinical applications using local, regional, and whole-body hyperthermia present a number of disadvantages, including limitations in achievable treatment depth, patient surface irregularities (head, arms, etc.), and overheating of adjacent normal tissue.[74, 75] Consequently, novel hyperthermic treatment options are of significant interest.[35] The employment of magnetic nanoparticles for localized oncotherapy is a novel and attractive treatment. However, some clinically relevant drugs which produces

resistance in some types of cancer have not been evaluated with this novel hyperthermic treatment and in addition, the mechanism by which magnetic fluid hyperthermia exert potentiation of anticancer drugs is unknown.

In an attempt to evaluate this treatment as a tool to improve the therapeutic effects of chemotherapeutics even when drug resistance have been developed, in this work we investigated the *in vitro* enhanced cytotoxicity of the anticancer drugs bortezomib and cisplatin when combined with magnetic fluid hyperthermia. The underlying cellular and molecular mechanisms by which such potentiation occurs were elucidated. In addition, preliminary *in vivo* studies were assessed using cisplatin in combination with MFH using ovarian cancer cells model. These results are significant because this approach could become a potentially effective anticancer therapy platform even in those cell lines that show intrinsic resistance to anticancer drugs.

1.3. Objectives

1.3.1. General objective

The overall objective of this work was to investigate the enhanced cytotoxicity of anticancer drugs caused by hyperthermia using magnetic nanoparticles (MFH) and the underlying cellular and molecular mechanisms by which such phenomena occurs.

1.3.2. Specific objectives

Study the potentiation of anticancer drugs by magnetic fluid hyperthermia

- Synthesis and characterization of magnetic nanoparticles covalently bound with carboxy methyl dextran.
- Determine cytocompatibility of magnetic nanoparticles for breast (MDA-

MB468, MCF-7), colon (Caco-2) and ovarian (A2780) cell lines in the absence of a magnetic field.

- Determine dose response and proteasome activity curves for BZ in MDA-MB468, MCF-7, Caco-2 and A2780 cell lines.
- Determine dose response curves for cDDP in the Caco-2 cell line.
- Investigate cell viability at short time after application of MFH combined with bortezomib in two BZ sensitive (Caco-2, MDA-MB468) and two BZ resistant (MCF-7, A2780) cell lines and compare the results with other type of hyperthermia such as hot water hyperthermia (HWH).
- Investigate cell viability after application of MFH combined with cisplatin at short and longer time in Caco-2 cells and compare the results with hot water hyperthermia (HWH).

Elucidate the potential mechanism involved in the hyperthermic potentiation of anticancer drugs using magnetic nanoparticles.

- Study membrane fluidity mechanism involved in the enhanced potentiation of cisplatin and magnetic fluid hyperthermia.
    - Measurement of Caco-2 cell response to cisplatin with or without copper using viability and clonogenic assays.
    - Conduction of platinum uptake studies
    - Test changes in membrane fluidity through fluorescence anisotropy measurements using trimethylamine-diphenylhexatriene (TMA-DPH).
    - Conduction of uptake studies with acridine orange by flow cytometry and confocal microscopy.

- Study the enhanced proteotoxic stress mechanism involved in the enhanced potentiation of BZ and magnetic fluid hyperthermia.
    - Measurement of MCF-7 cell response to bortezomib using DNA content profile, viability and clonogenic assays.
    - Determine aggresome formation and microtubules damage after hyperthermic treatment with or without BZ.

Preliminary in vivo studies

- Evaluate tumor remission after application of magnetic fluid hyperthermia in combination with cisplatin.

1.4. Overview of the Dissertation

The therapeutic enhancement of anticancer drugs by using heat dissipated by magnetic nanoparticles and the potential mechanisms to explain these observations were evaluated. In chapter two of this thesis hyperthermic potentiation of cisplatin by MFH at short and longer time and one of the mechanisms responsible for this potentiation in Caco-2 cells was elucidated. Direct and indirect measurements of cell membrane fluidity induced by MFH or HWH are presented. Taking advantage of the competitive binding effect of cisplatin and copper, cell response to cisplatin with or without copper was measured using viability and clonogenic assay. Platinum-uptake measurements are also presented. Finally, fluorescence anisotropy using TMA-DPH and acridine orange diffusion measurements were made to quantify the extent of membrane fluidity induced by MFH and HWH.

Chapter 3 focuses on the examination of magnetic fluid hyperthermia as an adjuvant to improve the therapeutic outcome of the proteasome inhibitor bortezomib, which has not shown promising results as a single agent.[26] Dose response curves for two BZ sensitive (Caco-2 and MDA-MB 468) and two BZ resistant (A2780 and MCF-7) cancer cell lines are presented. Proteasome inhibition curves as a function of BZ concentration were also evaluated, in order to determent BZ concentration to be used for subsequent experiments. Finally, cell response to BZ in combination with MFH at two different conditions (43ºC for 30 minutes and 45ºC for 30 minutes) was measured, an external source of heat as a control (HWH) was used.

Chapter 4 presents a potential mechanism to explain our observations of potentiation of the anti-cancer drug bortezomib using heat dissipated by magnetic nanoparticles in MCF-7 cell line. Cell response at short and long term was evaluated using DNA content profile, viability ratio ad clonogenic assay. Qualitative and quantitative analysis of aggresome formation is presented. Microtubules damage induced by hyperthermic treatments (MFH or HWH) is also evaluated in this chapter.

Chapter 5 presents preliminary in vivo studies in order to evaluate the therapeutic effects of cisplatin in combination with MFH in solid tumor xenograft models. Tumor volume T/C values are presented for control and experimental groups.

Chapter 6 presents final remarks and conclusions of this thesis.

1.5. References

1. Hildebrandt B, Wust P, Ahlers O, Dieing A, Sreenivasa G, Kerner T, et al. The Cellular and Molecular Basis of Hyperthermia. *Crit Rev Oncol Hematol*. **2002**; 43: 33-56.

2. Gao F, Ye Y, Zhang Y, Yang J. Water Bath Hyperthermia Reduces Stemness of Colon Cancer Cells. *Clin Biochem*. 46: 1747-1750.

3. Franckena M, Lutgens LC, Koper PC, Kleynen CE, van der Steen-Banasik EM, Jobsen JJ, et al. Radiotherapy and Hyperthermia for Treatment of Primary Locally Advanced Cervix Cancer: Results in 378 Patients. *Int J Radiat Oncol Biol Phys*. **2009**; 73: 242-250.

4. Hiraoka M, Masunaga S, Nishimura Y, Nagata Y, Jo S, Akuta K, et al. Regional Hyperthermia Combined with Radiotherapy in the Treatment of Lung Cancers. *Int J Radiat Oncol Biol Phys*. **1992**; 22: 1009-1014.

5. Pawlik A, Nowak JM, Grzanka D, Gackowska L, Michalkiewicz J, Grzanka A. Hyperthermia Induces Cytoskeletal Alterations and Mitotic Catastrophe in P53-Deficient H1299 Lung Cancer Cells. *Acta Histochem*. **2013**; 115: 8-15.

6. Habash RW, Bansal R, Krewski D, Alhafid HT. Thermal Therapy, Part 2: Hyperthermia Techniques. *Crit Rev Biomed Eng*. **2006**; 34: 491-542.

7. Wust P, Hildebrandt B, Sreenivasa G, Rau B, Gellermann J, Riess H, et al. Hyperthermia in Combined Treatment of Cancer. *Lancet Oncol*. **2002**; 3: 487-497.

8. Hobohm U. Fever and Cancer in Perspective. *Cancer Immunol Immunother*. **2001**; 50: 391-396.

9. Coley WB. The Treatment of Malignant Tumors by Repeated Inoculations of Erysipelas. With a Report of Ten Original Cases. 1893. *Clin Orthop Relat Res*. **1991**: 3-11.

10. Coley WB. The Treatment of Inoperable Sarcoma by Bacterial Toxins (the Mixed Toxins of the Streptococcus Erysipelas and the Bacillus Prodigiosus). *Proc R Soc Med*. **1910**; 3: 1-48.

11. Liang X, Zhou H, Liu X, He Y, Tang Y, Zhu G, et al. Effect of Local Hyperthermia on Lymphangiogenic Factors Vegf-C and -D in a Nude Mouse Xenograft Model of Tongue Squamous Cell Carcinoma. *Oral Oncol*. **2010**; 46: 111-115.

12. Ohguri T, Imada H, Yahara K, Moon SD, Yamaguchi S, Yatera K, et al. Re-Irradiation Plus Regional Hyperthermia for Recurrent Non-Small Cell Lung Cancer: A Potential Modality for Inducing Long-Term Survival in Selected Patients. *Lung Cancer*. **2012**; 77: 140-145.

13. Sapozink MD, Gibbs FA, Jr., Thomson JW, Eltringham JR, Stewart JR. A Comparison of Deep Regional Hyperthermia from an Annular Array and a Concentric Coil in the Same Patients. *Int J Radiat Oncol Biol Phys*. **1985**; 11: 179-190.

14. Katschinski DM, Wiedemann GJ, Longo W, d'Oleire FR, Spriggs D, Robins HI. Whole Body Hyperthermia Cytokine Induction: A Review, and Unifying Hypothesis for Myeloprotection in the Setting of Cytotoxic Therapy. *Cytokine Growth Factor Rev*. **1999**; 10: 93-97.

15. Richel O, Zum Vorde Sive Vording PJ, Rietbroek R, Van der Velden J, Van Dijk JD, Schilthuis MS, et al. Phase Ii Study of Carboplatin and Whole Body Hyperthermia (Wbh) in Recurrent and Metastatic Cervical Cancer. *Gynecol Oncol*. **2004**; 95: 680-685.

16. Pilepich MV, Myerson RJ, Emami BN, Perez CA, Leybovich L, von Gerichten D. Regional Hyperthermia: A Feasibility Analysis. *Int J Hyperthermia*. **1987**; 3: 347-351.

17. Pilepich MV, Myerson RJ, Emami BN, Perez CA, Straube W, von Gerichten D. Regional Hyperthermia--Assessment of Tolerance to Treatment. *Int J Radiat Oncol Biol Phys*. **1988**; 14: 347-352.

18. Emami B, Myerson RJ, Pilepich MV, Perez CA, Sathiaseelan V, Leybovich L, et al. Regional Hyperthermia in the Treatment of Recurrent Deep-Seated Tumors: Preliminary Analysis of Phase I Trial. *Strahlenther Onkol*. **1989**; 165: 709-711.

19. Xia H, Ikata T, Katoh S, Rokutan K, Saito S, Kawai T, et al. Whole Body Hyperthermia Selectively Induces Heat Shock Protein 72 in Neurons of the Rat Spinal Cord. *Neurosci Lett*. **1998**; 258: 151-154.

20. Gong B, Asimakis GK, Chen Z, Albrecht TB, Boor PJ, Pappas TC, et al. Whole-Body Hyperthermia Induces up-Regulation of Vascular Endothelial Growth Factor Accompanied by Neovascularization in Cardiac Tissue. *Life Sci*. **2006**; 79: 1781-1788.

21. Hahn GM, Li GC, Shiu E. Interaction of Amphotericin B and 43 Degrees Hyperthermia. *Cancer Res*. **1977**; 37: 761-764.

22. Torres-Lugo M, Rinaldi C. Thermal Potentiation of Chemotherapy by Magnetic Nanoparticles. *Nanomedicine (Lond)*. **2013**; 8: 1689-1707.

23. Mateos MV, San Miguel JF. Bortezomib in Multiple Myeloma. *Best Pract Res Clin Haematol*. **2007**; 20: 701-715.

24. Codony-Servat J, Tapia MA, Bosch M, Oliva C, Domingo-Domenech J, Mellado B, et al. Differential Cellular and Molecular Effects of Bortezomib, a Proteasome Inhibitor, in Human Breast Cancer Cells. *Mol Cancer Ther*. **2006**; 5: 665-675.

25. Mujtaba T, Dou QP. Advances in the Understanding of Mechanisms and Therapeutic Use of Bortezomib. *Discov Med*. 12: 471-480.

26. Xu H, Ju D, Jarois T, Xie Y. Diminished Feedback Regulation of Proteasome Expression and Resistance to Proteasome Inhibitors in Breast Cancer Cells. *Breast Cancer Res Treat*. **2008**; 107: 267-274.

27. Ling X, Calinski D, Chanan-Khan AA, Zhou M, Li F. Cancer Cell Sensitivity to Bortezomib Is Associated with Survivin Expression and P53 Status but Not Cancer Cell Types. *J Exp Clin Cancer Res*. **2010**; 29: 8.

28. Loeffler-Ragg J, Mueller D, Gamerith G, Auer T, Skvortsov S, Sarg B, et al. Proteomic Identification of Aldo-Keto Reductase Akr1b10 Induction after Treatment of Colorectal Cancer Cells with the Proteasome Inhibitor Bortezomib. *Mol Cancer Ther*. **2009**; 8: 1995-2006.

29. Bose RN. Biomolecular Targets for Platinum Antitumor Drugs. *Mini Rev Med Chem*. **2002**; 2: 103-111.

30. Liu S, Wang W, Zhou X, Gu R, Ding Z. Dose Responsive Effects of Cisplatin in L02 Cells Using Nmr-Based Metabolomics. *Environ Toxicol Pharmacol*. **2013**; 37: 150-157.

31. Ohno S, Siddik ZH, Kido Y, Zwelling LA, Bull JM. Thermal Enhancement of Drug Uptake and DNA Adducts as a Possible Mechanism for the Effect of Sequencing Hyperthermia on Cisplatin-Induced Cytotoxicity in L1210 Cells. *Cancer Chemother Pharmacol*. **1994**; 34: 302-306.

32. Wang D, Lippard SJ. Cellular Processing of Platinum Anticancer Drugs. *Nat Rev Drug Discov*. **2005**; 4: 307-320.

33. Zakris EL, Dewhirst MW, Riviere JE, Hoopes PJ, Page RL, Oleson JR. Pharmacokinetics and Toxicity of Intraperitoneal Cisplatin Combined with Regional Hyperthermia. *J Clin Oncol*. **1987**; 5: 1613-1620.

34. de Wit R, van der Zee J, van der Burg ME, Kruit WH, Logmans A, van Rhoon GC, et al. A Phase I/Ii Study of Combined Weekly Systemic Cisplatin and Locoregional Hyperthermia in Patients with Previously Irradiated Recurrent Carcinoma of the Uterine Cervix. *Br J Cancer*. **1999**; 80: 1387-1391.

35. van der Zee J. Heating the Patient: A Promising Approach? *Ann Oncol*. **2002**; 13: 1173-1184.

36. Rietbroek RC, Schilthuis MS, Bakker PJ, van Dijk JD, Postma AJ, Gonzalez Gonzalez D, et al. Phase Ii Trial of Weekly Locoregional Hyperthermia and Cisplatin in Patients with a Previously Irradiated Recurrent Carcinoma of the Uterine Cervix. *Cancer*. **1997**; 79: 935-943.

37. Ohno S, Siddik ZH, Baba H, Stephens LC, Strebel FR, Wondergem J, et al. Effect of Carboplatin Combined with Whole Body Hyperthermia on Normal Tissue and Tumor in Rats. *Cancer Res*. **1991**; 51: 2994-3000.

38. Branquinho LC, Carriao MS, Costa AS, Zufelato N, Sousa MH, Miotto R, et al. Effect of Magnetic Dipolar Interactions on Nanoparticle Heating Efficiency: Implications for Cancer Hyperthermia. *Sci Rep*. **2014**; 3: 2887.

39. Laurent S, Dutz S, Hafeli UO, Mahmoudi M. Magnetic Fluid Hyperthermia: Focus on Superparamagnetic Iron Oxide Nanoparticles. *Adv Colloid Interface Sci*. **2011**; 166: 8-23.

40. Latorre M, Rinaldi C. Applications of Magnetic Nanoparticles in Medicine: Magnetic Fluid Hyperthermia. *P R Health Sci J*. **2009**; 28: 227-238.

41. Barrera C, Herrera A, Zayas Y, Rinaldi C. Surface Modification of Magnetite Nanoparticles for Biomedical Applications. *Journal of Magnetism and Magnetic Materials*. **2009**; 321: 1397-1399.

42. Barrera C, Herrera AP, Rinaldi C. Colloidal Dispersions of Monodisperse Magnetite Nanoparticles Modified with Poly(Ethylene Glycol). *J Colloid Interface Sci*. **2009**; 329: 107-113.

43. Veiseh O, Gunn JW, Zhang M. Design and Fabrication of Magnetic Nanoparticles for Targeted Drug Delivery and Imaging. *Adv Drug Deliv Rev*. **2010**; 62: 284-304.

44. Farokhzad OC, Langer R. Impact of Nanotechnology on Drug Delivery. *ACS Nano*. **2009**; 3: 16-20.

45. Herrera AP, Barrera C, Zayas Y, Rinaldi C. Monitoring Colloidal Stability of Polymer-Coated Magnetic Nanoparticles Using Ac Susceptibility Measurements. *J Colloid Interface Sci*. 342: 540-549.

46. Alvarez-Berrios MP, Castillo A, Rinaldi C, Torres-Lugo M. Magnetic Fluid Hyperthermia Enhances Cytotoxicity of Bortezomib in Sensitive and Resistant Cancer Cell Lines. *Int J Nanomedicine*. **2013**; 9: 145-153.

47. Lee JS, Rodriguez-Luccioni HL, Mendez J, Sood AK, Lpez-Berestein G, Rinaldi C, et al. Hyperthermia Induced by Magnetic Nanoparticles Improves the Effectiveness of the Anticancer Drug Cis-Diamminedichloroplatinum. *J Nanosci Nanotechnol*. **2011**; 11: 4153-4157.

48. Rodriguez-Luccioni HL, Latorre-Esteves M, Mendez-Vega J, Soto O, Rodriguez AR, Rinaldi C, et al. Enhanced Reduction in Cell Viability by Hyperthermia Induced by Magnetic Nanoparticles. *Int J Nanomedicine*. 6: 373-380.

49. Creixell M, Bohorquez AC, Torres-Lugo M, Rinaldi C. Egfr-Targeted Magnetic Nanoparticle Heaters Kill Cancer Cells without a Perceptible Temperature Rise. *ACS Nano*. **2012**; 5: 7124-7129.

50. Domenech M, Marrero-Berrios I, Torres-Lugo M, Rinaldi C. Lysosomal Membrane Permeabilization by Targeted Magnetic Nanoparticles in Alternating Magnetic Fields. *ACS Nano*. **2013**; 7: 5091-5101.

51. Jordan A, Scholz R, Koch M, Lein M, Deger S, Roigas J, et al. Evaluation of Magnetic Fluid Hyperthermia in a Standard Rat Model of Prostate Cancer. *J Endourol*. **2004**; 18: 495-500.

52. Sadhukha T, Wiedmann TS, Panyam J. Inhalable Magnetic Nanoparticles for Targeted Hyperthermia in Lung Cancer Therapy. *Biomaterials*. **2013**; 34: 5163-5171.

53. Dennis CL, Jackson AJ, Borchers JA, Hoopes PJ, Strawbridge R, Foreman AR, et al. Nearly Complete Regression of Tumors Via Collective Behavior of Magnetic Nanoparticles in Hyperthermia. *Nanotechnology*. **2009**; 20: 395103.

54. Hilger I, Hiergeist R, Hergt R, Winnefeld K, Schubert H, Kaiser WA. Thermal Ablation of Tumors Using Magnetic Nanoparticles: An in Vivo Feasibility Study. *Invest Radiol*. **2002**; 37: 580-586.

55. Wang G, Xu D, Chai Q, Tan X, Zhang Y, Gu N, et al. Magnetic Fluid Hyperthermia Inhibits the Growth of Breast Carcinoma and Downregulates Vascular Endothelial Growth Factor Expression. *Oncology Letters*. **2014**; 7: 1370-1374.

56. Zhao Q, Wang L, Cheng R, Mao L, Arnold RD, Howerth EW, et al. Magnetic Nanoparticle-Based Hyperthermia for Head & Neck Cancer in Mouse Models. *Theranostics*. **2012**; 2: 113-121.

57. Balivada S, Rachakatla RS, Wang H, Samarakoon TN, Dani RK, Pyle M, et al. A/C Magnetic Hyperthermia of Melanoma Mediated by Iron(0)/Iron Oxide Core/Shell Magnetic Nanoparticles: A Mouse Study. *BMC Cancer*. **2010**; 10: 119.

58. Brusentsov NA, Brusentsova TN, Filinova EY, Jurchenko NY, Kupriyanov DA, Pirogov YA, et al. Magnetohydrodynamic Thermochemotherapy and Mri of Mouse Tumors. *Journal of Magnetism and Magnetic Materials*. **2007**; 311: 176-180.

59. Ren Y, Zhang H, Chen B, Cheng J, Cai X, Liu R, et al. Multifunctional Magnetic Fe3o4 Nanoparticles Combined with Chemotherapy and Hyperthermia to Overcome Multidrug Resistance. *Int J Nanomedicine*. **2012**; 7: 2261-2269.

60. Ito A, Saito H, Mitobe K, Minamiya Y, Takahashi N, Maruyama K, et al. Inhibition of Heat Shock Protein 90 Sensitizes Melanoma Cells to Thermosensitive Ferromagnetic Particle-Mediated Hyperthermia with Low Curie Temperature. *Cancer Sci*. **2009**; 100: 558-564.

61. Babincov M, Altanerov V, Altaner C, Bergemann C, Babinec P. In Vitro Analysis of Cisplatin Functionalized Magnetic Nanoparticles in Combined Cancer Chemotherapy and Electromagnetic Hyperthermia. *IEEE Trans Nanobioscience*. **2008**; 7: 15-19.

62. Petryk AA, Giustini AJ, Gottesman RE, Kaufman PA, Hoopes PJ. Magnetic Nanoparticle Hyperthermia Enhancement of Cisplatin Chemotherapy Cancer Treatment. *Int J Hyperthermia*. **2013**; 29: 845-851.

63. Eheman C, Henley SJ, Ballard-Barbash R, Jacobs EJ, Schymura MJ, Noone AM, et al. Annual Report to the Nation on the Status of Cancer, 1975-2008, Featuring Cancers Associated with Excess Weight and Lack of Sufficient Physical Activity. *Cancer*. 118: 2338-2366.

64. Cancer Facts & Figures 2014. *Atlanta:American Cancer Society*. **2014**.

65. Hanahan D, Weinberg RA. The Hallmarks of Cancer. *Cell*. **2000**; 100: 57-70.

66. Hanahan D, Weinberg RA. Hallmarks of Cancer: The Next Generation. *Cell*. **2011**; 144: 646-674.

67. Coolbrandt A, Van den Heede K, Vanhove E, De Bom A, Milisen K, Wildiers H. Immediate Versus Delayed Self-Reporting of Symptoms and Side Effects During Chemotherapy: Does Timing Matter? *European Journal of Oncology Nursing*. 15: 130-136.

68. Ketiku KK, Ajekigbe AT. Chemotherapy of Breast Cancer in Nigerians: Side-Effects and Quality of Life. *Clinical Oncology*. **1990**; 2: 153-155.

69. Luk KH, Francis ME, Perez CA, Johnson RJ. Combined Radiation and Hyperthermia: Comparison of Two Treatment Schedules Based on Data from a Registry Established by the Radiation Therapy Oncology Group (Rtog). *Int J Radiat Oncol Biol Phys*. **1984**; 10: 801-809.

70. Issels RD. Hyperthermia Adds to Chemotherapy. *Eur J Cancer*. **2008**; 44: 2546-2554.

71. Colombo R, Salonia A, Da Pozzo LF, Naspro R, Freschi M, Paroni R, et al. Combination of Intravesical Chemotherapy and Hyperthermia for the Treatment of Superficial Bladder Cancer: Preliminary Clinical Experience. *Crit Rev Oncol Hematol*. **2003**; 47: 127-139.

72. Falk MH, Issels RD. Hyperthermia in Oncology. *Int J Hyperthermia*. **2001**; 17: 1-18.

73. Hurwitz MD, Hansen JL, Prokopios-Davos S, Manola J, Wang Q, Bornstein BA, et al. Hyperthermia Combined with Radiation for the Treatment of Locally Advanced

Prostate Cancer: Long-Term Results from Dana-Farber Cancer Institute Study 94-153. *Cancer*. 117: 510-516.

74. Tae-Hee W, Minkyun Y, Wanghyun K, Youngwoo K, Young-Seek C, Jeiwon C, et al., editors. Non-Invasive Hyperthermic Ablation of Adipose Tissue Using Microwave. Antennas and Propagation Society International Symposium (APSURSI), 2010 IEEE; 11-17 July 2010.

75. Hand JW. Heat Delivery and Thermometry in Clinical Hyperthermia. *Recent Results Cancer Res*. **1987**; 104: 1-23.

`

Chapter 2

Hyperthermic Potentiation of Cisplatin by Magnetic Nanoparticle Heaters is Correlated with an Increase in Cell Membrane Fluidity

2.1. Introduction

Hyperthermic potentiation, defined as the improved effect obtained through a combination of heat and chemo/radiotherapy, has shown promising results in the treatment of cancer.[1,2] Over the years, an increasing number of reports regarding use of hyperthermia in conjunction with antineoplastic modalities have provided substantial evidence of its enhanced efficacy.[3] Nonetheless, current clinical applications using local, regional, and whole body hyperthermia have a number of disadvantages, including limitations in achievable treatment depth, complications due to patient surface irregularities (eg, head, arms), and overheating of adjacent normal tissue. Consequently, novel hyperthermic treatment options are of significant interest.[4]

The mechanisms involved in the hyperthermic potentiation of antineoplastic modalities are diverse. However, increased membrane fluidity has been proposed to be a reasonable cause of this potentiation.[5–7] Cis-diammine-dichloroplatinum (II) (cDDP, cisplatin) is a well characterized chemotherapeutic agent that has shown promising results when combined with hyperthermia, but its mechanisms of potentiation remain largely unknown.[8,9] Uptake of cDDP by the cell appears to be mediated by two distinct mechanisms, ie, active transport via copper transporter receptors and passive diffusion through the cellular membrane.[10] Currently, it is believed that active transport is the dominant mechanism of cDDP uptake.[11] Studies have

implicated regulators of copper homeostasis, including the primary human cell copper transporter (hCTR1), as being responsible for modulating the cytotoxic activity of cisplatin and other platinum-based drugs.[12] hCTR1 is rich in histidine and methionine residues, for which both copper and cisplatin have been shown to have high affinity and bind competitively.[13]

Numerous studies have highlighted the cytoprotective effects of copper in cDDP-exposed yeast and mammalian cells, emphasizing its dependence on hCTR receptors.[14–17] Although some groups report distinct molecular behaviors of the different members of the hCTR family, which appear to be cell-dependent, all reports agree that copper, due to its affinity with the hCTR receptor, affects receptor-mediated entry of cDDP negatively, resulting in improved cytotoxicity.[9,18–23]

Although copper receptors have a critical role in the uptake of cisplatin, one of the first studies that focused on the mechanisms of thermal enhancement of cDDP reported an increase in cell membrane fluidity, which in turn augmented the uptake of cDDP.[17,24,25] Therefore, the synergism of cDDP and hyperthermic treatment can potentially be explained in the context of membrane fluidity. However, the means by which hyperthermia is induced can also have additional effects on cells that must be taken into account.

The range of technologies by which hyperthermia is induced has expanded greatly in recent years. The use of magnetic nanoparticles to induce hyperthermia, so-called magnetic fluid hyperthermia, has shown promising in vitro and in vivo results.[26,27] Recent studies have also explored magnetic nanoparticles as a means of enhancing chemotherapeutic efficacy.[28] When inducing hyperthermia using magnetic nanoparticles, the physical mechanisms inherent in the dissipation of heat by these particles may exert an additional stress that goes beyond thermal effects and which results in enhanced potentiation of chemotherapeutics. Previously, we reported

that magnetic fluid hyperthermia resulted in enhanced cytotoxicity when compared with hot water hyperthermia alone in two separate cell lines, and subsequently we showed that magnetic fluid hyperthermia resulted in significantly enhanced cytotoxicity when combined with cDDP, as compared with hyperthermia using a water bath.[29,30]

In this study, we endeavored to characterize some of the differences in hyperthermic potentiation of cDDP using hot water hyperthermia and magnetic fluid hyperthermia. We hypothesized that magnetic fluid hyperthermia induces membrane fluidization by an additional thermal or physical stress on the cellular membrane, and that this in turn is responsible for increased intracellular accumulation of cDDP when compared with the effect of hot water hyperthermia. To test this hypothesis, we made direct and indirect measurements of cell membrane fluidity. First, the cell response to cDDP was measured using viability and clonogenic assays and platinum uptake measurements. To take advantage of the competitive binding effect of cisplatin and copper, we exposed a Caco-2 cell line to extracellular copper, thus hindering hCTR1-active receptor transport and permitting preferential passive diffusion via the cell membrane.[10,31] In addition, fluorescence anisotropy using trimethylamine-diphenylhexatriene (TMA-DPH) and acridine orange (Life Technologies, Carlsbad, CA, USA) diffusion measurements were done to quantify the extent of membrane fluidity induced by magnetic fluid hyperthermia and hot water hyperthermia. Our results show that cell membrane permeability induced by magnetic fluid hyperthermia is higher than that induced by hot water hyperthermia under similar temperature conditions. This increase in membrane fluidity induced by magnetic fluid hyperthermia is at least one of the mechanisms responsible for magnetic fluid hyperthermia potentiation of cDDP in Caco-2 cells.

2.2. Materials and methods

2.2.1. Caco-2 cell culture

Caco-2 cells were obtained from the American Type Culture Collection (ATCC) (Manassas, VA, USA). Cells were cultured in 75 cm^2 flasks (Costar, Corning, NY, USA) using Dulbecco's modified Eagle's medium (Sigma-Aldrich, St Louis, MO, USA) containing 10% fetal bovine serum (Life Technologies), 1% nonessential amino acids (Life Technologies), 100 U/mL penicillin (Sigma-Aldrich), and 100 μg/mL streptomycin (Sigma-Aldrich), supplemented with 2 mM L-glutamine and 24 mM sodium bicarbonate. Cells were maintained at 37°C, 95% relative humidity, and 5% CO2. Cell passages were performed weekly, while testing for mycoplasma contamination monthly.

2.2.2. Nanoparticle Suspension

The nanoparticles used in this study are from the same batch used in a previous study by Rodriguez-Luccioni et al.[29] For expedience, we summarize their preparation and characterization. Briefly, the iron oxide (IO) nanoparticles were synthesized by the coprecipitation method. An aqueous solution of ferric chloride and ferrous chloride with ammonium hydroxide at 80°C was mixed and stirred for 1 hour at pH 8.0 with bubbling nitrogen. After cooling to room temperature, the solution was centrifuged at 1800 rpm for 5 minutes to precipitate the nanoparticles. Nanoparticles were peptized with 0.5 M HNO3, centrifuged for 15 minutes at 3500 rpm, and resuspended in water. Afterwards, the IO nanoparticles were functionalized with carboxymethyl dextran and characterized. The content of IO in the nanoparticles was determined using a thermogravimetric analyzer (TA-2950; TA

Instruments, Newcastle, DE, USA). The hydrodynamic diameter was determined by dynamic light scattering using a particle size analyzer (BI-90 Plus; Brookhaven Instrument Corp, Holtsville, NY, USA). The specific absorption rate was measured by placing a suspension of nanoparticles at a concentration of 0.6 mg IO/ mL in an induction heater instrument (RDO Enterprises Inc, Washington, NJ, USA) and applying a magnetic field of 20 kA/m and 238 kHz.[29]

The nanoparticles were autoclaved for 60 minutes at a temperature of 121 °C and 15 psi. The autoclaved particles were characterized to verify particle integrity, dispersion, and stability. Once characterized the particles were suspended in Dulbecco's modified Eagle's medium prior to in vitro testing. The final particle concentration was 2 mg particles per mL (0.6 mg IO/mL).

2.2.3. IC50 determination

IC_{50} values were determined using Cell Titer Blue™ cell viability (Promega, Madison, WI, USA) and clonogenic assays. The cells were seeded in 96-well plates (Thermo Fisher Waltham, MA, USA) and allowed to adhere for 48 hours in Dulbecco's modified Eagle's medium. Adherent cells were exposed to increasing concentrations of cDDP (0.3–200 μM; Sigma-Aldrich) with and without 5 μM Cu^{2+} (Sigma-Aldrich) for 2.5 hours. Cells were then washed twice with Hank's balanced salt solution (Sigma-Aldrich) buffer and allowed to recover in Dulbecco's modified Eagle's medium for one week at 37° and 5% CO. After this recovery period the Dulbecco's modified Eagle's medium was discarded and the cells were washed twice with Hank's balanced salt solution, stained with CellTiter Blue, and analyzed fluorometrically (Spectra MAX Gemini EM; Molecular Devices, Sunnyvale, CA, USA). For clonogenic assay, the cells ($5 \times 10\underline{5}$ cells suspended in 2.5 mL of complete Dulbecco's modified Eagle's medium) were exposed to increasing concentrations of cDDP (0.3-200 μM) with and without 5

μM Cu^{2+} for 2.5 hours. Subsequently, the cells were washed by centrifugation and counted manually using Trypan blue (Sigma-Aldrich).

Different cell dilutions (2000-7000 cells) were seeded in six-well plates (Thermo Fisher Scientific) and allowed to form colonies for 10 days. After this time, the colonies were fixed stained with crystal violet, and counted in the manner reported by Franken et al.[32]

2.2.4. Synergism studies

2.2.4.1. Hot water hyperthermia (HWH)

Approximately 5×10^5 cells suspended in 2.5 mL of complete Dulbecco's modified Eagle's medium were transferred to 10 mL glass tubes and placed in a temperature-regulated water bath. Further temperature assessment was performed using a thermometer at 15-minute intervals. Control tubes were half-sealed to allow CO_2 exchange and remained in the incubator at 37°C for a period of 2.5 hours. Caco-2 cell samples were either treated or not treated with cisplatin (5 μM),Cu^{2+} (5 μM), or both, and heated to 41°C for 30 minutes. We decided to use mild hyperthermia (41°C) in order to distinguish better the synergistic effect between hyperthermia and cDDP. Application of higher temperatures would lead to signifcant decreases in cell viability, precluding differentiation of cell response to the various treatments. After treatment, the cells were incubated for a further 2 hours at 37°C. The cells were subsequently centrifuged for 10 minutes, the treatment medium was discarded and the cells were resuspended in 2.5 mL of drug-free medium. The cells were seeded in a 25 cm^2 flask (Costar) for 48 hours at 37°C and 5% CO_2. The cells were then trypsinized and cell viability was measured using Trypan blue. The surviving fraction was assessed by clonogenic assay as explained above.

2.2.4.2. Magnetic fluid hyperthermia (MFH)

Approximately 5×10^5 cells (in 2.5 mL final Dulbecco's modifed Eagle's medium suspension) were transferred to 10 mL glass tubes and treated with cDDP (5 μM), copper (5 μM), neither or both, concomitantly with a concentration of 2 mg/ mL of autoclaved IO carboxymethyl dextran nanoparticles. The tubes were then placed in the coil of the heat induction equipment and exposed to an alternating magnetic field. The environment surrounding the sample was kept at 37°C using an incubator enclosure. The sample temperature increased to 41°C due to energy dissipation by the nanoparticles and was held at that temperature for 30 minutes. A frequency of 237 kHz and a magnetic field of 20 kA/m were applied during the treatment period. After treatment, the cells were incubated for a further 2 hours at 37°C. The cells were then spun down for 10 minutes and the treatment medium was discarded. The cells were resuspended in 2.5 mL of Dulbecco's modified Eagle's medium. The viability fraction and surviving fraction were assessed as previously described.

2.2.5. cDDP uptake studies

Approximately 1×10^6 cells were exposed to either cDDP (5 μM), copper (5 μM) or both, and treated for 30 minutes with magnetic fluid hyperthermia or hot water hyperthermia at 41°C. The samples were subsequently placed in the incubator at 37°C for a period of 2 hours. At the end of the treatment period the cells were removed from the test tubes and centrifuged at 800 g for 10 minutes in order to remove the drug. The pellets were washed three times with phosphate-buffered saline at 4°C. After the final wash, the supernatant was aspirated and the pellet was frozen at −20°C, while awaiting uptake assay. The pelleted cells were resuspended in 200 μL of ultrapure water to obtain a homogeneous cell suspension. The suspended cells were

transferred into glass tubes containing 70% HNO3 and then mineralized until completely dried at 80°C. The mineralized sample was dissolved in 2 mL of 2% HNO3 containing 50 μg/L of indium (used as the internal standard). The samples were further disrupted by means of sonication for 10 minutes, resulting in a clear solution.[33] Sample analysis for platinum content was made using an inductively coupled plasma-mass spectrometer (X5 Series; Thermo Optek, Cinisello Balsamo, Italy). Concentration values were corrected to the indium signal.[33]

2.2.6. Membrane Fluidization Studies

Membrane fluidity was determined by measuring fluorescence anisotropy using TMA-DPH. After the cell samples had undergone treatment, TMA-DPH was added to a final concentration of 5 μM and the samples were allowed to incubate for 5 minutes prior to measurements. Fluorescence intensity measurements parallel or perpendicular to the direction of the excitation beam were read using a fluorescence spectrometer (USB4000; Ocean Optics, Henderson, NV, USA) with an external excitation source (100 mW, excitation wavelength 405 nm, emission 430 nm; Wicked Lasers, Hong Kong, People's Republic of China). Fluorescence anisotropy values are inversely proportional to cell membrane fluidity and are quantified according to:

$$r = \frac{I_{vv} - I_{vh}}{I_{vv} + 2I_{vh}}$$

where I_{vv} is the fluorescence intensity emitted parallel to the direction of excitation light, and I_{vh} is fluorescence intensity emitted perpendicular to excitation light.[34]

2.2.7. Flow cytometer

Cells (5×10^5) were stained with acridine orange immediately after hyperthermic treatment to a concentration of 1 μg/mL for a period of 5 minutes, then washed and resuspended in phosphate-buffered saline. Green (500-550 nm, FL1 channel) fluorescence, which was illuminated with blue (488 nm) light excitation, was measured using a flow cytometer (Accuri C6; Becton Dickinson, Ann Arbor, MI, USA).

2.2.8. Confocal microscopy

Cells stained with acridine orange were washed and resuspended in phosphate-buffered saline. Next, 20 μL of the cell suspension was aliquoted onto a microscope slide and immediately overlayed with a cover slip. Pictures were obtained with a spinning disk (Intelligent Imaging Innovations Inc, Denver, CO, USA) confocal microscope (Olympus IX81; Olympus America, Center Valley, PA, USA) equipped with a Xenon Fl source for visualization. Images were captured using a 60× oil immersion objective and Rolera EM-C2 camera (Quantitative Imaging Corporation, Cary, NC, USA). Experiments were repeated twice, and two images were obtained for each sample analyzed. All pictures were taken with an identical exposure time.

2.2.9. Statistical analysis

The sample size was n = 3 for all experiments except for confocal imaging (n = 2) and the control group in platinum uptake analysis (n = 4). Statistical analyses were conducted using the Student's *t*-test (two-tailed distribution, two-sample with unequal variances). Differences were considered significant at $P < 0.05$. The standard error and surviving fraction for clonogenic assay studies were determined using the approach established by Gupta et al.[35]

2.3. Results

2.3.1. Nanoparticle characterization

The nanoparticles used in this study were the same batch used by Rodriguez-Luccioni et al.[29] In that study, the hydro-dynamic diameter of the IO nanoparticles was determined to be 72 ± 4 nm by dynamic light scattering. The inorganic core content was found to be 27% by weight, as determined by thermogravimetric analysis. A specific absorption rate value of 245 W/g was determined at a magnetic field amplitude of 20 kA/m and a frequency of 238 kHz. Considering that specific absorption rate values generally depend on the magnetic field amplitude and frequency, nanoparticle structure (size and shape), and magnetic properties, the specific absorption rate value obtained for nanoparticles used in this study is consistent with data reported in the literature.[26,27] For example, IO nanoparticles exposed to a magnetic field amplitude of 24.5 kA/m and frequency of 400 kHz had a specific absorption rate value of 447 W/g.[26,36] On the other hand, Dennis et al synthesized and studied two different batches of IO nanoparticles coated with dextran. When they were exposed to a magnetic field amplitude of 85.9 kA/m and a frequency of 150 kHz, nanoparticles with lower saturation magnetization had a specific absorption rate value of 209 W/g, whereas nanoparticles with higher saturation magnetization had a specific absorption rate value of 537 W/g.[37,38]

2.3.2. Effect of extracellular Cu on cDDP-induced cell death

hCTR1-mediated uptake of cDDP into cells has been extensively documented.[9–14,19–24] It is widely accepted as the primary mechanism of influx of this platinum-based drug in cells.[10,11] To assess the effect of extracellular copper on this form of drug transport, the surviving

fraction and viability ratio of Caco-2 cells was studied by exposing cells to a mixture of 5 μM copper and increasing concentrations of cDDP for 2.5 hours. The concentration of copper was chosen based on its reported binding constant (K_m) value. Because K_m is defined as the copper concentration when the rate of transport through the hCTR1receptor is half of its maximum value, we chose a copper concentration above the K_m in order to hinder the hCTR1 receptor.[39] The surviving fraction of samples began to deviate significantly at cDDP concentrations above 5 μM, after which the fraction of surviving cells treated without copper dropped dramatically (Figure 2.1). On the other hand, we observed statistically significant differences in the viability ratio of cells treated with copper at concentrations of cDDP above 40 μM (Figure 2.1). The IC_{50}value of cDDP in the absence of copper was approximately 80 μM for both experimental methods. In the presence of copper, this value increased by approximately 30%. Mild hyperthermia is known to significantly enhance cDDP potentiation, leading to a significant increase in cell death. Consequently, we chose a lower drug concentration of 5 μM for subsequent experiments.

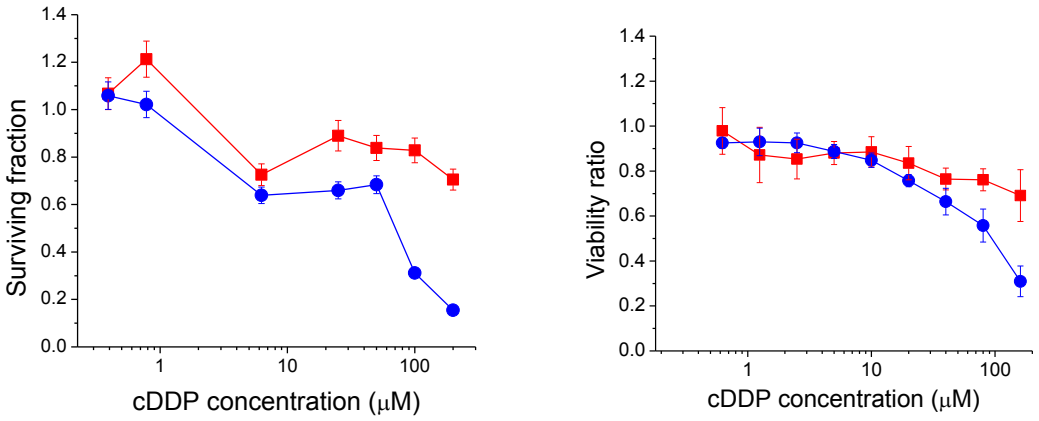

Figure 2. 1. Surviving fraction and viability ratio of Caco2 cells as a function of concentration of cDDP for an exposure period of 2.5h with Cu (squares) and without Cu (circles). Error bars represent the standard error of the mean of three independent experiments.

Because the magnetic fluid hyperthermia setup requires use of IO carboxymethyl dextran nanoparticles to induce heat, the cells were treated with the required concentration of these nanoparticles (0.6 mg IO/mL) in order to evaluate nanoparticle-induced cytotoxicity. Previous work by our group has shown that this concentration of nanoparticles used during magnetic fluid hyperthermia treatment does not induce cell cytotoxicity on its own.[29]

2.3.3. Effect of Cu on cDDP-induced cell death after treatment with hyperthermia

In an initial attempt to explain the differences in enhanced cytotoxicity between both forms of hyperthermic treatment, Caco-2 cells were treated for 30 minutes at 37°C or at 41°C using either hot water hyperthermia or magnetic fluid hyperthermia in combination with cDDP or cDDP + copper. After heat treatment, the cells were further exposed to cDDP or cDDP + copper for an additional 2 hours. This treatment sequence was chosen because an independent study had concluded that cDDP potentiation was most effective when the drug and hyperthermic treatment were applied simultaneously, followed by 2 hours of exposure to the drug at 37°C.[29] Cell viability and clonogenicity were quantified. The cytotoxic effects of hot water hyperthermia and magnetic fluid hyperthermia were evident using both assays (Figure 2.2). Interestingly, the surviving fraction determined using a clonogenic assay was consistently higher than viability ratio determined using trypan blue exclusion test, except for the cells treated with a combination of magnetic fluid hyperthermia and cDDP, with and without copper. The combination of magnetic fluid hyperthermia and cDDP proved to be most effective in reducing Caco-2 viability and clonogenicity, resulting in a statistically significant difference in viability ratio and surviving fractions relative to untreated cells and those treated with hot water hyperthermia (Figure 2.2, cDDP). In a similar manner, magnetic fluid hyperthermia was most effective in treating cells concomitantly with cDDP and copper (Figure 2.2, cDDP + copper).

The presence of extracellular copper resulted in a statistically significant difference in the surviving fraction for cells treated with hot water hyperthermia. In contrast, copper appeared to have little or no effect on Caco-2 cell survival in the context of magnetic fluid hyperthermia (Figure 2.2, cDDP versus cDDP + copper).

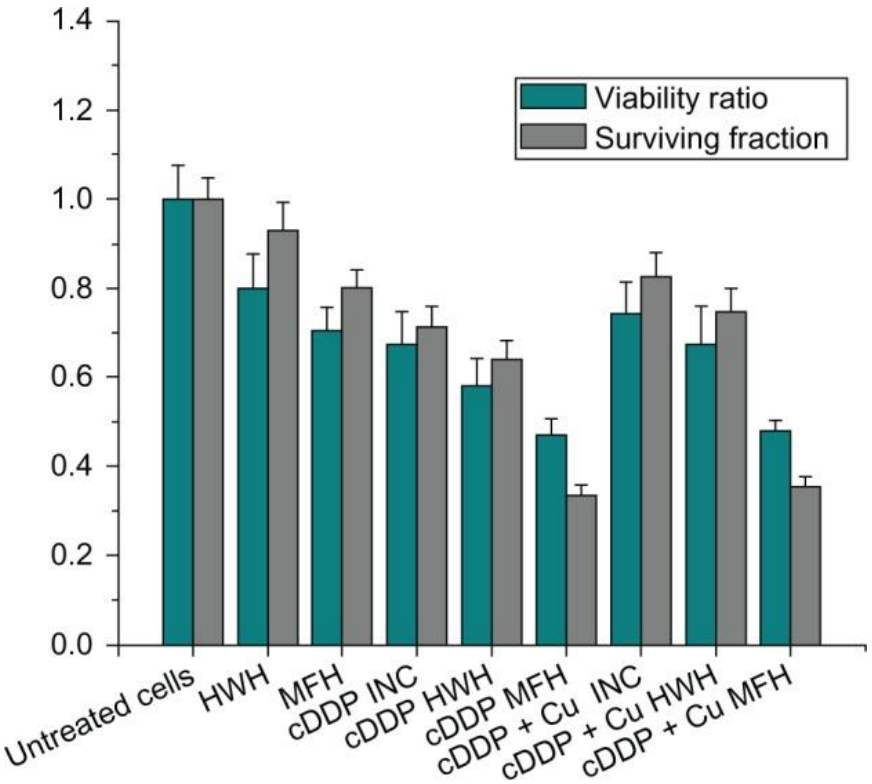

Figure 2. 2. Surviving fraction and viability ratio of Caco-2 cells treated with 5 µM cDDP with and without copper for 2.5 hours at 37°C, and with hot water hyperthermia or magnetic fluid hyperthermia, both at 41°C.

Notes: Untreated cells, cells maintained in the incubator; cDDP, cells with cisplatin; cDDP + Cu, cells with cisplatin and copper. Error bars represent the standard error of the mean of three independent experiments.

Abbreviation: cDDP, Cis-diammine-dichloroplatinum (II); HWH, hot water hyperthermia; INC, incubator; MFH, magnetic fluid hyperthermia; Cu, copper.

2.3.4. cDDP accumulation in vitro

The uptake of platinum in the context of hyperthermia, in the presence and absence of copper, was measured as a means to elucidate the mechanism of cell death induced by hyperthermia and cDDP (Figure 2.3). Immediately after treatment, the cells were washed three times with cold phosphate-buffered saline by centrifugation, then pelleted and frozen until the samples were ready to be quantified. The use of magnetic fluid hyperthermia and hot water hyperthermia in the presence of cDDP increased platinum uptake significantly when compared with control cells (cells with cDDP in the incubator versus cells with cDDP treated with hot water hyperthermia and those treated with cDDP and magnetic fluid hyperthermia). Furthermore, platinum uptake in cells treated with magnetic fluid hyperthermia was significantly greater than that in cells treated with hot water hyperthermia (cDDP hot water hyperthermia versus cDDP with magnetic fluid hyperthermia). Whereas the presence of extracellular copper served a protective role in our control cells, this was not evident in cells treated with cDDP in combination with either magnetic fluid hyperthermia or hot water hyperthermia. However, the surviving fraction of cells treated with magnetic fluid hyperthermia and cDDP in the presence of copper was lower than that of cells treated with hot water hyperthermia under the same conditions (Figure 2.2). Taken together, these results show that magnetic fluid hyperthermia promotes higher cDDP uptake than hot water hyperthermia at the same temperature of 41°C. Furthermore, no statistically significant differences in uptake of platinum by hyperthermia-treated cells in the presence of extracellular copper were observed, which suggests that both mild heat treatments are able to increase cell membrane fluidity, such that the protective role of copper is no longer apparent under these conditions. In light of these results, we hypothesized that differences in membrane fluidity induced by both forms of hyperthermic treatment could

explain the disparities in platinum uptake, and thereby surviving fraction and viability ratio, among the conditions evaluated. In order to test this hypothesis we conducted fluorescence polarization studies using a membranebound TMA-DPH probe.

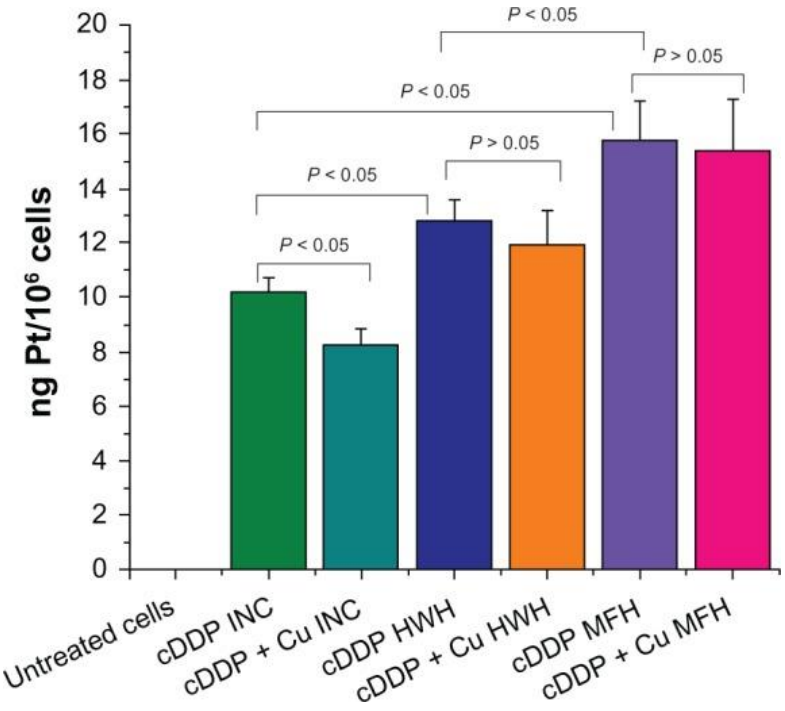

Figure 2. 3. Platinum uptake in Caco-2 cells treated with different thermal modalities in conjunction with Cu and cDDP. Values represent the mean ± SE from n = 3 for experimental samples and n = 4 for controls.

Abbreviation: cDDP, Cis-diammine-dichloroplatinum (II); HWH, hot water hyperthermia; INC, incubator; MFH, magnetic fluid hyperthermia; CU, copper.

2.3.5. Increased membrane fluidity in cells treated with magnetic fluid hyperthermia

TMA-DPH is a cationic derivative of the classic fluorescence polarization probe DPH, and has significant specificity for the cell plasma membrane, by anchoring its charged trimethylammonium group at the polar heads of the phospholipid bilayers and the apolar DPH

moiety placed between the fatty acid chains.[34] TMA-DPH has been used to label the outer leaflet of lipid bilayers in order to follow changes in membrane arrangements by fluorescence anisotropy measurements. These measurements have been shown to correlate with the rotational capability of the probe.[40]

Previous studies have shown that the heat shock response of cells involves an increase in cell membrane fluidity.[5–7] We hypothesized that cells that have undergone a mild treatment of hyperthermia (41°C and 30 minutes) using magnetic nanoparticles would suffer an additional mechanical stress on their cell membrane, induced by the presence of rotating and/or vibrating nanoparticles in solution, resulting in a higher membrane fluidity than those cells treated with hot water hyperthermia under the same temperature and for the same duration. Consequently, differences in fluorescence anisotropy induced by TMA-DPH would be observed.

Our results showed significant differences in membrane arrangements for both hyperthermic conditions relative to the control, as seen by a decrease in their fluorescence anisotropy reading, with magnetic fluid hyperthermia-treated cells showing significantly greater membrane fluidity than hot water hyperthermia-treated cells (Figure 2.4). This result suggests that magnetic fluid hyperthermia can induce an additional stress on the cellular membrane, either absent or not as significant in hot water hyperthermia-treated cells, that promotes higher membrane fluidity and which may be responsible for differences in cDDP uptake (Figure 2.3). In order to determine whether or not the concentration of cDDP used in this study induces membrane fluidity, we quantified changes in anisotropy for Caco-2 cells exposed to cDDP 5 μM at 37°C for 30 minutes, followed by TMA-DPH labeling. As shown in Figure 2.4 (red), cDDP-treated cells did not show any significant increase in membrane fluidity compared with the control.

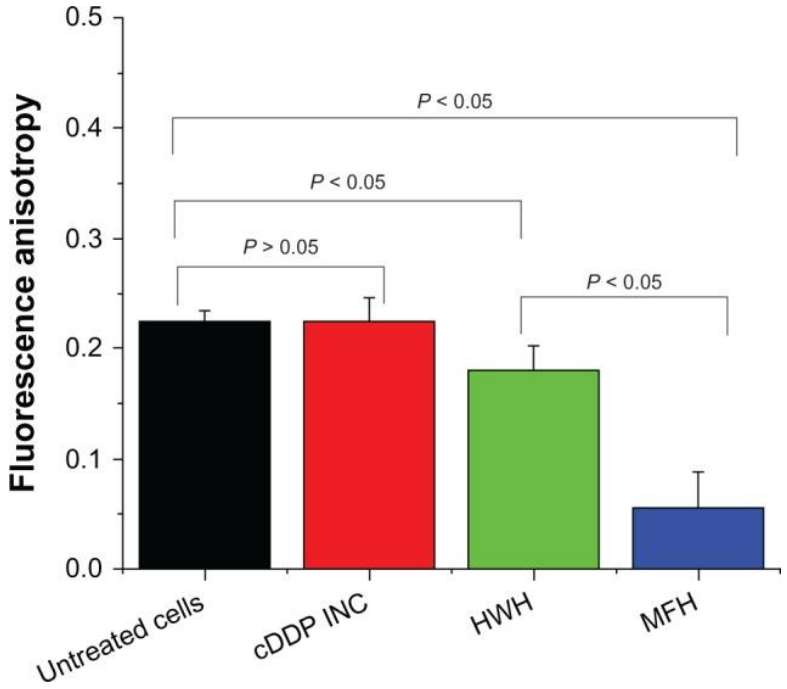

Figure 2. 4. Fluorescence anisotropy changes in cells treated with mild hyperthermia (41°C) as detected by TMA-DPH.

Notes: Caco-2 cells suspended in phosphate-buffered saline were treated at 41°C for 30 minutes, or left at 37°C, and labeled with TMA-DPH. The fluorescence anisotropy measurements were made at 430 nm. Data correspond to the mean ± SE for n = 3.

Abbreviations: TMA-DPH, trimethylamine-diphenylhexatriene; SE, standard error of the mean; INC, incubator; HWH, hot water hyperthermia; MFH, magnetic fluid hyperthermia; cDDP, cis-diammine-dichloroplatinum (II).

2.3.6. Enhanced passive transport of acridine orange in magnetic fluid hyperthermia-treated cells

An alternative indirect approach was used to evaluate changes in membrane fluidity of treated cells relative to untreated cells, by measuring the fluorescence intensity of cells exposed to acridine orange (Figure 2.5). Green fluorescence intensity measurements (as measured using a flow cytometer) were significantly higher in cells treated with mild hyperthermia relative to untreated cells (Figure 2.5). Furthermore, the green fluorescence intensity of cells treated with

magnetic fluid hyperthermia was significantly higher than that of cells treated with hot water hyperthermia. As shown in Table 2.1, the fold increases in fluorescence intensity observed between magnetic fluid hyperthermia and hot water hyperthermia were statistically different (Table 2.1). Finally, qualitative imaging of samples (Figure 2.6) showed incorporation of acridine orange. In agreement with flow cytometry measurements, an increase in green fluorescence is more apparent in cells treated with mild hyperthermia, with magnetic fluid hyperthermia-treated cells showing the most significant incorporation of the weak base. These results suggest that the rate of passive diffusion of acridine orange had greater enhancement in magnetic fluid hyperthermia-treated cells, presumably due to an increase in cell membrane fluidity.

Table 2. 1. Fold increase in fluorescence intensity of treated cells (HWH and MFH) relative to untreated cells

	HWH treated cells	MFH treated cells
	FL1 intensity	FL1 intensity
Mean	1.32*	1.87**
SD	0.08	0.05
SE	0.05	0.03

Notes: * Statistically different when compared to **. The numbers represent the mean of 3 independent experiments.

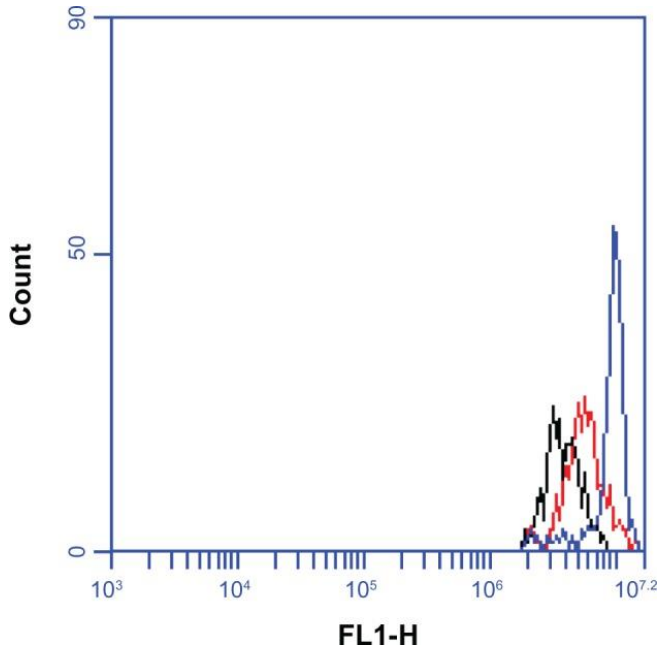

Figure 2. 5. Effect of mild hyperthermia on the fluorescence intensity (as measured by FL1 channel) in acridine orange-stained cells (blue: magnetic fluid hyperthermia and red: hot water hyperthermia), relative to untreated cells (black).

Note: Three independent experiments were done.

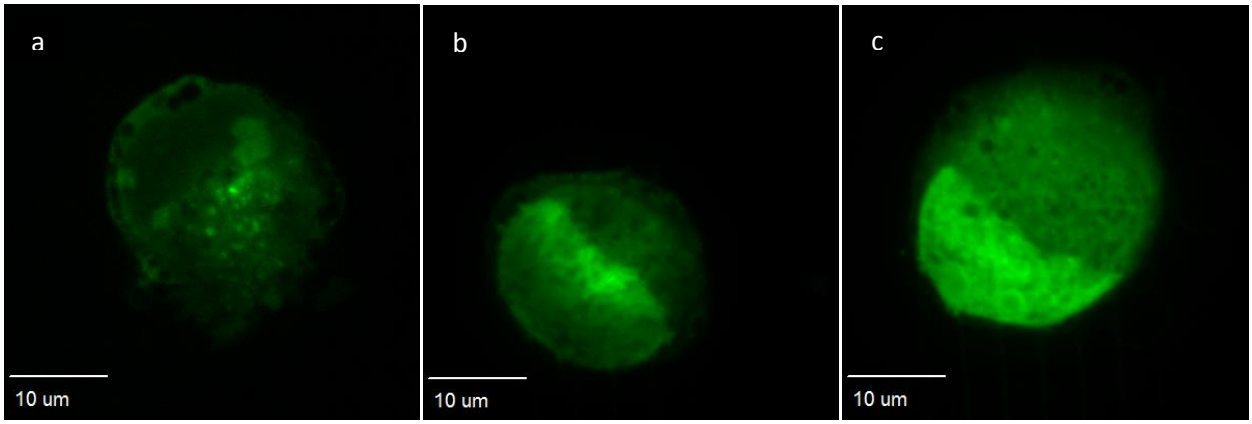

Figure 2. 6. Acridine orange incorporation in cells treated with mild hyperthermia (41°C). a. Untreated cells. b. Cells treated with water bath hyperthermia for 30 minutes. c. Cells treated with MFH for 30 minutes (two independent experiments).

2.4. Discussion

In the present work, we have shown that the presence of extracellular copper at a concentration close to the K_m value of hCTR1 reduces cDDP-induced cytotoxicity in Caco-2 cells at cisplatin concentrations above 5 μM (Figure 2.1).[39] In order to determine whether the aforementioned concentration of extracellular copper is able to affect mild hyperthermic-induced cell toxicity, we treated Caco-2 cells with cDDP at 41°C with either magnetic fluid hyperthermia or hot water hyperthermia, in the presence and absence of extracellular copper (Figure 2.2). We had previously reported differences in cell viability after combined treatment of cDDP and mild hot water hyperthermia or magnetic fluid hyperthermia at 41°C.[30] At the aforementioned temperature, differences in drug potentiation could be observed without compromising the fate of our entire cell sample.

Our results show that while copper serves a protective role in the context of long-term clonogenic survival when cells are treated concomitantly with hot water hyperthermia and cDDP, this protective role is not evident when magnetic fluid hyperthermia is used instead. No protective role in short-term cell viability was observed under our experimental conditions. These results suggest that the synergistic potentiation of cDDP with magnetic fluid hyperthermia differs from that of cDDP with hot water hyperthermia through a mechanism that appears to be independent of hCTR1-mediated drug influx. It is possible that the presence of extracellular copper is inhibiting the amount of cDDP that is being incorporated into cells exposed to hot water hyperthermia and control cells through a competitive binding interaction with hCTR1. In the case of cells treated with cDDP and magnetic fluid hyperthermia, the absence of a protective role by copper in the surviving fraction of cells suggests that this hyperthermic treatment might allow cDDP incorporation via an alternative route. Mild hyperthermia has been shown to

increase cell membrane fluidity in different cell lines.[41,42] In this study, we have shown that hyperthermia-induced cell membrane fluidity is one of the mechanisms responsible for cDDP potentiation in cancer cells and that the extent of drug potentiation and membrane fluidity varies greatly between the two forms of hyperthermia application, ie, magnetic fluid hyperthermia and hot water hyperthermia. cDDP potentiation using magnetic fluid hyperthermia is caused, at least in part, by an increase in cell membrane fluidity. Cells treated concomitantly with cDDP and magnetic fluid hyperthermia or hot water hyperthermia had higher platinum uptake than control cells. Cells treated at 41°C with magnetic fluid hyperthermia had a higher platinum uptake compared with cells treated with hot water hyperthermia at the same temperature. These results point to the possibility that magnetic fluid hyperthermia-induced cell membrane fluidity was more significant than that induced by hot water hyperthermia, allowing a higher uptake of cDDP to be transported passively across the cell membrane. In order to assess this possibility, we performed two independent experiments aimed at characterizing the membrane fluidity of cells exposed to magnetic fluid hyperthermia and hot water hyperthermia (Figure 2.4). Statistically significant differences in fluorescence anisotropy were observed between untreated cells and cells treated at 41°C. Furthermore, a significant reduction in fluorescence anisotropy was observed in cells treated with magnetic fluid hyperthermia compared with hot water hyperthermia, suggesting that magnetic fluid hyperthermia increases cell membrane fluidity more dramatically. We also saw no significant differences in cDDP-induced membrane fluidity at the drug concentration used in this work. Finally, we quantified the amount of acridine orange which diffused into cells right after treatment with either magnetic fluid hyperthermia or hot water hyperthermia. Acridine orange is a weak base that can passively diffuse through the cell membrane. It fluoresces green when located in the cytoplasm and nucleus.[43] Its fluorescence

intensity is directly proportional to the amount of acridine orange that has entered into the cytoplasm and nucleus. Previous studies suggest that internalization of acridine orange into cells is mainly passive, so we hypothesized that its diffusion into cells would differ between treatments that affect the fluidity of the cell membrane.[44] The fluorescence intensity of cells was analyzed quantitatively and qualitatively using flow cytometry and confocal microscopy, respectively. Statistically significant differences in fluorescence intensity were observed between cells treated with magnetic fluid hyperthermia and hot water hyperthermia (Table 2.1). Furthermore, qualitative differences in fluorescence intensity after exposure to acridine orange were observed for cells exposed to magnetic fluid hyperthermia and hot water hyperthermia.

2.5. Conclusion

To our knowledge, this work provides the first direct evidence of a mechanistic difference in the hyperthermic potentiation of a chemotherapeutic agent by hot water and magnetic fluid hyperthermia. Specifically, we have demonstrated that magnetic fluid hyperthermia enhances cDDP activity in cancer cells by enhancing passive uptake due to an increase in membrane fluidity. This mechanism was demonstrated by comparison of the reduction in cell viability and cDDP uptake in cells treated with magnetic fluid hyperthermia or hot water hyperthermia and cDDP with and without blocking active uptake through the CTR1 transporter. These studies demonstrated enhanced activity and uptake of cDDP in cells treated with magnetic fluid hyperthermia, regardless of the status of the CTR1 transporter. Further experiments demonstrated increased membrane fluidity and passive uptake of the diffusing species in cells treated with magnetic fluid hyperthermia. Although demonstrated in the context of cDDP, the demonstrated mechanism of enhanced passive uptake could find application in potentiation of other chemotherapeutics.

2.6. References

1. Hahn GM, Li GC, Shiu E. Interaction of amphotericin B and 43 degrees hyperthermia. Cancer Res.**1977**;37(3):761–764.

2. Hurwitz MD, Hansen JL, Prokopios-Davos S, et al. Hyperthermia combined with radiation for the treatment of locally advanced prostate cancer: long-term results from Dana-Farber Cancer Institute study 94-153. *Cancer*. **2011**;117(3):510–516.

3. Vanakoski J, Seppala T. Heat exposure and drugs. A review of the effects of hyperthermia on pharmacokinetics. *Clin Pharmacokinet*. **1998**;34(4):311–322.

4. van der Zee J. Heating the patient: a promising approach? *Ann Oncol*. **2002**;13(8):1173–1184.

5. Rock E, Motta C, Vignon X, Kozak-Ribbens G. Fluidity state of lymphocyte plasma membrane in malignant hyperthermia susceptible pigs and humans. *Acta Anaesthesiol Scand*. **1993**;37(5):488–492.

6. Dynlacht JR, Fox MH. The effect of 45 degrees C hyperthermia on the membrane fluidity of cells of several lines. Radiat Res. **1992**;130(1):55–60.

7. Kawamoto M, Fujii K, Kikuchi H, Morio M. Increased membrane fluidity of erythrocytes in a case with malignant hyperthermia. *J Anesth*. **1987**;1(1):88–92.

8. Rao W, Deng ZS, Liu J. A review of hyperthermia combined with radiotherapy/chemotherapy on malignant tumors. *Crit Rev Biomed Eng*. **2010**;38(1):101–116.

9. Kuo MT, Chen HH, Song IS, Savaraj N, Ishikawa T. The roles of copper transporters in cisplatin resistance. *Cancer Metastasis Rev*. **2007**;26(1):71–83.

10. Wang D, Lippard SJ. Cllular processing of platinum anticancer drugs. *Nat Rev Drug* Discov.**2005**;4(4):307–320.

11. Safaei R, Howell SB. Copper transporters regulate the cellular pharmacology and sensitivity to Pt drugs. Crit Rev Oncol Hematol. **2005**;53(1):13–23.

12. Safaei R. Role of copper transporters in the uptake and efflux of platinum containing drugs. *Cancer Lett*. **2006**;234(1):34–39.

13. Lee J, Pena MM, Nose Y, Thiele DJ. Biochemical characterization of the human copper transporter Ctr1. *J Biol Chem*. **2002**;277(6):4380–4387.

14. Ishida S, Lee J, Thiele DJ, Herskowitz I. Uptake of the anticancer drug cisplatin mediated by the copper transporter Ctr1 in yeast and mammals. *Proc Natl Acad Sci U S A.* **2002**;99(22):14298–14302.

15. Ohashi K, Kajiya K, Inaba S, et al. Copper(II) protects yeast against the toxicity of cisplatin independently of the induction of metallothionein and the inhibition of platinum uptake. *Biochem Biophys Res Commun*. **2003**;310(1):148–152.

16. Ishida S, McCormick F, Smith-McCune K, Hanahan D. Enhancing tumor-specific uptake of the anticancer drug cisplatin with a copper chelator. *Cancer Cell*. **2010**;17(6):574–583.

17. Holzer AK, Katano K, Klomp LW, Howell SB. Cisplatin rapidly down-regulates its own influx transporter hCTR1 in cultured human ovarian carcinoma cells. *Clin Cancer Res*. **2004**;10(19):6744–6749.

18. Molloy SA, Kaplan JH. Copper-dependent recycling of hCTR1, the human high affinity copper transporter. *J Biol Chem*. **2009**;284(43):29704–29713.

19. Sinani D, Adle DJ, Kim H, Lee J. Distinct mechanisms for Ctr1-mediated copper and cisplatin transport. *J Biol Chem*. **2007**;282(37):26775–26785.

20. Blair BG, Larson CA, Safaei R, Howell SB. Copper transporter 2 regulates the cellular accumulation and cytotoxicity of cisplatin and carboplatin. *Clin Cancer Res*. **2009**;15(13):4312–4321.

21. Blair BG, Larson CA, Adams PL, Abada PB, Safaei R, Howell SB. Regulation of copper transporter 2 expression by copper and cisplatin in human ovarian carcinoma cells. *Mol Pharmacol*. **2010**;77(6):912–921.

22. Jandial DD, Farshchi-Heydari S, Larson CA, Elliott GI, Wrasidlo WJ, Howell SB. Enhanced delivery of cisplatin to intraperitoneal ovarian carcinomas mediated by the effects of bortezomib on the human copper transporter 1. *Clin Cancer Res*. **2009**;15(2):553–560.

23. Holzer AK, Varki NM, Le QT, Gibson MA, Naredi P, Howell SB. Expression of the human copper influx transporter 1 in normal and malignant human tissues. *J Histochem Cytochem*.**2006**;54(9):1041–1049.

24. Eisses JF, Chi Y, Kaplan JH. Stable plasma membrane levels of hCTR1 mediate cellular copper uptake. J Biol Chem. **2005**;280(10):9635–9639.

25. Hettinga J V, Lemstra W, De Vries EG, Konings AW, Kampinga HH. Sensitization to cisplatin action by step-down heating in cDDP-sensitive and -resistant cells. *Int J Cancer*. **1995**;61(5):722–726.

26. Kumar CS, Mohammad F. Magnetic nanomaterials for hyperthermia-based therapy and controlled drug delivery. *Adv Drug Deliv Rev*. **2011**;63(9):789–808.

27. Lee JH, Jang JT, Choi JS, et al. Exchange-coupled magnetic nanoparticles for efficient heat induction. *Nat Nanotechnol*. **2011**;6(7):418–422.

28. Banerjee R, Katsenovich Y, Lagos L, McIintosh M, Zhang X, Li CZ. Nanomedicine: magnetic nanoparticles and their biomedical applications. Curr Med Chem. 2010;17(27):3120–3141.

29. Rodriguez-Luccioni HL, Latorre-Esteves M, Mendez-Vega J, et al. Enhanced reduction in cell viability by hyperthermia induced by magnetic nanoparticles. Int J Nanomedicine. 2011;6:373–380.

30. Lee JS, Rodriguez-Luccioni HL, Mendez J, et al. Hyperthermia induced by magnetic nanoparticles improves the effectiveness of the anticancer drug cis-diamminedichloroplatinum. J Nanosci Nanotechnol. 2011;11(5):4153–4157.

31. Howell SB, Safaei R, Larson CA, Sailor MJ. Copper transporters and the cellular pharmacology of the platinum-containing cancer drugs. Mol Pharmacol. 2010;77(6):887–894.

32. Franken NA, Rodermond HM, Stap J, Haveman J, van Bree C. Clonogenic assay of cells in vitro.Nat Protoc. 2006;1(5):2315–2319.

33. Ghezzi A, Aceto M, Cassino C, Gabano E, Osella D. Uptake of antitumor platinum(II)-complexes by cancer cells, assayed by inductively coupled plasma mass spectrometry (ICP-MS). J Inorg Biochem.2004;98(1):73–78.

34. Gantet P, Hubac C, Brown SC. Flow Cytometric Fluorescence Anisotropy of Lipophilic Probes in Epidermal and Mesophyll Protoplasts from Water-Stressed Lupinus albus L. Plant Physiol.1990;94(2):729–737.

35. Gupta N, Lamborn K, Deen DF. A statistical approach for analyzing clonogenic survival data. Radiat Res. 1996;145(5):636–640.

36. Gonzales-Weimuller M, Zeisberger M, Krishnan KM. Size-dependant heating rates of iron oxide nanoparticles for magnetic fluid hyperthermia. J Magn Mag Mater. 2009;321(13):1947–1950.

37. Dennis CL, Jackson AJ, Borchers JA, et al. The influence of magnetic and physiological behaviour on the effectiveness of iron oxide nanoparticles for hyperthermia. J Phys D: Appl Phys.2008;41(13):134020.

38. Dennis CL, Jackson AJ, Borchers JA, et al. The infuence of collective behavior on the magnetic and heating properties of iron oxide nanoparticles. J Appl Phys. 2008;10307(7):A319.

39. Eisses JF, Kaplan JH. Molecular characterization of hCTR1, the human copper uptake protein. J Biol Chem. 2002;277(32):29162–29171.

40. Azenabor AA, Job G, Adedokun OO. Chlamydia pneumoniae infected macrophages exhibit enhanced plasma membrane fluidity and show increased adherence to endothelial cells. Mol Cell Biochem. 2005;269(1–2):69–84.

41. Balogh G, Horvath I, Nagy E, et al. The hyperfluidization of mammalian cell membranes acts as a signal to initiate the heat shock protein response. FEBS J. 2005;272(23):6077–6086.

42. Moulin M, Carpentier S, Levade T, Arrigo AP. Potential roles of membrane fluidity and ceramide in hyperthermia and alcohol stimulation of TRAIL apoptosis. Apoptosis. 2007;12(9):1703–1720.

43. Paglin S, Hollister T, Delohery T, et al. A novel response of cancer cells to radiation involves autophagy and formation of acidic vesicles. Cancer Res. 2001;61(2):439–444.

44. Dechsupa N, Mankhetkorn S. P-Glycoprotein-Mediated Efflux and Drug Sequestration in Lysosomes Confer Advantages of K562 Multi-drug Resistance Sublines to Survive Prolonged Exposure to Cytotoxic Agents. Am J Appl Sci. 2009;6(9):1637–1646.

Chapter 3

Magnetic Fluid Hyperthermia Enhances Bortezomib Cytotoxicity in Sensitive and Resistant Cancer Cells lines

3.1. Introduction

The proteasome, a multisubunit proteinase machinery, is in charge of degrading 80%–90% of all nuclear and cytosolic proteins in cells[1–3] and plays an essential role in regulating the intracellular concentration of specific proteins, thereby maintaining homeostasis within the cell.[1,4,5] Inhibition of the 26S proteasome prevents this targeted proteolysis, which can affect multiple signaling cascades within the cell, leading to cell death.[1,6] As such, proteasome inhibition has become an attractive target for cancer treatment.[7]

Bortezomib (BZ), a drug approved by the US Food and Drug Administration, is a reversible inhibitor of the chymotrypsin-like activity of the 26S proteasome in mammalian cells. It has been tested as a potential therapeutic agent for the treatment of several types of cancer including breast, colon, ovarian, lung, and certain hematologic neoplasms.[8] Unfortunately, some of these types of cancer do not respond to its therapeutic effect, because they have intrinsic or acquired BZ resistance.[9–13] The reason for this phenomenon is still unknown, but some molecular mechanisms have been proposed. de Wilt et al demonstrated that intrinsic BZ resistance of non-small-cell lung cancer is related to increased proteasome activity.[14] On the other hand, acquired resistance was associated with mutation of the β5 subunit, which is the proteasome subunit

where BZ binds.[14] Overexpression of antiapoptotic protein Bcl-2 and heat-shock proteins 27, 70, and 90 is also considered a mechanism of acquired BZ resistance.[15,16]

Recent studies have provided evidence of enhanced efficacy of BZ when used in combination with hyperthermia.[11,17–19] Xu et al showed that hyperthermia using a water bath sensitized resistant breast cancer cells to BZ, resulting in enhanced cell death.[11] Similar observations were made with HT1080, HeLa, H1299, and HCT116 cells exposed to BZ and hyperthermia.[18,19] The mechanism by which hyperthermia enhances BZ cytotoxicity has not been elucidated. However, protein unfolding and subsequent aggregation induced by hyperthermia is considered one of the mechanisms by which hyperthermia sensitizes cells to proteasome inhibition.[20]

Although in vitro studies of hyperthermia with BZ have shown promising results, translation to the clinic has been limited due to challenges regarding application of hyperthermia as a treatment modality. These include avoidance of nonspecific damage to adjacent tissues, occurrence of tachycardia and malaise, and a detrimental impact on tissue metabolism, blood flow, organ function, and tissue repair.[21,22] For these reasons, alternative hyperthermia application approaches are being actively pursued.

The use of magnetic nanoparticles for localized thermal oncotherapy is a novel and attractive approach.[23] This approach, commonly called magnetic fluid hyperthermia (MFH), takes advantage of the deposition of thermal and mechanical energy by magnetic particles under an applied alternating magnetic field, resulting in local heating of cancerous tissue.[24] Recently, we have demonstrated that application of MFH to treat a human epithelial colorectal adenocarcinoma cell line (Caco-2) was more effective in reducing cell viability when compared with hot water hyperthermia (HWH) at similar thermal doses.[25] Also, combination treatment

using cisdiamminedichloroplatinum(II) and MFH induced significant cytotoxicity in the Caco-2 cell model, and was more effective than a combination of the drug with hyperthermia using a hot water bath.[26] Subsequently, it was demonstrated that one of the mechanisms explaining why MFH is significantly more effective in combination with cisdiamminedichloroplatinum(II) than HWH is an increase in membrane fluidity which allows higher intracellular drug accumulation.[27]

Our past work motivated us to search for other anticancer drugs that could potentially be enhanced by the application of MFH, particularly in cases of intrinsic or acquired chemoresistance. Given the expectation that delivery of thermal energy to the interior of a cell could result in enhanced protein denaturation, we hypothesized that proteasome inhibitors in combination with MFH should possess enhanced cytotoxicity that is greater than each individual treatment. In order to test this hypothesis, dose response curves and proteasome activity curves, as a function of BZ concentration were conducted. The following cell lines were selected to conduct the experiments: human epithelial breast carcinoma cells (MDA-MB-468), heterogeneous human colorectal adenocarcinoma cells derived from colon carcinoma (Caco-2), and human epithelial ovarian cancer cells established from the tumor tissue of an untreated patient (A2780). Two of these are BZ-sensitive (MDA-MB-468, Caco-2) and one is BZ-resistant (A2780). The cell response to BZ in combination with MFH at two different conditions (43°C for 30 minutes and 45°C for 30 minutes) was then measured and the combined cytotoxicity was compared with that of HWH and BZ. Results indicated that enhancement of cytotoxicity between MFH and BZ is greater than the effect produced by HWH and BZ at similar thermal doses. Our results confirm the effectiveness of MFH for potentiation of BZ, even in cell lines that show intrinsic resistance to this drug, making this an attractive approach for enhancing the effectiveness of a drug already approved by the US Food and Drug Administration.

3.2. Material and Methods

3.2.1. Cell culture

MDA-MB-468 and Caco-2 cells were obtained from the American Type Culture Collection (Manassas, VA, USA). The cells were cultured in 75 cm^2 flasks (Costar, Corning, NY, USA) using Dulbecco's modified Eagle's medium (Sigma, St Louis, MO, USA) containing 10% fetal bovine serum (Invitrogen, Carlsbad, CA, USA), 1% nonessential amino acids (Invitrogen), 100 units/mL of penicillin (Sigma), and 100 μg/mL of streptomycin (Sigma), and supplemented with 2 mM L-glutamine and 24 mM sodium bicarbonate. The cells were maintained at 37°C, 95% relative humidity, and 5% CO_2. A2780 cells were donated by Dr Anil K Sood from the MD Anderson Cancer Center, Houston, TX, USA. They were cultured in Roswell Park Memorial Institute medium (Sigma) with 15% fetal bovine serum and 0.1% gentamicin (Sigma) at 37°C under 5% CO_2.

3.2.2. Drug

BZ (LC Laboratories, Woburn, MA, USA) was dissolved in dimethylsulfoxide (Sigma), aliquoted, and stored at −20°C. Aliquots were thawed and diluted in Dulbecco's modified Eagle's medium before use.

3.2.3. Synthesis of iron oxide nanoparticles

Iron oxide nanoparticles were synthesized by the coprecipitation method and coated with carboxymethyl dextran, as described previously.[28] An aqueous iron solution (Fe^{+3}:$2Fe^{+2}$) and an ammonium hydroxide solution were mixed at 80°C. The pH of this reaction mixture was

maintained at 8.0 while stirring for one hour with bubbling nitrogen. After this reaction period, the solution was centrifuged at 1,500 rpm for 5 minutes, the supernatant was discarded, and the magnetic nanoparticles were peptized with tetramethyl ammonium hydroxide (1 M). The peptized nanoparticles were dried at 65°C using a vacuum oven. Next, 1.125 g of peptized iron oxide nanoparticles were functionalized with 3-aminopropyltriethoxysilane (APS) in a solution containing 75 mL dimethylsulfoxide, 5 mL of APS, 1.25 mL of water, and 100 μL of acetic acid. This solution was stirred for 36 hours in a shaker at 150 rpm and room temperature. At the end of the reaction, the nanoparticles were washed four times with ethanol by centrifugation and left to dry at room temperature. The iron oxide nanoparticles coated with APS were then functionalized with carboxymethyl dextran via reaction with N,N-(3-dimethylaminopropyl)-N'-ethyl-carbodiimide hydrochloride (EDC)/N-hydroxysuccinimide (NHS) in order to form covalent bonds between APS and carboxymethyl dextran. This reaction was achieved by mixing a solution containing 1 g of carboxymethyl dextran, 10 mL of deionized water, 12.25 mg of EDC, and 7.25 mg of NHS at pH 4.5–5 with 0.1 g of IO-APS dissolved in 10 mL of deionized water at pH 4.5–5. This mixture was stirred at 150 rpm for 36 hours at room temperature. After this reaction period, the nanoparticles were washed three times with ethanol by centrifugation and left to dry in a vacuum oven at 65°C.[29]

The nanoparticles were sterilized at a temperature of 121°C and 15 psi for 60 minutes before the in vitro experiments. They were then characterized and suspended in Dulbecco's modified Eagle's medium prior to the experiments. The final particle concentration was 3.848 mg particles per mL (0.5 mg IO/mL).

3.2.4. Characterization of Nanoparticles

The physical size and morphology of the iron oxide nanoparticles were determined using an energy-filtered transmission electron microscope (LEO 922 Omega, Carl Zeiss Meditec AG, Jena, Germany) at 200 kV. The hydrodynamic diameter of the synthesized and functionalized nanoparticles suspended in deionized water was determined by dynamic light scattering using a particle size analyzer (BI-90 Plus, Brookhaven Instrument Corporation, Holtsville, NY, USA). Inorganic core content was estimated using a thermogravimetric analyzer (TGA/DSC1, Mettler Toledo Inc, Columbus, OH, USA). The magnetic properties of the nanoparticles were determined using a SQUID magnetometer (MPMS XL-7, Quantum Design Inc., San Diego, CA, USA). The specific absorption rate of the iron oxide nanoparticles was obtained by placing a solution of nanoparticles in deionized water at a concentration of 0.5 mg IO/mL in an induction heater (HFI 3 KW RF heating system, RDO Induction LLC, Washington, NJ, USA) with magnetic field intensities ranging from 24.18 kA/m to 34.73 kA/m. The specific absorption rate is reported as watt per gram of iron oxide.

3.2.5. Bortezomib Dose-Response Curve

MDA-MB-468 and Caco-2 cells were seeded in 96-well plates (Fisher Scientific, Suwanee, GA, USA) and allowed to adhere for 48 hours in Dulbecco's modified Eagle's medium solution. A2780 cells were allowed to adhere for 24 hours in Roswell Park Memorial Institute medium. These time periods were chosen to ensure that the cells were in log phase growth before treatment. After this incubation period, the cells were exposed to varying concentrations of BZ (2–1,000 nM) for 48 hours. The cells were then washed twice with phosphate-buffered saline (Sigma), stained with Cell Titer Blue™ (Promega, Madison, WI,

USA) and analyzed fluorometrically (Spectra MAX Gemini EM, Molecular Devices, Sunnyvale, CA, USA).

3.2.6. Proteasome activity

Cells were seeded in 96-well plates (10,000 cells per well) and allowed to adhere in medium solution as described before. Adhered cells were exposed to various concentrations of BZ (2–1,000 nM) for 3 hours. Next, 100 μL of Proteasome-Glo™ Chymotrypsin-Like Assay (Promega), containing a substrate which luminesces when recognized and degraded by the proteasome, was added per well and allowed to react at room temperature for 15 minutes in the dark. After this period, luminescence measurements were made in a spectrofluorometer (Spectra MAX Gemini EM).

3.2.7.Combined Hyperthermia Treatment

Approximately 5×10^5 cells were transferred to 10 mL glass tubes. Cells to be treated by HWH were suspended in 2.5 mL of complete medium with and without BZ. Next, samples in the presence of BZ were left in the incubator for 3 hours to promote proteasome inhibition before hyperthermic treatment. After pretreatment, the samples were placed in a temperature-regulated water bath for 30 minutes at 43°C or 45°C. Cells to be treated by MFH were suspended in 2.5 mL of DMEM solution with or without BZ, concomitantly with a concentration of 3.8 mg/mL of auto claved carboxymethyl dextran-coated magnetite nanoparticles. Samples containing BZ were incubated for 3 hours prior to applying the alternating magnetic field. The samples were then placed in an induction heater coil (HFI 3 KW RF heating system) and magnetically heated to 43°C or 45°C for 30 minutes. A magnetic field of 29.39 kA/m or 34.73 kA/m was applied to maintain the sample temperature at 43°C or 45°C, respectively. A frequency of 233 kHz was

applied at both temperature conditions. Control tubes had the same dimethylsulfoxide concentration as the experimental group (0.1%) but remained in the incubator at 37°C. After treatment, 100,000 cells were transferred to six-well plates (Fisher Scientific) exposing cells continuously to the drug to maintain a constant proteasome inhibition for an additional of 48 hours at 37°C and 5% CO_2. After incubation, the cells were trypsinized and cell viability was measured using the trypan blue exclusion method (Sigma). Our previous work using anticancer drugs such as cisplatin in combination with hyperthermia has shown similar tendencies between viability ratio and surviving fraction using trypan blue and clonogenic survival fraction respectively. For this reason, we only determined the viability ratio in this study.

3.2.8. Statistical analysis

Unless otherwise stated, the sample size was n=3. Statistical analyses were conducted using the Student's t-test (two-tailed distribution, two samples with unequal variances). Differences were considered to be statistically significant at $P<0.05$.

3.3. Results

3.3.1. Nanoparticle characterization

The cluster size of the synthesized magnetic nanoparticles determined by transmission electron microscopy was approximately 69±4 nm, consisting of primary nanoparticles 11 nm in diameter (Figure 3.1A shows a representative image of a cluster of particles). The hydrodynamic diameter of the iron oxide nanoparticles coated with carboxymethyl dextran determined by dynamic light scattering was ~70 nm (Figure 3.1B), with some aggregates of ~300 nm visible in the volume-weighted diameter distribution. The inorganic mass was determined by

thermogravimetric analysis (Figure 3.1C), and was determined to be 14% by weight. The specific absorption rate of the nanoparticles was 46.9 W/g of iron oxide at a magnetic field amplitude of 34.73 kA/m and frequency of 233 kHz. Finally, SQUID magnetization measurements showed the nanoparticles to be superparamagnetic, with a saturation magnetization of ~58 Am^2/kg at 300 K (Figure 3.1D). The nanoparticles used in this study were not cytotoxic at a concentration of up to 0.5 mg IO/mL (data not shown).

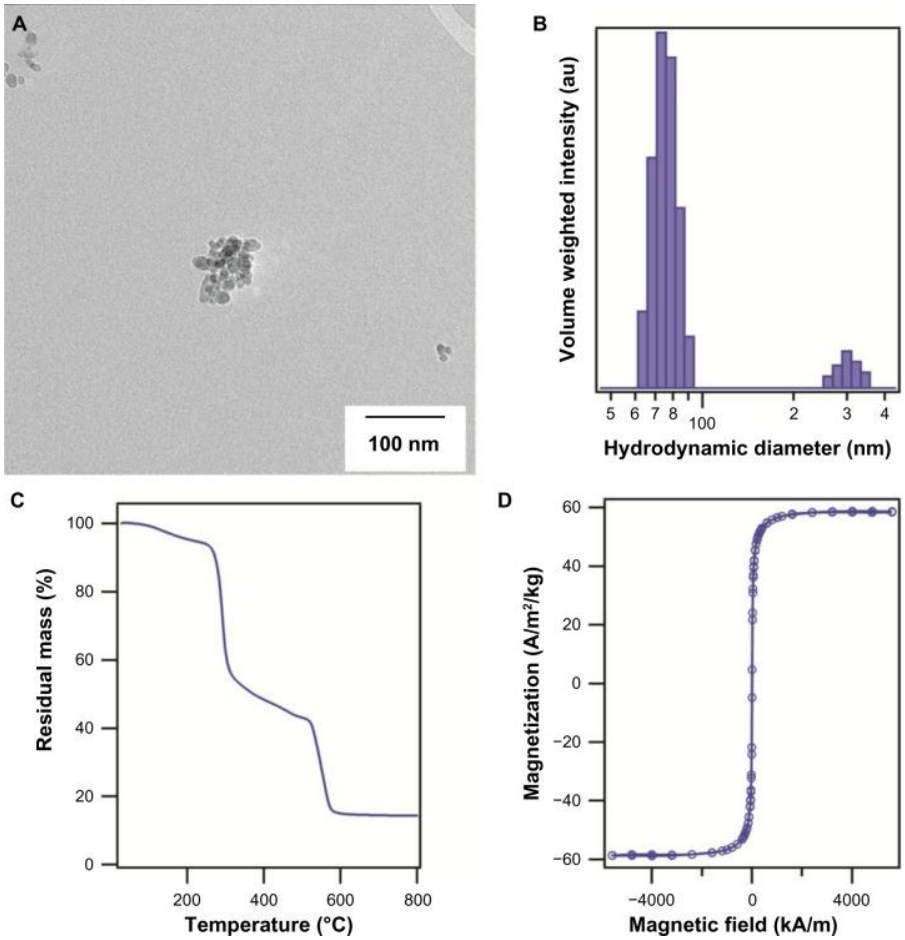

Figure 3. 1. (A) Representative transmission electron microscopy image of magnetic nanoparticles synthesized by the coprecipitation method and coated with carboxymethyl dextran. (B) Volume-weighted hydrodynamic diameter distribution. (C) Remnant mass as a function of temperature for carboxymethyl dextran-coated iron oxide nanoparticles determined by thermogravimetric analysis. (D) Equilibrium magnetization as a function of field at room temperature.

3.3.2. Sensitivity of cancer cells to BZ

Recent studies have shown that the sensitivity of cancer cells to BZ is cell line-dependent.[8,9,12,13] To assess the sensitivity of different cancer cell lines to the therapeutic effect of BZ, the viability of three different cell lines (Caco-2, MDA-MB-468, and A2780) was determined after exposing the cells to increasing concentrations of BZ for 48 hours.

The Caco-2 and MDA-MB-468 cell lines were significantly more sensitive to BZ than A2780 cell lines, showing half maximal inhibitory concentrations of 15 nM, 9 nM, and 250 nM, respectively (Figure 3.2). This result confirms that A2780 has intrinsic BZ resistance. For subsequent experiments, the maximum BZ concentration was kept at 100 nM, because this is the maximum concentration clinically achieved in the plasma of patients treated with BZ.[13]

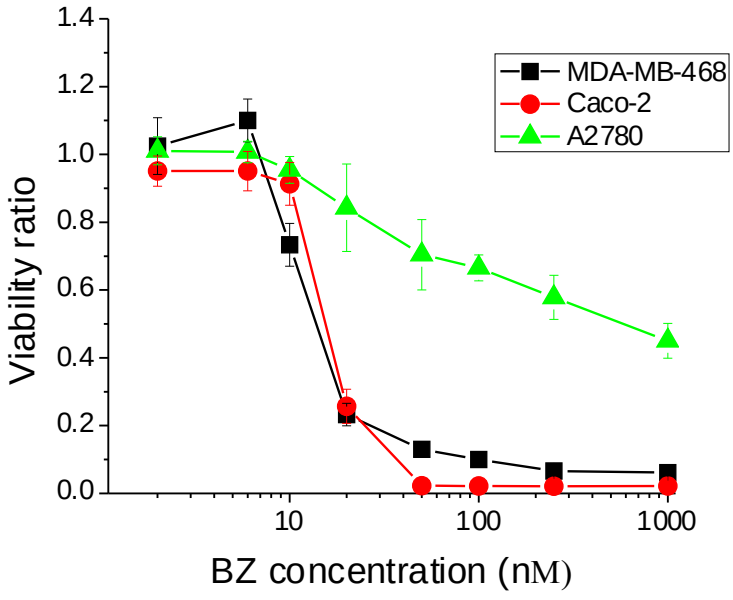

Figure 3. 2. Dose-response curve for MDA-MB-468, Caco-2, and A2780 cell lines. Cells were exposed to BZ concentrations of 2–1,000 nM for 48 hours. Error bars represent the standard error of eight independent experiments.

3.3.3. Proteasome activity curves

BZ is a reversible proteasome inhibitor and a modified dipeptidyl boronic acid specifically designed to fit the active sites of the proteasome.[9] Proteasome inhibition is a function of exposure time and concentration of the drug. To evaluate the effect of hyperthermia in combination with BZ for BZ-sensitive and BZ-resistant cells under the same conditions, it is necessary to choose a BZ concentration that achieves the same proteasome inhibition before applying hyperthermic treatment. Therefore, proteasome inhibition curves, as a function of BZ concentration, were determined by exposing cells to the drug for 3 hours. Proteasome activity was measured after this incubation period.

The proteasome activity curve for Caco-2 cells (Figure 3.3) illustrates that, above 10 nM BZ, proteasome activity does not change further for this exposure time. Proteasome inhibition is approximately 57% at 6 nM BZ. Proteasome activity also decreases in MDA-MB-468 and A2780 cell lines as a function of drug concentration. At 10 nM BZ, the proteasome activity is 59% for MDA-MB-468, while for A2780 at 30 nM the proteasome activity is 56%. It was observed that A2780 cells showed greater proteasome activity than the other cell lines at a given concentration of BZ. In order to verify enhanced cytotoxicity using BZ and hyperthermia in BZ-sensitive and BZ-resistant cells under the same conditions, for subsequent experiments we exposed cells to a lower drug concentration which produced approximately the same level of proteasome inhibition for a pre-exposure time of 3 hours in all cell lines. The concentrations used were 10 nM, 6 nM, and 30 nM for MDA-MB-468, Caco-2, and A2780 cells, respectively.

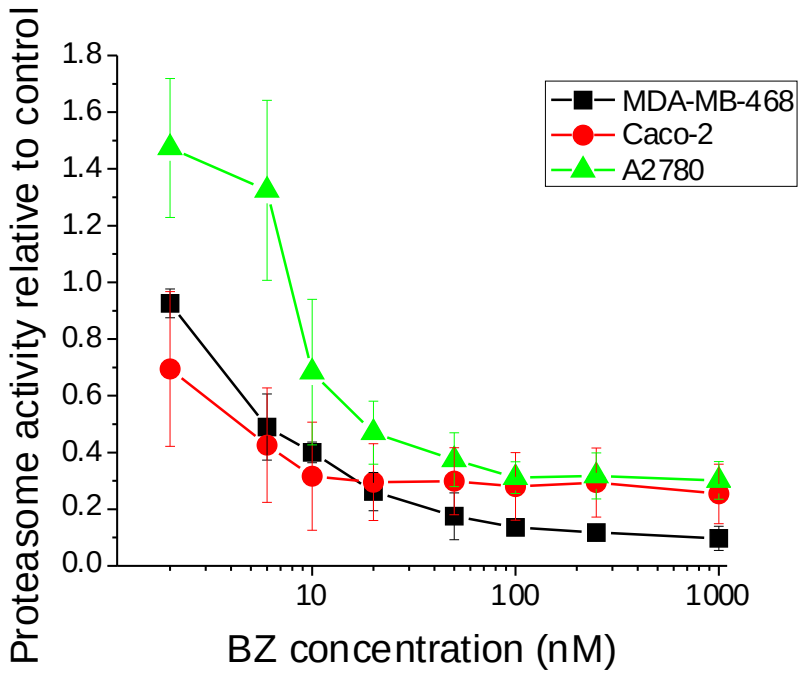

Figure 3. 3. Proteasome activity for MDA-MB-468, Caco-2, and A2780 cell lines treated with different concentrations of BZ (2–1,000 nM) for 3 hours of exposure time. Error bars represent the standard error of three independent experiments.

3.3.4. Enhanced potentiation between MFH and BZ in sensitive and resistant cells

Recent studies have reported enhanced potentiation using hyperthermia and proteasome inhibitors in cancer cells.[18,30] In an effort to assess this enhanced cytotoxicity, studies using BZ in combination with MFH in two BZ-sensitive (MDA-MB-468, Caco-2) and one BZ-resistant (A2780) cancer cell line were performed and compared with potentiation using HWH. Cells were pretreated with BZ for 3 hours, followed by exposure to hyperthermic treatment for 30 minutes at 43°C or 45°C. To achieve this, HWH samples were placed in a water bath at the target temperature for 30 minutes and MFH samples were placed in an alternating magnetic field of sufficient amplitude to achieve temperatures of 43°C (29.39 kA/m) and 45°C (34.73 kA/m) for 30 minutes. Experiments with a similar target temperature had similar temperature-time

profiles, hence the samples were subjected to similar thermal doses as quantified using the cumulative equivalent minutes dose metric of Dewey *et al*.[31] After treatment, the cell samples were allowed to recover for a period of 48 hours. Cell viability was then measured by cell counting. BZ concentrations were chosen individually for each cell line based on the amount of drug that would result in similar proteasome inhibition (6 nM for Caco-2, 10 nM for MDA-MB-468, and 30 nM for A2780).

Enhanced cytotoxicity was evident when BZ was combined with either type of hyperthermic treatment (Figure 3.4). Cell death was not observed when Caco-2 cells were exposed to 6 nM BZ for as long as 48 hours at 37°C (Figure 3.4A). However, when BZ was combined with hyperthermia, this resulted in a significant decrease in cell viability, as shown by the results at 43°C (89%±5.6% reduction for BZ + MFH and 60%±10% reduction for BZ + HWH, $P<0.05$) and 45°C (~99%±1.2% reduction for BZ + MFH and 94%±2.3% reduction for BZ + HWH, $P<0.05$). Consistent with prior observations,[26] MFH showed significantly more cell death than HWH for both temperature conditions. Similarly, both types of hyperthermia enhanced BZ cytotoxicity in MDA-MB-468 cells (Figure 3.4B). Cells treated with MFH or HWH in combination with BZ showed more cell death when compared with cells treated with BZ alone at 37°C. Again, MFH was significantly more effective in inducing cell death than HWH under the same temperature conditions, as shown by the results at 43°C (76%±7% reduction for BZ + MFH and 55%±8% reduction for BZ + HWH, $P<0.05$) and 45°C (~88%±2% reduction for MFH + BZ and 78%±4% reduction for HWH + BZ, $P<0.05$). Finally, as previously noted, A2780 cells were resistant to BZ, with approximately 60%±4% of cells viable even at 100 nM BZ (Figure 3.2). At 30 nM BZ when treated in an incubator, these cells demonstrated no significant cytotoxic response. Interestingly, the effect of BZ was greatly enhanced in the

presence of hyperthermia, with MFH treatment showing the greatest response (Figure 3.4C). At 43°C, cell death was evident (91%±4.9% reduction for BZ + MFH and 70%±10% reduction for BZ + HWH, $P<0.05$). However, when hyperthermia was applied for 30 minutes at 45°C to pretreated samples with BZ, almost complete eradication of cell viability was observed (~99.7%±0.6% reduction for BZ + MFH and 98%±0.5% reduction for BZ + HWH, $P<0.05$). Taken together, these results demonstrate enhancement of cytotoxicity by BZ with hyperthermia in both sensitive and resistant cell lines and that MFH is more effective than HWH at enhancing BZ cytotoxicity under the same temperature conditions.

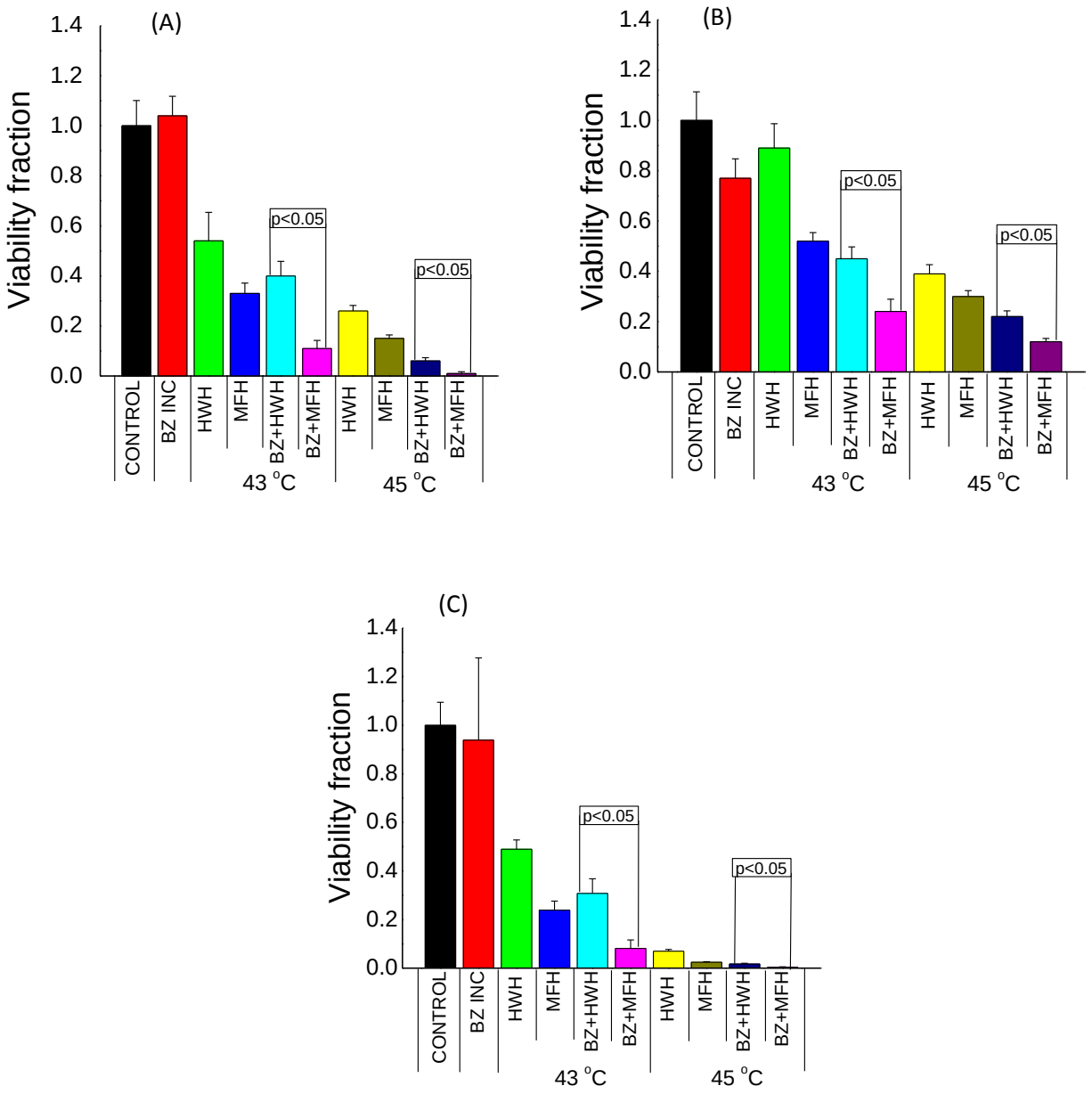

Figure 3. 4. Viability ratio for BZ-sensitive and BZ-resistant cell lines pretreated for 3 hours with BZ, exposed to hyperthermic treatment (MFH and HWH) at 43°C and 45°C for 30 minutes, and incubated for a recovery period of 48 hours in the presence of BZ. (A) Caco-2 viability ratio using 6 nM of BZ.(B) Viability ratio for MDA-MB-468 cell line using 10 nM of BZ. (C) A2780 viability ratio using 30 nM of BZ. Error bars represent the standard error of three independent experiments.

Abbreviations: Control, cells maintained in the incubator; BZ Inc, cells with BZ in incubator; HWH, cells treated by hot water hyperthermia; MFH, cells treated by magnetic fluid hyperthermia; BZ, bortezomib.

3.4. Discussion

Caco-2 and MDA-MB-468 cells exhibited greater sensitivity to BZ, while A2780 showed a minimal response to BZ, with half maximal inhibitory concentrations of 15 nM, 9 nM, and 250 nM, respectively. This result suggests that the A2780 cell line possesses intrinsic BZ resistance, while Caco-2 and MDA-MB-468 are sensitive to the therapeutic effect of BZ. Although it was to be expected that the response to BZ would be cell type-dependent, this expectation had not been tested for Caco-2, MDA-MB-468, and A2780 cell lines before. This difference in sensitivity to proteasome inhibitors remains poorly understood. However, some studies have reported that intrinsic BZ resistance is related to high proteasome activity, implying that BZ-resistant cell lines need a higher BZ concentration to produce the same proteasome inhibition compared with BZ-sensitive cell lines.[14] For example, Xu et al demonstrated that the proteasome activity of BZ-sensitive cells was less than that of BZ-resistant cells under the same conditions.[11]

Proteasome activity curves were determined in order to assess the effect of BZ concentration in all the cell lines. Proteasome activity results revealed that the A2780 cell line, which is resistant to BZ as reported in Figure 3.2, demonstrated higher proteasome activity than the other two BZ-sensitive cell lines (Figure 3.3). This result is consistent with reports in the literature mentioned above.[11]

It is known that hyperthermia can sensitize cells to some anticancer drugs, thereby enhancing their efficacy.[18,19,26,30] This has been attributed to cellular events triggered by hyperthermia, such as changes in membrane fluidity which produce alterations in intracellular drug concentration, cytoskeletal, lysosomal and endoplasmic reticulum changes, inhibition of repair enzymes, impairment of RNA/DNA synthesis, unfolding, and subsequent protein

aggregation.[20,32–34] The way in which hyperthermia is applied can intensify some of these cellular events.[27,35]

In this study, we tested the effect of hyperthermia induced in two different ways (using a water bath and using magnetic nanoparticles) in combination with BZ in cells sensitive and resistant to BZ. To evaluate the effect of hyperthermia in combination with BZ under the same conditions, we used a BZ concentration that resulted in a similar proteasome inhibition in all cell lines prior to application of hyperthermia. Our results confirm that hyperthermia enhanced the effectiveness of the drug in all cell lines. We observed that MFH in combination with BZ produced more cell death than HWH under the same conditions. Although BZ-sensitive and BZ-resistant cells showed similar levels of proteasome inhibition, thermal sensitization induced by MFH in combination with BZ in cells resistant to BZ resulted in significant cell death.

The mechanisms of the enhanced cytotoxicity seen with MFH and BZ are yet to be elucidated. A recent study by our group demonstrated that MFH induced significant membrane fluidity with better subsequent intracellular accumulation of cisplatin.[27] While the therapeutic effect of cisplatin is limited by transport into the cell, BZ does not appear to have this limitation. BZ has rapid effects on the cell, as shown by pharmacokinetic and pharmacodynamic evaluation.[8] Additionally, several studies have suggested that BZ is not affected by the efflux pumps involved in multidrug resistance.[36–39] However, it is possible that the membrane fluidity induced by MFH can enhance intracellular accumulation of BZ, and we will explore this possibility in future research.

It is known that hyperthermia (40°C–46°C) causes proteins to unfold, exposing hydrophobic groups that can interact to form aggregates.[20] Recent studies have shown that hyperthermia using a water bath interrupts protein homeostasis in the cell.[18] Taking into account

the fact that MFH produces marked effects on the cell as shown by recent studies,[27,35] one potential cause of this enhanced cytotoxicity could be related to increased production of unfolded proteins and their subsequent aggregation induced by heat delivered by the magnetic nanoparticles, drastically affecting protein homeostasis.

Overall, our results are significant because they demonstrate the enhanced potential of MFH to sensitize resistant and nonresistant cancer cells to the drug BZ. Future work will explore possible causes of this enhanced potentiation, such as interruption of protein homeostasis, differences in uptake of magnetic nanoparticles, and morphologic changes induced by hyperthermic treatments.

3.5. Conclusion

Our findings demonstrate that combined treatment of BZ and MFH results in greater cell death in BZ-sensitive and BZ-resistant cells, as compared with MFH or BZ alone, or BZ in combination with HWH. The fact that MFH induced greater BZ cytotoxicity than HWH in BZ-sensitive and BZ-resistant cancer cell lines makes it an attractive method for inducing local hyperthermia without causing discomfort and the side effects associated with other types of hyperthermia. Additionally, the combination of MFH and BZ could enable treatment of cancers that are sensitive and resistant to the proteasome inhibitor BZ. We believe that this enhanced potentiation between MFH and BZ is due to denaturation of proteins and their subsequent aggregation caused by the heat dissipated by the magnetic nanoparticles in MFH.

3.6. References

1. Wolf DH, Hilt W. The proteasome: a proteolytic nanomachine of cell regulation and waste disposal.Biochim Biophys Acta. **2004**;1695(1–3):19–31.

2. Miller J, Gordon C. The regulation of proteasome degradation by multi-ubiquitin chain binding proteins. FEBS Lett. **2005**;579(15):3224–3230.

3. Crews CM. Feeding the machine: mechanisms of proteasome-catalyzed degradation of ubiquitinated proteins. Curr Opin Chem Biol. **2003**;7(5):534–539.

4. Kim HM, Yu Y, Cheng Y. Structure characterization of the 26S proteasome. Biochim Biophys Acta.**2011**;1809(2):67–79.

5. Frankland-Searby S, Bhaumik SR. The 26S proteasome complex: an attractive target for cancer therapy. Biochim Biophys Acta. **2012**;1825(1):64–76.

6. Wu WKK, Cho CH, Lee CW, et al. Proteasome inhibition: a new therapeutic strategy to cancer treatment. Cancer Lett. **2010**;293(1):15–22.

7. Farras R, Bossis G, Andermarcher E, Jariel-Encontre I, Piechaczyk M. Mechanisms of delivery of ubiquitylated proteins to the proteasome: new target for anti-cancer therapy? Crit Rev Oncol Hematol.**2005**;54(1):31–51.

8. Mateos MV, San Miguel JF. Bortezomib in multiple myeloma. Best Pract Res Clin Haematol.**2007**;20(4):701–715.

9. Codony-Servat J, Tapia MA, Bosch M, et al. Differential cellular and molecular effects of bortezomib, a proteasome inhibitor, in human breast cancer cells. Mol Cancer Ther. **2006**;5(3):665–675.

10. Mujtaba T, Dou QP. Advances in the understanding of mechanisms and therapeutic use of bortezomib. Discov Med. **2011**;12(67):471–480.

11. Xu H, Ju D, Jarois T, Xie Y. Diminished feedback regulation of proteasome expression and resistance to proteasome inhibitors in breast cancer cells. Breast Cancer Res Treat. **2008**;107(2):267–274.

12. Ling X, Calinski D, Chanan-Khan AA, Zhou M, Li F. Cancer cell sensitivity to bortezomib is associated with survivin expression and p53 status but not cancer cell types. J Exp Clin Cancer Res.**2010**;29:8.

13. Loeffler-Ragg J, Mueller D, Gamerith G, et al. Proteomic identification of aldo-keto reductase AKR1B10 induction after treatment of colorectal cancer cells with the proteasome inhibitor bortezomib.Mol Cancer Ther. **2009**;8(7):1995–2006.

14. de Wilt LH, Jansen G, Assaraf YG, et al. Proteasome-based mechanisms of intrinsic and acquired bortezomib resistance in non-small cell lung cancer. Biochem Pharmacol. **2012**;83(2):207–217.

15. Smith AJ, Dai H, Correia C, et al. Noxa/Bcl-2 protein interactions contribute to bortezomib resistance in human lymphoid cells. J Biol Chem. **2011**;286(20):17682–17692.

16. Shringarpure R, Catley L, Bhole D, et al. Gene expression analysis of B-lymphoma cells resistant and sensitive to bortezomib. Br J Haematol. **2006**;134(2):145–156.

17. Vanakoski J, Seppala T. Heat exposure and drugs. A review of the effects of hyperthermia on pharmacokinetics. Clin Pharmacokinet. **1998**;34(4):311–322.

18. Neznanov N, Komarov AP, Neznanova L, Stanhope-Baker P, Gudkov AV. Proteotoxic stress targeted therapy (PSTT): induction of protein misfolding enhances the antitumor effect of the proteasome inhibitor bortezomib. Oncotarget. **2011**;2(3):209–221.

19. Milani V, Lorenz M, Weinkauf M, et al. Combination of hyperthermia and bortezomib results in additive killing in mantle cell lymphoma cells. Int J Hyperthermia. **2009**;25(4):262–272.

20. Roti Roti JL. Cellular responses to hyperthermia (40–46 degrees C): cell killing and molecular events. Int J Hyperthermia. **2008**;24(1):3–15.

21. Wust P, Hildebrandt B, Sreenivasa G, et al. Hyperthermia in combined treatment of cancer. Lancet Oncol. **2002**;3(8):487–497.

22. Habash RW, Bansal R, Krewski D, Alhafid HT. Thermal therapy, part 2: hyperthermia techniques.Crit Rev Biomed Eng. **2006**;34(6):491–542.

23. Banerjee R, Katsenovich Y, Lagos L, McIintosh M, Zhang X, Li CZ. Nanomedicine: magnetic nanoparticles and their biomedical applications. Curr Med Chem. **2010**;17(27):3120–3141.

24. Latorre M, Rinaldi C. Applications of magnetic nanoparticles in medicine: magnetic fluid hyperthermia. P R Health Sci J. **2009**;28(3):227–238.

25. Rodriguez-Luccioni HL, Latorre-Esteves M, Mendez-Vega J, et al. Enhanced reduction in cell viability by hyperthermia induced by magnetic nanoparticles. Int J Nanomedicine. **2011**;6:373–380.

26. Lee JS, Rodriguez-Luccioni HL, Mendez J, et al. Hyperthermia induced by magnetic nanoparticles improves the effectiveness of the anticancer drug cis-diamminedichloroplatinum. J Nanosci Nanotechnol. **2011**;11(5):4153–4157.

27. Alvarez-Berrios MP, Castillo A, Rinaldi C, Soto O, Rinaldi C, Torres-Lugo M. Hyperthermic potentiation of cisplatin by magnetic nanoparticle heaters is correlated with an increase in cell membrane fluidity. Int J Nanomedicine. **2013**;8:1–11.

28. Herrera AP, Barrera C, Rinaldi C. Synthesis and functionalization of magnetite nanoparticles with aminopropylsilane and carboxymethyldextran. J Mater Chem. **2008**;18(31):3650–3654.

29. Creixell M, Bohorquez AC, Torres-Lugo M, Rinaldi C. EGFR-targeted magnetic nanoparticle heaters kill cancer cells without a perceptible temperature rise. ACS Nano. **2011**;5(9):7124–7129.

30. Pajonk F, van Ophoven A, McBride WH. Hyperthermia-induced proteasome inhibition and loss of androgen receptor expression in human prostate cancer cells. Cancer Res. **2005**;65(11):4836–4843.

31. Sapareto SA, Dewey WC. Thermal dose determination in cancer therapy. Int J Radiat Oncol Biol Phys. **1984**;10(6):787–800.

32. Bodell WJ, Cleaver JE, Roti Roti JL. Inhibition by hyperthermia of repair synthesis and chromatin reassembly of ultraviolet-induced damage to DNA. Radiat Res. **1984**;100(1):87–95.

33. Cummings M. Increased c-fos expression associated with hyperthermia-induced apoptosis of a Burkitt lymphoma cell line. Int J Radiat Biol. **1995**;68(6):687–692.

34. Hildebrandt B, Wust P, Ahlers O, et al. The cellular and molecular basis of hyperthermia. Crit Rev Oncol Hematol. **2002**;43(1):33–56.

35. Domenech M, Marrero-Berrios I, Torres-Lugo M, Rinaldi C. Lysosomal membrane permeabilization by targeted magnetic nanoparticles in alternating magnetic fields. ACS Nano. **2013**;7(6):5091–5101.

36. Oerlemans R, Franke NE, Assaraf YG, et al. Molecular basis of bortezomib resistance: proteasome subunit Î²5 (PSMB5) gene mutation and overexpression of PSMB5 protein. Blood. **2008**;112(6):2489–2499.

37. Minderman H, Zhou Y, O'Loughlin K, Baer M. Bortezomib activity and in vitro interactions with anthracyclines and cytarabine in acute myeloid leukemia cells are independent of multidrug resistance mechanisms and p53 status. Cancer Chemother Pharmacol. **2007**;60(2):245–255.

38. Williamson MJ, Silva MD, Terkelsen J, et al. The relationship among tumor architecture, pharmacokinetics, pharmacodynamics, and efficacy of bortezomib in mouse xenograft models. Mol Cancer Ther. **2009**;8(12):3234–3243.

39. Zheng B, Zhou R, Gong Y, Yang X, Shan Q. Proteasome inhibitor bortezomib overcomes P-gp-mediated multidrug resistance in resistant leukemic cell lines. Int J Lab Hematol. **2012**;34(3):237–247.

Chapter 4

Enhanced Proteotoxic Stress is Responsible for Hyperthermic Potentiation of the Proteasome Inhibitor Bortezomib Using Magnetic Nanoparticles

4.1. Introduction

The use of magnetic nanoparticles to induce hyperthermia, also known as magnetic fluid hyperthermia (MFH), in conjunction with anticancer drugs has shown promising results in the treatment of cancer. [1-3] Recently, we have demonstrated that the *in vitro* therapeutic effects of the combination treatment of bortezomib (BZ) and heat were greater when heat was applied through MFH when compared to conventional hot water hyperthermia (HWH). [4] The explanation of this phenomenon is intriguing. A recent study proposed that induction and subsequent aggregation of misfolded proteins, which results in an increase in the toxicity of the proteotoxic stress (enhanced proteotoxic stress) in the cell, is a potential cause for the enhanced potentiation of BZ using hyperthermia.[5]

Bortezomib (BZ) is a reversible inhibitor, specifically designed to fit the active sites of the proteasome. The proteasome is responsible for degradation of non-functional or misfolded proteins, preventing their aggregation and accumulation within the cell.[5-8] Aggregated proteins increase the toxicity of the proteotoxic stress, which can lead to programmed cell death. To protect the cell from accumulation of such aggregates, they are transported via microtubules to an aggregate deposition site located near the microtubule-organizing centre (MTOC) and named the aggresome.[9-11] BZ is attractive as a drug that increases the toxicity of proteotoxic stress in

cancer cells, because such cells produce significant amounts of misfolded and non-functional proteins, such that alternative mechanisms of cell protection against proteotoxic stress can be overwhelmed.[5, 10] Recent studies have indicated that BZ induces an enhanced proteotoxic stress by promoting the accumulation and subsequent aggregation of ubiquitinated proteins in MDA-MB-231, MDA-MD-453, and HT1080 cancer cell lines.[12, 13]

Magnetic fluid hyperthermia is an attractive method to induce local hyperthermia without causing damage to adjacent tissues.[14-16] Essentially, it takes advantage of the dissipation of magnetic field energy in the form of heat caused by the physical rotation or internal dipole reorientation of magnetic particles in an alternating magnetic field. This heat is deposited into nearby tissues, raising their temperature above 37°C. Recent studies have shown that magnetic fluid hyperthermia produces marked cellular effects, possibly due to additional stress induced by magnetic nanoparticles, beyond thermal effects.[1, 2, 17] Alvarez-Berrios *et al* showed that MFH induces higher membrane fluidity than hot water hyperthermia under the same temperature conditions.[1] When HeLa cells were exposed to hyperthermia via magnetic nanoparticles, high levels of microtubule damage were observed, resulting in significant cell death.[18] Studies have postulated that hyperthermia induces significant protein damage and this is one of the possible causes of cell death.[19-21] These cellular effects can significantly enhance the action of anticancer drugs. [3, 22]

In this study we have tried to elucidate the mechanisms of potentiation between MFH and BZ. We hypothesized that MFH in combination with BZ can significantly increase the toxicity of the proteotoxic stress by a combination of microtubule damage, an increase in the amount of aggregated proteins, and their subsequent accumulation in the cytosol. To test this hypothesis we first determined cell response to BZ in combination with MFH at 43 ºC or 45 ºC as a function of

recovery time by measuring DNA content profile, cell viability and clonogenic potential of the cells. Results were compared with those obtained using HWH. Measurements of aggresome formation and microtubule stability as a function of recovery time were made to evaluate the increase in aggregated proteins and interruption of their transport to the perinuclear area induced by hyperthermic treatment (MFH or HWH). Our results indicate that the combination of cellular effects induced by MFH, such as microtubule disruption and protein damage, induces progressive enhanced proteotoxic stress, which accelerates cell death and is one of the mechanisms responsible for the improved potentiation between MFH and BZ in the MCF-7 cell line.

4.2. Materials & methods

4.2.1. Cell culture and drug preparation

MCF-7 cells were generously donated by Dr. Edna Mora from the UPR Comprehensive Cancer Center. Cells were cultured on 75cm^2 flasks (Costar, Corning, NY) with Dulbecco's modified Eagle medium (Sigma, St. Louis, MO) containing 10% fetal bovine serum (Invitrogen, Carlsbad, CA), 1% nonessential aminoacids (Invitrogen, Carlsbad, CA),100 units/mL of penicillin (Sigma, St. Louis, MO), 100 μg/mL of ampothericin B (Sigma, St. Louis, MO), 2 mM L-glutamine and 24 mM sodium bicarbonate. Cells were maintained at 37°C, under 5% CO_2 and 95% relative humidity. Cell passages were performed 48 hours before all experiments to ensure cells in log phase growth. The proteasome inhibitor bortezomib (LC laboratories, Woburn, MA) was dissolved in DMSO (Sigma, St. Louis, MO) to a final concentration of 100mM. Then, this solution was aliquoted and stored at -20 °C. Aliquots were thawed, and diluted in Dulbecco's modified Eagle medium before experiments.

4.2.2. Synthesis and characterization of nanoparticles

Nanoparticles used in this study are the same as those used in our previous study.[4] Below we summarize their preparation and characterization. Nanoparticles were synthesized by the co-precipitation method using an aqueous solution of ferric and ferrous salts at a molar ratio of 1:2, in combination with an ammonium hydroxide solution. This mixture was maintained at 80 °C and a pH of 8 over a period of one hour. The solution was bubbled with nitrogen during the reaction. After this period, nanoparticles were recovered by centrifugation and peptized with tetramethyl ammonium hydroxide (1 M). Then, peptized nanoparticles were functionalized with APS solution consisting of 5 ml of 3-aminopropyltriethoxysilane (APS), 75 ml DMSO, 1.25 ml of water, and 100 ul of acetic acid. The reaction proceeded for 36 hr at room temperature. Afterwards nanoparticles were washed 4 times with ethanol and stored in a vacuum oven until completely dry. Nanoparticles coated with APS were functionalized with carboxymethyl dextran (CMDx) via reaction with 1-Ethyl-3-[3-dimethylaminopropyl] carbodiimide hydrochloride (EDC) / N-hydroxysuccinimide (NHS). The hydrodynamic diameter of the nanoparticles was determined using dynamic light scattering (DLS) (BI-90 Plus, Brookhaven Instrument Corp, Holtsville, NY, USA).[16] The iron oxide content was determined by thermogravimetric analysis (TGA/DSC1, Mettler Toledo Inc, Columbus,OH).[23] Magnetic properties were estimated using a SQUID magnetometer (MPMS XL-7, Quantum Design,Inc, San Diego, CA, USA) and the specific absorption rate (SAR) was obtained by measuring the increase in temperature as a function of time for nanoparticles in deionized water at a concentration of 0.5 mg IO/ml using an induction heater (RDO Induction, Washington, NJ, USA) with magnetic field intensities ranging from 24.18 kA/m to 34.73 kA/m.[23, 24] Before each experiment nanoparticles were sterilized at a temperature of 121°C and 15 psi for 60 minutes.

Then they were suspended in DMEM at a final concentration of 10mg particles/ml. The final particle concentration used for *in vitro* experiments was 3.848 mg particle/mL (0.5 mg IO/mL).

4.2.3. Dose-response curve for BZ

Cells ($1x10^3$) were seeded in 96-well plates (Fisher Scientific, Suwanee, GA) for 48h in DMEM solution. Adhered cells were exposed to BZ concentrations ranging between 2-1000 nM for 48h. Subsequently, cells were washed twice with HBSS buffer, stained with CellTiter Blue™ (Promega, Madison, WI) and analyzed using a spectrofluorometer (Spectra MAX Gemini EM, molecular devices, Sunnyvale, California).[4]

4.2.4. Proteasome activity

Proteasome activity was determined using a fluorogenic substrate.[4] Briefly, cells ($1x10^3$) were seeded in 96 well-plates for 48h in DMEM solution. Then, cells were exposed to concentrations of bortezomib between 2nM and 1000nM for 3h. After this incubation period, 100 µL Proteasome-Glo™ Chymotrypsin-Like Assay solution (Promega, Madison, WI) was added and samples were incubated for 15 minutes in the dark at room temperature. Afterwards, luminescence was measured in a spectrofluorometer (Spectra MAX Gemini EM, molecular devices, Sunnyvale, California).

4.2.5. Combination treatment

Cells to be treated by HWH ($5x10^5$ cells in suspension) were transferred to a glass tube, then, BZ was added to obtain a final concentration of 100 nM in a final volume of 2.5 ml (DMEM solution was added to obtain the final volume). For MFH experiments, samples contained 3.848 mg particle/mL in a final volume of 2.5 ml. Cells with or without BZ were

maintained in an incubator for 3 hours; after this period, samples with or without BZ were exposed to hyperthermic treatment for 30 minutes at 43 ºC or 45 ºC. This treatment combination schedule was chosen to ensure proteasome inhibition before heat application. Cells treated by hot water hyperthermia with or without BZ were placed in a temperature-regulated water bath for the conditions mentioned above. On the other hand, cells treated by MFH were placed in the coil of the heat induction equipment and exposed to a magnetic field of 29.39 kA/m or 34.73 kA/m and a frequency of 233 kHz. Control tubes had the same DMSO concentration as the experimental group (0.1% DMSO) and they remained in the incubator at 37°C. After treatment, cells were left in an incubator at 37°C and 5% CO_2 for a recovery time of 30 minutes, 2.5 hr or 48 hr in the presence of bortezomib in order to maintain constant proteasome inhibition. Cells (at 30minutes or 2.5 hr of recovery time) were washed with PBS and fixed in 70 % ethanol at 4 ºC for 2 hours. After this period, cells were washed with PBS and resuspended in a solution of PBS containing 40 µg/ml RNase A, 0.2 % triton-100 and 25 µg/ml propidium iodide for 15 minutes at 37 ºC. Cells were stored at 4 ºC and analyzed in the FL2 channel of an Accuri c6 Flow cytometer (BD, Ann Arbor, MI). Apoptotic cells were identified by the sub G1 peak (evidence of fractional DNA content) localized left of the G1 peak in the DNA content profile. DNA content profile using propidium iodide was used as a reliable method for these early recovery times, because it does not depend on characteristic cell changes (membrane fluidity). In first instance we tried to use trypan blue exclusion method; however, at 30 minutes of recovery time all cells treated by MFH incorporated trypan blue, suggesting detrimental membrane disruption (data not shown). Previous studies by our group have demonstrated that MFH induces increased membrane fluidity[25], which may be the reason why trypan blue is incorporatedrapidly after 30 minutes of MFH application.

After 48 hours of incubation, cells were trypsinized and cell viability was measured by cell counting using trypan blue (Sigma, St. Louis, MO). For clonogenic assays, the drug was removed after a period of 48 hours and cells were seeded with different dilutions into six-well tissue culture plates in absence of the drug. Colonies formed were fixed, stained with crystal violet, and counted after 10 days of incubation.[26]

4.2.6. Aggresome formation

Cells (1×10^6) in log phase were pretreated with BZ for 3 hours, exposed to hyperthermia in combination with BZ for 30 minutes at 43 °C or 45 °C and left in an incubator for a recovery time of 30 minutes or 2.5 hours in presence of BZ. Cells untreated with BZ were left in incubator for 3 hours, then exposed to hyperthermia treatment and incubated for a recovery time of 30 minutes and 2.5 hours. This recovery time was chosen in order to evaluate aggresome formation as a function of time. After recovery, cells were washed twice with PBS (sigma, St. Louis, MO), fixed in 4 % paraformaldehyde (Sigma, St. Louis, MO) in PBS for 30 minutes, washed with PBS and resuspended in permeabilizing solution (0.5% Triton X-100(Sigma, St. Louis, MO), 3 mM EDTA(Sigma, St. Louis, MO), pH 8) for 30 minutes on ice. Then, cells were washed with PBS and resuspended in ProteoStat®Aggresome solution (Enzo Life Sciences, Inc. Plymouth Meeting, PA). For cell analysis by flow cytometer, samples were resuspended in 500 µl ProteoStat solution and incubated for 30 minutes at room temperature, protected from light. No washing was required for samples for flow cytometric analysis. Then, fluorescence was measured in the FL2 channel using an Accuri c6 Flow cytometer (BD, Ann Arbor, MI). For cell analysis by confocal microscopy, samples were resuspended in 100 µl of Dual Detection Reagent (Enzo Life Sciences, Inc. Plymouth Meeting, PA) (prepared according to kit instructions) and incubated for 30 minutes at room temperature, protected from light. Cells were then washed and

resuspended in PBS buffer and 20 µL of the cell suspension were aliquoted onto a microscope slide and immediately overlaid with a cover slip. Pictures were captured with an Olympus Spinning Disk (3i system, Dever, CO) Confocal Microscope (Olympus IX81, Denver, CO) equipped with a Xenon Fl source for visualization. Images were obtained using a 60X oil immersion objective and Rolera EM-C2 camera (Quantitative Imaging Corporation). Two independent experiments were done and two images were captured for each sample with identical exposure time.

4.2.7. Microtubule damage determination

Cells (1×10^6) in log phase were exposed to hyperthermia for 30 minutes at 43 ºC and 45ºC and incubated at 37 ºC for a recovery time of 30 minutes and 2.5 hours. Afterwards, cells were washed by centrifugation with PBS, fixed in 4 % paraformaldehyde in PBS for 10 minutes at 37 ºC. Then, paraformaldehyde solution was removed by centrifugation. Cells were resuspended in PBS and chilled on ice for 1 minute. Ice-cold methanol was added to chilled cells to a final concentration of 90% methanol and incubated for 30 minutes on ice. After this period, methanol solution was removed; cells were washed twice with 0.5 % of bovine serum albumin in PBS (incubation buffer), resuspended in 100 µl of incubation buffer, and incubated for 10 minutes at room temperature. After this period, incubation buffer was discarded; cells were resuspended in 50 µl of a 1:50 dilution of α/β-Tubulin Antibody (Cell signaling Technology, Danvers, MA) in incubation buffer and incubated for 1 hour at room temperature. Then, cells were washed twice with incubation buffer and resuspended in 500 µl of a 1:1000 dilution of Anti-rabbit IgG (H+L), F(ab')2 Fragment (Alexa Fluor® 488 Conjugate)(Cell Signaling Technology, Danvers, MA) in incubation buffer and Incubated for 30 minutes at room temperature. Afterwards, samples were further rinsed as before in incubation buffer, resuspended

in 0.5 ml PBS and analyzed in the FL1 channel using an Accuri c6 Flow cytometer (BD, Ann Arbor, MI).

4.2.8. Statistical analysis

The sample size was n = 3 for all experiments except for confocal images (n = 2) and dose response curve (n = 8). Statistical analyses were conducted using Student's test (two-tailed distribution, two samples with unequal variances). Differences were considered significant at $P < 0.05$. Standard error and surviving fraction for clonogenic assay studies were determined using the approach described by Gupta *et.al.*[27] Aggresome formation data determined by flow cytometry was analyzed by comparison of the aggresome propensity factor (APF). APF is a measurement of the amount of aggregated proteins that are accumulated within the aggresome or inclusion bodies in the presence and absence of proteasome inhibitors or other inducers of aggresome and protein aggregation. This unitless term is defined as:

$$\left(\frac{MFI_{treated} - MFI_{control}}{MFI_{treated}}\right) \times 100$$

Where, $MFI_{treated}$ is the mean fluorescence intensity of treated samples and $MFI_{control}$ is the mean fluorescence intensity of untreated cells. APF values higher than 25 are considered as indicative of aggresome formation (a significant amount of aggregated proteins were produced and accumulated within the aggresome).[28]

4.3. Results

4.3.1. Nanoparticle characterization

Nanoparticles used in this study are from the same batch used in our past work.[4] These consisted of iron oxide nanoparticles, with primary diameters of ~11 nm according to transmission electron microscopy, coated with the polysaccharide carboxymethyl dextran and with a hydrodynamic diameter of ~70nm, determined by dynamic light scattering. We've demonstrated that particles produced by our methods are colloidally stable in cell culture media and possess low cytotoxicity in the absence of applied alternating magnetic fields [29]. Thermo-gravimetric analysis indicated that the iron content was 14% by weight. At a magnetic field amplitude of 34.73 kA/m and frequency of 233 kHz the specific absorption rate (SAR) value of the nanoparticles was 46.9W/g. The saturation magnetization of the nanoparticles was determined to be ~58 Am^2/kg at 300 K using SQUID magnetization measurements.

4.3.2. Cell response to the therapeutic effect of BZ

To assess the response of MCF-7 cells to BZ, cells were exposed to BZ concentrations ranging between 2-1000 nM for 48 hours. After this period, cell viability as a function of BZ concentration was measured (see Figure 4.1). The MCF-7 cells had a low response to BZ in the concentration range between 2-30 nM. However, above 30 nM cell viability showed a significant decrease, with a minimum cell viability of approximately 40% at 1000 nM. MCF-7 cells showed an IC_{50} value of 100 nM, which coincides with previous studies.[13]

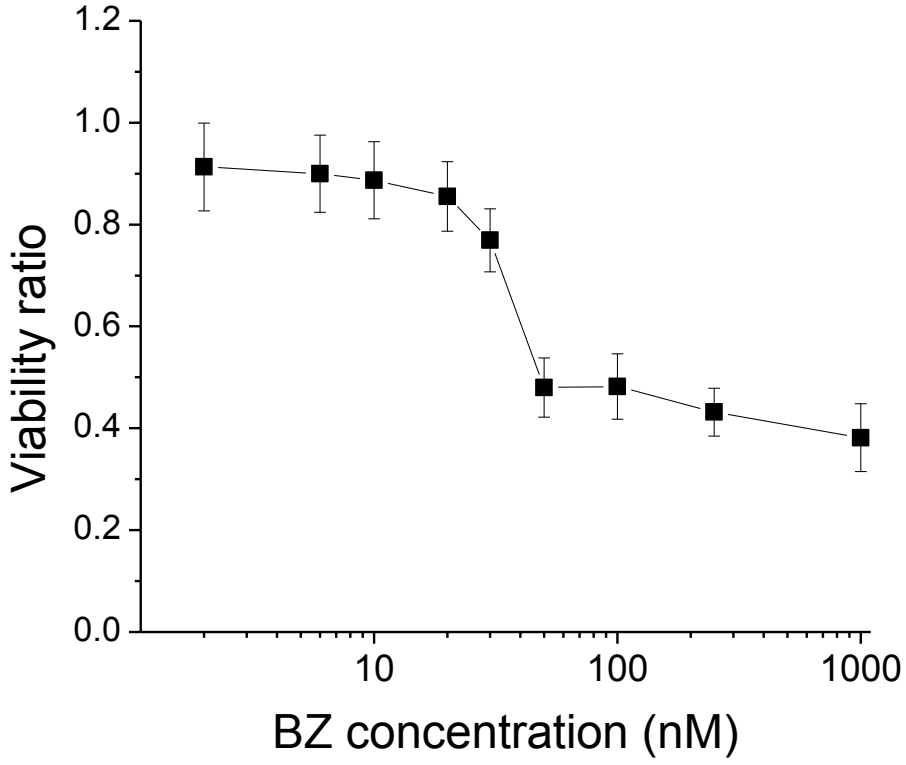

Figure 4. 1. Dose- response curve for MCF-7 cells after exposure for 48 hours to various BZ concentrations (2-1000nM). Error bars represent the standard error of eight independent experiments.

4.3.3. Proteasome activity as a function of BZ concentration

To obtain a BZ concentration that significantly inhibits the activity of the proteasome before hyperthermic treatment, MCF-7 cells were exposed to various BZ concentrations (2-1000nM) for 3 hours. Then, proteasome activity was measured at these conditions. Proteasome activity is concentration dependent, as illustrated in Figure 4.2. Higher BZ concentrations produced higher inhibition of the proteasome. For example, for this particular case, proteasome inhibition at a concentration of 2 nM was approximately 25%, whereas at 1000 nM it was found to be 70%. This behavior in proteasome activity as a function of BZ concentration is in

agreement with past studies, however at higher BZ concentration the viability is significantly affected.[4, 30] For subsequent experiments, the IC_{50} concentration (100 nM) was employed.

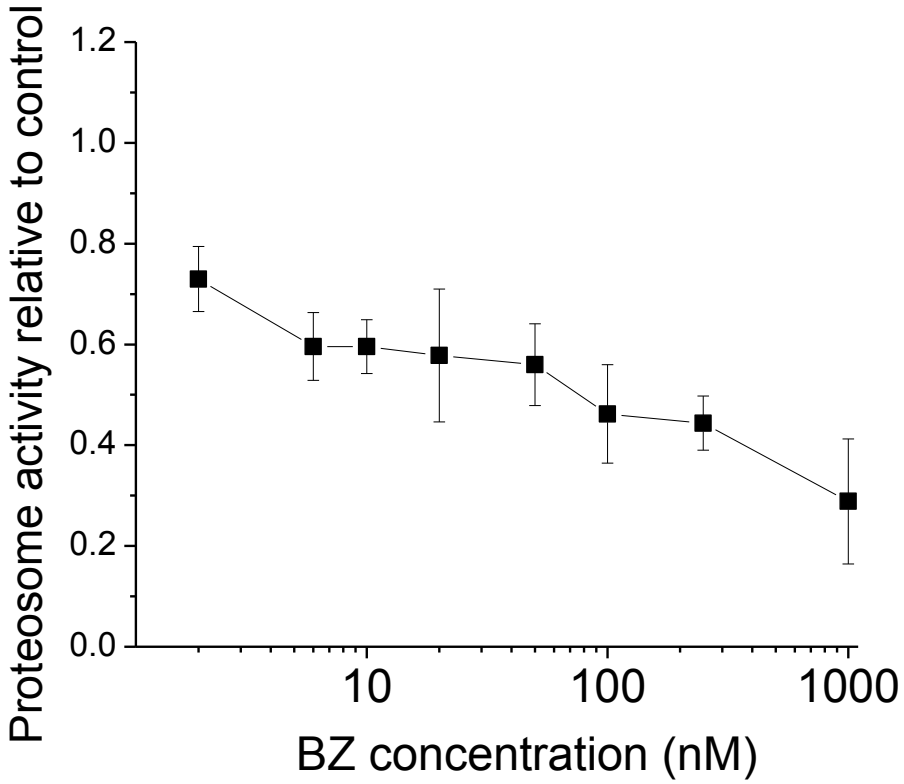

Figure 4. 2. Proteasome activity curve as a function of BZ concentration for an exposure time of 3 hours. Error bars represent the standard error of the mean of three independent experiments.

4.3.4. Enhanced potentiation between MFH and BZ

To assess cell response to combined treatment between hyperthermia and BZ as a function of recovery time, cells were exposed to BZ for 3 hours. Afterwards, hyperthermic treatment for 30 minutes at 43 ºC or 45 ºC was applied in presence of BZ. Samples were incubated for additional periods of 30 minutes, 2.5 hours, or 48 hours in the presence of BZ. Then, propidium iodide was used to evaluate the percentage of apoptotic cells at 30 min or 2.5

hours of recovery time, trypan blue exclusion method was used to determine viability ratio at 48 hours of recovery time, and surviving fraction was determined by clonogenic assay at 10 days of recovery time in absence of BZ.

Propidine iodide assay results indicated that exposing cells to BZ alone, HWH, or MFH resulted in increased cell death over untreated cells (Table 4.1). At 43 ºC and 30 minutes of recovery time we did not observe a statistically significant difference between MFH and HWH. However, at 2.5 hr of recovery time a statistically significant difference between hyperthermic treatments was observed. At 45ºC and 30 minutes of recovery time a statistically significant difference between MFH and HWH was observed, and at 2.5 hr of recovery time MFH also induced higher cell death than HWH. BZ combined with hyperthermia induced higher cell death than BZ alone or hyperthermia alone at the recovery times assessed (Table 4.1). At 43°C and 30 minutes or 2.5 hr of recovery time, MFH + BZ induced higher percentage of apoptotic cells than HWH+BZ (at 30 minutes of recovery time: 10 ± 0.4% of apoptotic cells for cells treated by MFH+BZ and 7.33 ± 0.32% for cells treated by HWH+BZ, statistically different with $p<0.05$; at 2.5 hours of recovery time: 12.80±0.85% of apoptotic cells for MFH+BZ and 8.73±0.12% for HWH+BZ; statistically different with $p<0.05$). This behavior was also observed at 45 ºC (at 30 minutes of recovery time: 14.27±1.3% of apoptotic cells for MFH+BZ and 10.97±0.2% for HWH+BZ; statistically different with $p<0.05$; at 2.5 hours of recovery time: 20.17±0.76% of apoptotic cells for MFH+BZ and 17.80±0.90% for HWH+BZ, statistically different with $p<0.05$).

Table 4. 1 Cell death analysis by DNA content profile.

	Percentage of apoptotic cells at 43 ºC		Percentage of apoptotic cells at 45º C	
	30 minutes of recovery time	**2.5 hours of recovery time**	**30 minutes of recovery time**	**2.5 hours of recovery time**
Untreated cells	2.70±0.1%	2.70±0.1%	2.63±0.06%	2.63±0.06%
BZ	3.83±0.15%	5.63±1%	3.70±0.1%	5.87±0.61%
HWH	4.97±0.49%	6.30±0.56%	6.67±0.06%	10±0.26%
MFH	6.43±0.1%	8.73±0.67%	9.27±0.25%	12.81±0.51%
HWH+BZ	7.33±0.55%*	8.73±0.21%**	10.97±0.35%***	17.80±0.35%****
MFH+BZ	10.00±0.7%*	12.80±1.47%**	14.27±0.83%***	20.17±1%****

Percentage of apoptotic cells for MCF-7 cells untreated or treated with BZ for 3 hours, exposed to hyperthermia for 30 minutes at 43 ºC or 45 ºC in presence of BZ, and left to incubate for a recovery time of 30 minutes or 2.5 hours. * Statistically different with $P<0.05$. ** Statistically different with $P<0.05$. *** Statistically different with $P<0.05$. **** Statistically different with $P<0.05$. The numbers represent the average and standard deviation of three independent experiments.

On the other hand, when viability was measured after 48 hours of recovery time using trypan blue exclusion method, cell death was much greater for those samples treated by MFH or HWH in combination with BZ (Figure 4.3). At 43 ºC the viability ratio was 28 ± 10% for HWH+BZ and 17 ± 3% for MFH+BZ (statistically different with $p<0.05$) and at 45 ºC the viability ratio was 8 ± 1.7% for HWH+BZ and 3 ± 2.4% for MFH+BZ (statistically different with $p<0.05$). Cell death using trypan blue exclusion method is greater than propidium iodide assay because of the time that was needed for cells to recover which is higher for the first method.

The clonogenic assay determines the ability of unlimited division of a single cell, that is, its ability to form colonies.[26] This assay is the gold standard for measuring cell response to

cytotoxic agents.[27] For that reason, surviving fraction results are often considered more relevant in terms of evaluating anti-cancer potential of anticancer drugs. Our results showed that there is not a statistically significant difference between untreated cells and cells treated with BZ according to clonogenic assays, indicating that cells were able to recover in the absence of BZ (Figure 4.3.). Nevertheless, when BZ was combined with hyperthermia the anticlonogenic effect was evident and cells were unable to recover, as shown by results at 43 ºC, for which the surviving fraction was approximately 33±1.33% for cells treated with HWH+BZ and 20±0.82% for cells treated with MFH+BZ (statistically different with $p<0.05$) and at 45 ºC, for which the surviving fraction was 8±0.42% for cells treated with HWH+BZ and 2±0.1% for cells treated with MFH+BZ, statistically different with $p<0.05$).

Results for apoptotic cell death, viability ratio, and colony forming capacity indicated that MFH in combination with BZ produces higher cytotoxicity in MCF-7 cells than HWH in combination with BZ, at both temperature conditions tested. In order to understand this enhanced potentiation between MFH and BZ studies of microtubule disruption and aggresome formation were performed.

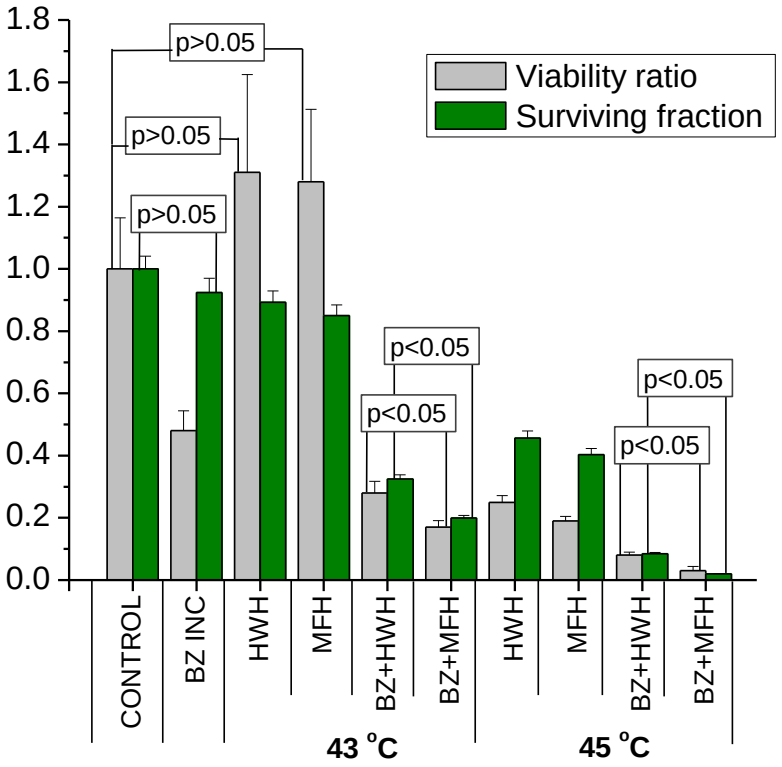

Figure 4. 3. Surviving fraction and viability ratio for MCF-7 cells treated or untreated with 100 nM of BZ for 3 hours, exposed to hyperthermia with or without BZ at 43 ºC or 45 ºC for 30 minutes. Error bars represent the standard error of three independent experiments.

4.3.5. Aggresome formation in MCF-7 cells is interrupted by MFH

To assess if there is an increase in the amount of aggregated proteins induced by hyperthermic treatment, a qualitative and quantitative analysis of aggresome formation was carried out by confocal microscopy and flow cytometry. Samples were tested at 30min and 2.5h recovery times in order to evaluate the progressive increase in aggregated proteins.

Confocal images of aggregated protein vesicles (red), produced during aggresome formation, are shown in Figure 4.4. In these images, the agregated protein vesicles appear in

close proximity of the nucleus (blue, DAPI stain) of the MCF-7 cells, suggesting that at the time the cell samples were fixed (pretreated or untreated for 3 hours with BZ, exposed to heat treatment, and left in incubator for 30 minutes or 2.5 hr of recovery time) the aggregated protein vesicles were already transported to the MTOC near the nucleus. Increased aggresome formation was evident as a function of time for cells treated with BZ. Cells treated with MFH or BZ+MFH at 43 ºC and 30 minutes of recovery time showed more protein aggregates surrounding the nucleus, compared to HWH or HWH+ BZ respectively. However, at 2.5 h recovery time we did not observe an increase in these aggregated proteins when compared to 30 minutes of recovery time for MFH or MFH+BZ treated cells. At 45 ºC the quantity of aggregated protein vesicles around the nucleus was lower than at 43 ºC, particularly after 2.5 h recovery. At this temperature condition confocal microscopy also revealed that cells treated with MFH+BZ had nuclear fragmentation at 2.5 hour of recovery time, indicative of cell death and in agreement with results from the propidium iodide assay (Table 4.1).

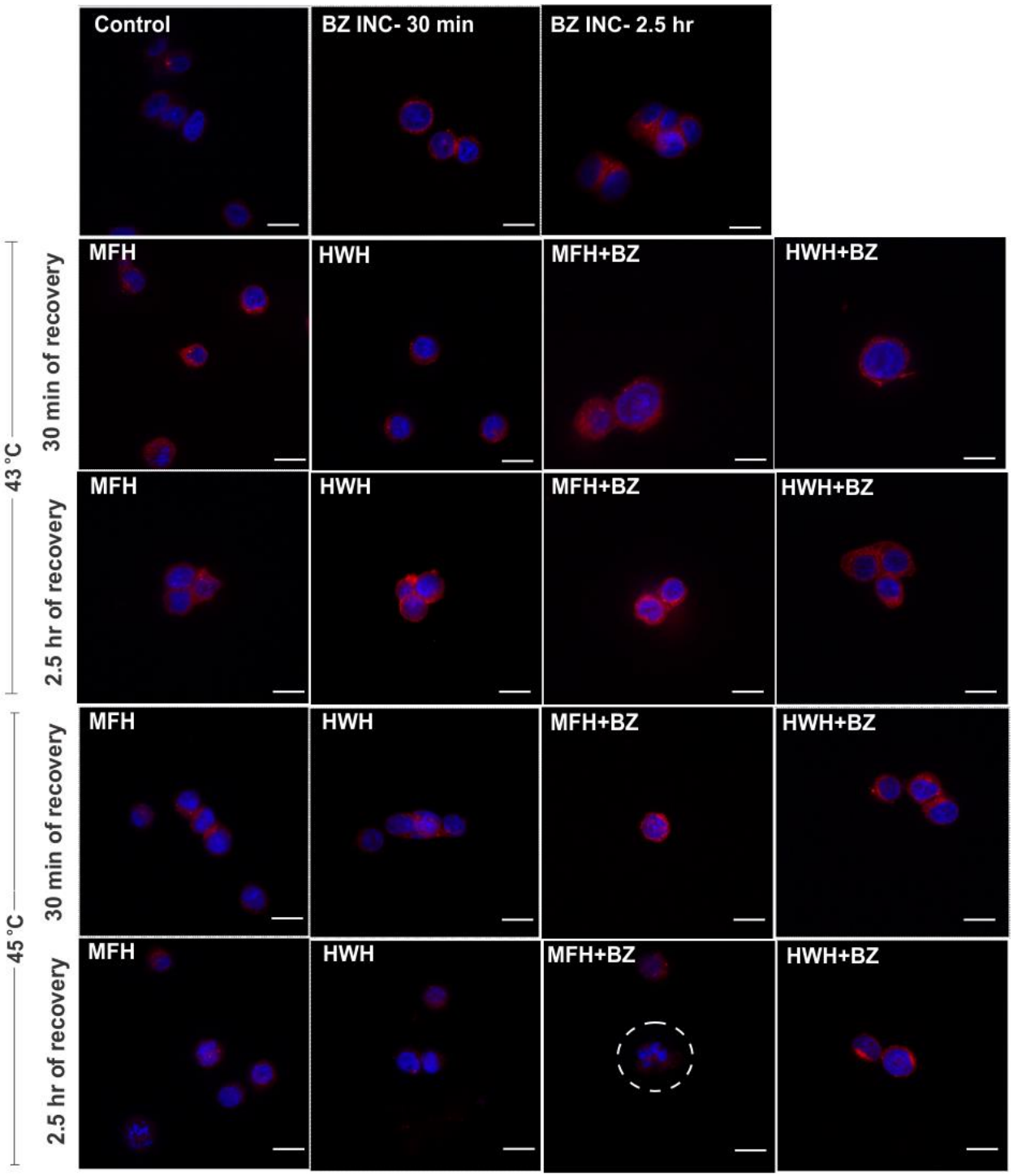

Figure 4. 4. Confocal images captured for MCF-7 cells after hyperthermic treatment in combination with 100 nM of bortezomib. Pictures were obtained at 30 minutes or 2.5 hours of recovery time. Aggresome (red), nucleus (blue). Dashed line shows nucleus fragmentation. Scale bars represent 10 μm.

Flow cytometer measurements were analyzed using the aggresome propensity factor (APF), which is a measure of the amount of aggregated proteins that have been packed in the aggresome in the presence or absence of an inducer of aggregated proteins. APF values higher than 25 mean that significant quantities of aggregated proteins have been transported to the perinuclear area to be packed within the aggresome. The resulting values are shown in Table 4.2. At 43º C hyperthermic treatments with or without BZ induced aggresome formation (APF>25) at both recovery times assessed. At 30 minutes of recovery time, aggresome was not formed in cells treated by BZ alone; in contrast, HWH and MFH induced aggresome formation at this condition. After 2.5 hr recovery time aggresome formation for cells treated with BZ in the incubator was evident (APF>25). However, cells treated with HWH showed higher aggresome formation than BZ treated cells. At this time point, we did not observe a significant difference in aggresome formation between cells treated with MFH and cells treated with BZ alone. After 30 minutes of recovery time MFH induced higher aggresome formation than HWH. But, after 2.5 hr of recovery time the opposite was observed, cells treated by HWH showed higher aggresome formation than those treated by MFH. When bortezomib was combined with hyperthermia at 43 ºC aggresome formation was evident. At 30 minutes of recovery time, MFH+BZ or BZ+HWH induced higher aggresome formation than BZ alone. On the other hand, cells treated by MFH+BZ showed higher aggresome formation than cells treated by MFH alone. However, no statistically significant difference in aggresome formation was observed between HWH and HWH+BZ at this time point. At 2.5 hr of recovery time we did not observe a significant difference in aggresome formation for BZ in combination with MFH treated cells when compared to MFH or BZ alone. At this recovery time significant differences between cells treated with HWH+BZ and BZ alone were observed, however we did not observe differences

between cells treated by HWH and HWH+BZ. Cells treated by MFH + BZ showed higher aggresome formation than those treated by HWH + BZ after 30 minutes of recovery time. At longer recovery time (at 2.5 hr of recovery time) HWH+BZ induced higher aggresome formation than MFH+BZ. Finally, no statistically significant difference was observed between 30 minutes and 2.5 hours of recovery time for those cells treated by MFH or MFH+BZ. However, samples treated by HWH or HWH+BZ had an increase in aggresome formation after recovery for 2.5 hr when compared to 30 minutes. Samples treated at 45 ºC did not show a significant difference in aggresome formation for both recovery times assessed.

The results above suggest the possibility that the transport of aggregated proteins to the perinuclear area (aggresome) is being interrupted by an additional effect induced by MFH, which results in an enhanced proteotoxic stress due to significant accumulation of aggregated proteins in the cytosol. To evaluate this possibility, microtubule damage as a function of recovery time was assessed.

Table 4. 2. Aggresome propensity factor (APF) measurements.

	APF at 43 ºC		APF at 45º C	
	30 minutes of recovery time	**2.5 hours of recovery time**	**30 minutes of recovery time**	**2.5 hours of recovery time**
BZ	21±5	31±4	21±5	31±4
HWH	27±7	46±3	25±22	24±10
MFH	41±4	40±26	12±5	23±2
HWH+BZ	42±11*	71±12**	32±23****	30±14****
MFH+BZ	61±9**	61±16***	29±1****	30±2****

Aggresome determination for cells pretreated or untreated with BZ for 3 hours, exposed to hyperthermia (30 minutes at 43 ºC or 45 ºC) using HWH and MFH and left in incubator for 30 minutes and 2.5 hr of recovery time. * Statistically different with $P<0.05$ when compared to**. ** Statistically equal with $P>0.05$ when compared to ***. **** Statistically equal with $P>0.05$ when compared between them. The numbers represent the average and standard deviation of three independent experiments.

4.3.6. Hyperthermia induced microtubule disruption in MCF-7 cells

When proteasomes are overwhelmed or inhibited, aggregated proteins are transported through microtubules to the perinuclear area, forming aggresomes.[9-11] If microtubule dynamics are lost, the transport of aggregated proteins is interrupted and they accumulate in the cytosol.[9] To evaluate the possible interruption of transport of aggregated proteins to the perinuclear area in MCF-7 cells, microtubule damage was determined as a function of recovery time. Cells were exposed to hyperthermia treatment at 43 ºC or 45 ºC for 30 minutes, incubated for a recovery time of 30 minutes or 2.5 hours and then anti-tubulin fluorescence was determined by flow cytometer. Results were normalized to the control fluorescence. Microtubule disruption is related to a decrease in anti-tubulin fluorescence relative to the control. For that reason, values lower than 1 in Figure 4.5 indicate microtubule damage.

Both heat treatments (MFH and HWH) induced microtubule disruption. Normalized anti-tubulin fluorescence for HWH and MFH at both 43°C and 45°C are equal at both temperatures for the recovery time periods assessed, except after 2.5 hour of recovery at 43°C. At 43 ºC with a recovery time of 30 minutes no significant microtubule disruption was induced by either hyperthermic treatment (HWH and MFH). However, at 2.5 hour of recovery time microtubule damaged induced by MFH was evident; samples treated by HWH showed intact microtubules at this condition. At 45°C similar damage to microtubules at both recovery times was observed for MFH and HWH. This may be attributed to the fact that the temperature is relatively high; causing extensive damage that precludes distinguishing the two forms of heat application. These results suggest that microtubule damage can play a significant role in the mechanisms by which MFH enhances BZ cytotoxicity. We speculate that the combination of microtubule damage and increased protein aggregation can explain the thermal enhancement of BZ.

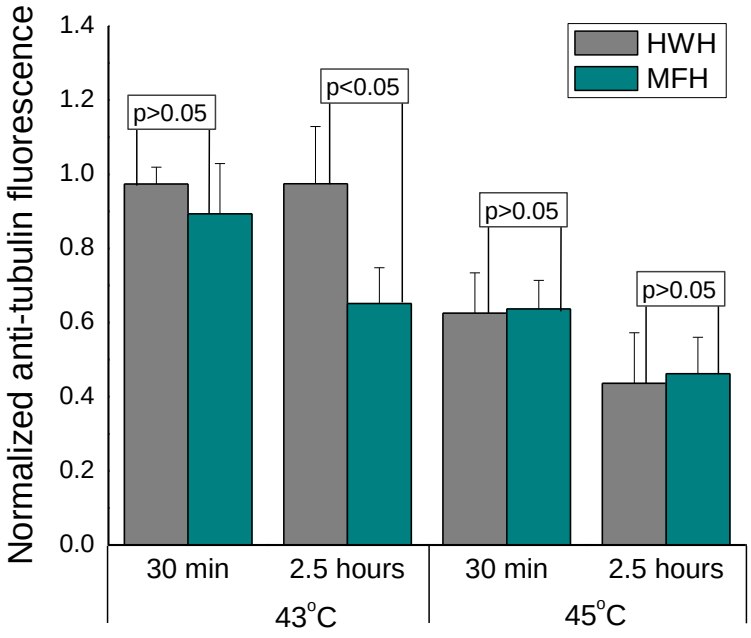

Figure 4. 5. Microtubule damage determination: Flow cytometer analysis for cells untreated with BZ, incubated for 3 hours, exposed to heat treatment (30 minutes at 43 ºC and 45 ºC) using HWH and MFH and left in incubator for 30 minutes and 2.5 hr of recovery time. Numbers were normalized to the control fluorescence. Error bars represent the standard deviation of the mean of three independent experiments.

4.4. Discussion

The results presented above show that application of hyperthermia (30 minutes at 43ºC or 30 minutes at 45ºC) promoted time-dependent cell death in BZ pretreated cells. Apoptotic cells were detectable after 30 minutes of heat treatment application and they increased with recovery time (Table 4.1). At 48 hours of recovery in the presence of BZ, cell death increased significantly, as shown by viability ratio results. Even when BZ was withdrawn after 48 hours recovery time and cells were left to form colonies for 10 days, those cells treated with hyperthermia in combination with BZ were unable to recover. For all these recovery times, BZ

potentiation was higher using MFH. This progressive cell death induced by MFH is likely due to a time-dependent increase in the toxicity of the proteotoxic stress.

Hyperthermia has been shown to increase the toxicity of the proteotoxic stress in cancer cells.[5, 21] In this study we found that in addition to protein damage, hyperthermia caused by magnetic nanoparticles also induces microtubule damage, which can intensify this proteotoxic stress. These cellular effects and BZ potentiation vary between HWH and MFH. We hypothesized that the combination of microtubule disruption and an increase in the amount of aggregated proteins are responsible for BZ potentiation using MFH; consequently, the cell has greater concentration of aggregated proteins in the cytosol, accelerating cell death. To test this hypothesis, we first determined aggresome formation as a measurement of protein damage induced by the two hyperthermic treatments (HWH and MFH) at two conditions (30 minutes at 43 ºC and 30 minutes at 45 ºC) as a function of recovery time (30 minutes or 2.5hr of recovery time). Total quantity of aggregated proteins in the cytosol was not measured in this study, only the formation and accumulation of aggresomes in the perinuclear region.

Results indicated that BZ alone did not induce aggresome formation at 30 minutes of recovery time (APF <25) (Table 4.2). However, at 2.5 hr of recovery time an APF value of 31 ± 4 was observed, indicating that at this period of time a significant quantity of aggregated proteins had been transported to the perinuclear area to form aggresomes. At 43 ºC and 30 minutes of recovery time cells treated by MFH had higher aggresome formation than cells treated by HWH. This same trend was observed for cells treated by MFH+BZ when compared to HWH+BZ treated cells. Aggresome formation increased as recovery time passed for those cells treated with HWH or HWH+BZ, as shown by results at 2.5 hr recovery time. Nevertheless, we did not observe a difference in aggresome formation between 30 minutes and 2.5 hr of recovery time for

cells treated by MFH or MFH+BZ. Although cell death induced at 45 ºC is detrimental, aggresome formation was less evident than at 43 ºC. These results suggest that an additional cellular effect induced by hyperthermic treatments interrupts transport of aggregated proteins to the perinuclear area, and probably accelerates cell death by their accumulation in the cytosol. This transport interruption was more evident when MFH was applied as shown by results at 43ºC (Table 4.2).

Microtubules play an important role in the transport of aggregated proteins to the aggresome.[9] The literature proposes that aggregated proteins are first produced throughout the cytoplasm of the cell, after which they are quickly transported through microtubules towards the microtubule organizing center (MTOC), found close to the cell nucleus, where they are packed into the aggresome.[9-11] Microtubule disruption interrupts the motility of aggregated proteins to the aggresome, allowing their accumulation throughout the cytosol.[9] Hyperthermia induces microtubule damage (mass loss and dynamic instability interruption) as established by previous studies.[18, 31, 32] We speculated that MFH induces significant damage to microtubules, interrupting the transport of aggregated proteins to the aggresome. This additional cellular effect could explain our observations of aggresome formation and BZ potentiation. To assess this possibility, microtubule disruption studies for both hyperthermic treatments were performed (Figure 4.5). Our results suggest that microtubule disruption is temperature and recovery time dependent under both hyperthermic treatments. At 45°C, the temperature is so detrimental to the cells that similar damage to microtubules is observed, regardless of the type of hyperthermic treatment used. This damage is more evident as time passes by, coinciding with previous reports where the loss of microtubule dynamics is progressive.[18, 32] In contrast, at 43°C and short recovery times there was no difference in microtubule damage between MFH and HWH, whereas a difference

emerged at longer recovery times, with MFH showing greater damage. This suggests that MFH affects microtubules, which in turn can slow formation of aggresomes and results in greater concentration of misfolded and aggregated proteins in the cytoplasm, leading to greater enhanced proteotoxic stress.

Our hypothesis is supported by analyzing together aggresome formation and microtubule stability measurements. When cells are exposed to conditions that disrupt protein homeostasis, and microtubules are not compromised, aggresome formation becomes a direct measurement of aggregated proteins.[9, 10] At 43 ºC and 30 minutes of recovery time MFH or MFH+BZ induced higher aggresome formation than HWH or HWH+BZ respectively (Table 4.2), at this condition both hyperthermic treatments did not induce significant microtubule damage (Figure 4.5), suggesting that MFH induces higher protein damage than HWH. HWH or HWH+BZ treated cells showed an increase in aggresome formation as 2.5 hr recovery time passed; at this point microtubule damage induced by HWH was not evident. Moreover, we see that at this condition aggresome formation for MFH or MFH+BZ treated cells did not show a statistically significant difference when compared to 30 minutes recovery time. At 2.5 hour recovery time a significant decrease in normalized anti-tubulin fluorescence is also observed for MFH treated cells, suggesting that microtubule disruption is responsible for these differences in aggresome formation. That is, aggregated proteins cannot go through microtubules to the perinuclear area in order to be packed into the aggresome.

Although we observed differences in normalized anti-tubulin fluorescence at 45°C between 30min and 2.5 hour of recovery time for both MFH and HWH, aggresome formation for BZ+MFH and BZ+HWH was statistically similar at both time points. This suggests that the microtubule disruption attained at 30 minutes of recovery time was enough to impact aggresome

formation. Overall our results suggest that combined treatment with MFH and BZ induces a progressive enhanced proteotoxic stress by combination of an increase in the amount of aggregated proteins and microtubule instability. Aggregated proteins accumulated in the cytosol cannot be transported through microtubules to the perinuclear area to form aggresome, resulting in greater concentration of misfolded and aggregated proteins in the cytoplams leading to greater enhanced proteotoxic stress and cell death.

4.5. Conclusion

Our work presents evidence of one of the mechanisms involved in the hyperthermic potentiation of the anti-cancer bortezomib by heat released using magnetic nanoparticles. Our results suggest that MFH improves BZ cytotoxicity due to the increase of the toxicity of proteotoxic stress by the combination of microtubule damage, an increase in the amount of aggregated proteins, and their subsequent accumulation in the cytosol. This mechanism was evaluated by comparison of cellular effects such as microtubule damage and aggresome formation in cells treated by MFH or HWH with or without BZ. These results showed that these cellular effects were more evident when hyperthermia was induced by magnetic nanoparticles, compared to hyperthermia using a water bath. The combination of nanoscale heat delivery using magnetic nanoparticles and the anti-cancer drug bortezomib resulted impaired transport of aggregated proteins to the aggresomes, hence causing their accumulation in the cytosol and enhancing the toxicity of proteotoxic stress.

4.6. References

1. Alvarez-Berrios MP, Castillo A, Mendez J, Soto O, Rinaldi C, Torres-Lugo M. Hyperthermic Potentiation of Cisplatin by Magnetic Nanoparticle Heaters Is Correlated with an Increase in Cell Membrane Fluidity. *Int J Nanomedicine*. **2013**; 8: 1003-1013.

2. Torres-Lugo M, Rinaldi C. Thermal Potentiation of Chemotherapy by Magnetic Nanoparticles. *Nanomedicine (Lond)*. **2013**; 8: 1689-1707.

3. Lee JS, Rodriguez-Luccioni HL, Mendez J, Sood AK, Lpez-Berestein G, Rinaldi C, et al. Hyperthermia Induced by Magnetic Nanoparticles Improves the Effectiveness of the Anticancer Drug Cis-Diamminedichloroplatinum. *J Nanosci Nanotechnol*. **2011**; 11: 4153-4157.

4. Alvarez-Berrios MP, Castillo A, Rinaldi C, Torres-Lugo M. Magnetic Fluid Hyperthermia Enhances Cytotoxicity of Bortezomib in Sensitive and Resistant Cancer Cell Lines. *Int J Nanomedicine*. **2013**; 9: 145-153.

5. Neznanov N, Komarov AP, Neznanova L, Stanhope-Baker P, Gudkov AV. Proteotoxic Stress Targeted Therapy (Pstt): Induction of Protein Misfolding Enhances the Antitumor Effect of the Proteasome Inhibitor Bortezomib. *Oncotarget*. 2: 209-221.

6. Thompson SJ, Loftus LT, Ashley MD, Meller R. Ubiquitin-Proteasome System as a Modulator of Cell Fate. *Curr Opin Pharmacol*. **2008**; 8: 90-95.

7. Wolf DH, Hilt W. The Proteasome: A Proteolytic Nanomachine of Cell Regulation and Waste Disposal. *Biochim Biophys Acta*. **2004**; 1695: 19-31.

8. Fusco C, Micale L, Egorov M, Monti M, D'Addetta EV, Augello B, et al. The E3-Ubiquitin Ligase Trim50 Interacts with Hdac6 and P62, and Promotes the Sequestration and Clearance of Ubiquitinated Proteins into the Aggresome. *PLoS One*. 7: e40440.

9. Johnston JA, Ward CL, Kopito RR. Aggresomes: A Cellular Response to Misfolded Proteins. *J Cell Biol*. **1998**; 143: 1883-1898.

10. Markossian KA, Kurganov BI. Protein Folding, Misfolding, and Aggregation. Formation of Inclusion Bodies and Aggresomes. *Biochemistry (Mosc)*. **2004**; 69: 971-984.

11. Zaarur N, Meriin AB, Gabai VL, Sherman MY. Triggering Aggresome Formation. Dissecting Aggresome-Targeting and Aggregation Signals in Synphilin 1. *J Biol Chem*. **2008**; 283: 27575-27584.

12. Nawrocki ST, Carew JS, Dunner K, Jr., Boise LH, Chiao PJ, Huang P, et al. Bortezomib Inhibits Pkr-Like Endoplasmic Reticulum (Er) Kinase and Induces Apoptosis Via Er Stress in Human Pancreatic Cancer Cells. *Cancer Res*. **2005**; 65: 11510-11519.

13. Xu H, Ju D, Jarois T,Xie Y. Diminished Feedback Regulation of Proteasome Expression and Resistance to Proteasome Inhibitors in Breast Cancer Cells. *Breast Cancer Res Treat*. **2008**; 107: 267-274.

14. Banerjee R, Katsenovich Y, Lagos L, McIintosh M, Zhang X, Li CZ. Nanomedicine: Magnetic Nanoparticles and Their Biomedical Applications. *Curr Med Chem*. 17: 3120-3141.

15. Latorre M, Rinaldi C. Applications of Magnetic Nanoparticles in Medicine: Magnetic Fluid Hyperthermia. *P R Health Sci J*. **2009**; 28: 227-238.

16. Rodriguez-Luccioni HL, Latorre-Esteves M, Mendez-Vega J, Soto O, Rodriguez AR, Rinaldi C, et al. Enhanced Reduction in Cell Viability by Hyperthermia Induced by Magnetic Nanoparticles. *Int J Nanomedicine*. 6: 373-380.

17. Domenech M, Marrero-Berrios I, Torres-Lugo M, Rinaldi C. Lysosomal Membrane Permeabilization by Targeted Magnetic Nanoparticles in Alternating Magnetic Fields. *ACS Nano*. **2013**.

18. Prasad NK, Rathinasamy K, Panda D, Bahadur D. Mechanism of Cell Death Induced by Magnetic Hyperthermia with Nanoparticles of [Gamma]-Mnxfe2-Xo3 Synthesized by a Single Step Process. *Journal of Materials Chemistry*. **2007**; 17: 5042-5051.

19. Dewey WC, Hopwood LE, Sapareto SA, Gerweck LE. Cellular Responses to Combinations of Hyperthermia and Radiation. *Radiology*. **1977**; 123: 463-474.

20. Hildebrandt B, Wust P, Ahlers O, Dieing A, Sreenivasa G, Kerner T, et al. The Cellular and Molecular Basis of Hyperthermia. *Crit Rev Oncol Hematol*. **2002**; 43: 33-56.

21. Roti Roti JL. Cellular Responses to Hyperthermia (40-46 Degrees C): Cell Killing and Molecular Events. *Int J Hyperthermia*. **2008**; 24: 3-15.

22. Wust P, Hildebrandt B, Sreenivasa G, Rau B,Gellermann J, Riess H, et al. Hyperthermia in Combined Treatment of Cancer. *Lancet Oncol*. **2002**; 3: 487-497.

23. Creixell M, Herrera AP, Latorre-Esteves M, Ayala V, Torres-Lugo M, Rinaldi C. The Effect of Grafting Method on the Colloidal Stability and in Vitro Cytotoxicity of Carboxymethyl Dextran Coated Magnetic Nanoparticles. *Journal of Materials Chemistry*. 20: 8539-8547.

24. Herrera AP, Barrera C, Rinaldi C. Synthesis and Functionalization of Magnetite Nanoparticles with Aminopropylsilane and Carboxymethyldextran. *Journal of Materials Chemistry*. **2008**; 18: 3650-3654.

25. Alvarez-Berrios MP, Castillo A, Mendez J, Soto O, Rinaldi C, Torres-Lugo M. Hyperthermic Potentiation of Cisplatin by Magnetic Nanoparticle Heaters Is Correlated with an Increase in Cell Membrane Fluidity. *Int J Nanomedicine*. 8: 1003-1013.

26. Franken NA, Rodermond HM, Stap J, Haveman J, van Bree C. Clonogenic Assay of Cells in Vitro. *Nat Protoc*. **2006**; 1: 2315-2319.

27. Gupta N, Lamborn K, Deen DF. A Statistical Approach for Analyzing Clonogenic Survival Data. *Radiat Res*. **1996**; 145: 636-640.

28. Shen D, Coleman J, Chan E, Nicholson TP,Dai L, Sheppard PW, et al. Novel Cell- and Tissue-Based Assays for Detecting Misfolded and Aggregated Protein Accumulation within Aggresomes and Inclusion Bodies. *Cell Biochem Biophys*. 60: 173-185.

29. Creixell M, Herrera AP, Latorre-Esteves M, Ayala V,Torres-Lugo M, Rinaldi C. The Effect of Grafting Method on the Colloidal Stability and in Vitro Cytotoxicity of Carboxymethyl Dextran Coated Magnetic Nanoparticles. Journal of Materials Chemistry. 2010; 20: 8539-8547.

30. Codony-Servat J, Tapia MA, Bosch M, Oliva C, Domingo-Domenech J, Mellado B, et al. Differential Cellular and Molecular Effects of Bortezomib, a Proteasome Inhibitor, in Human Breast Cancer Cells. *Mol Cancer Ther*. **2006**; 5: 665-675.

31. Huang SH,Yang KJ,Wu JC,Chang KJ,Wang SM. Effects of Hyperthermia on the Cytoskeleton and Focal Adhesion Proteins in a Human Thyroid Carcinoma Cell Line. *J Cell Biochem*. **1999**; 75: 327-337.

32. Pawlik A,Nowak JM,Grzanka D,Gackowska L,Michalkiewicz J,Grzanka A. Hyperthermia Induces Cytoskeletal Alterations and Mitotic Catastrophe in P53-Deficient H1299 Lung Cancer Cells. *Acta Histochem*. 115: 8-15.

Chapter 5

Magnetic Fluid Hyperthermia Enhances the In Vivo Therapeutic Effect of Cisplatin

5.1. Introduction

Recently, magnetic fluid hyperthermia (MFH) has gained great interest as an alternative treatment to treat cancer.[1-5] Studies have demonstrated that this novel therapeutic approach can promote cell death *in vitro* and tumor remission *in vivo*.[5-11] *Jordan et al*, confirmed that MFH was a feasible method in a rat prostate carcinoma model.[12] Other studies also showed the effectiveness of this treatment to inhibit tumor growth.[5, 7, 13, 14] For example, *Dennis et al*, demonstrated that breast cancer tumors had nearly complete regression after magnetic fluid hyperthermia application.[5] Similarly, Hilger *et al.* and Wang *et al*. reported that hyperthermia using iron oxide nanoparticles inhibited breast tumor growth in mice and rats respectively.[13, 14]

It is known that heat improves the therapeutic effects of chemotherapeutic agents, even those with limited clinical use.[15] The platinum based drug cisplatin is an anticancer drug used to treat many forms of cancer, however it induces significant side effects and some types of cancer develop drug resistance, limiting the therapeutic effect of this drug.[16-19] Ohno *et al*. showed that the effect of cisplatin in combination with whole body hyperthermia was significantly improved in fibrosarcoma models.[20] Additional animal and clinical studies also revealed that the therapeutic outcome of cisplatin in ovarian cancer was potentiated by hyperthermia using microwave and hot water tubes respectively.[21, 22] However, these types of hyperthermic treatments were painful and invasive. They also induced a significant amount of side effects such

as metabolic or hematologic toxicities, nausea and vomiting. These effects had limited the clinical use of conventional hyperthermia as an adjutant to improve the therapeutic outcome of anticancer drugs.[15]

Recently, MFH has been explored as an adjuvant to enhance the cytotoxicity of chemotherapeutics agents to overcome limitations, such as severe side effects and drug resistance.[15] This treatment is attractive because it can generate targeted heat without causing damage to adjacent tissues.[15, 23] Li *et al.* showed that inducing hyperthermia via magnetic nanopowder in combination with carboplatin produced significant tumor inhibition in a liver carcinoma model without obvious side-effects.[23] Combining MFH with geldanamycin resulted in antitumor effect in a mouse melanoma model.[24] *In vitro* and *in vivo* studies also have demonstrated that MFH enhances the therapeutic effect of cisplatin.[9, 15, 25, 26] Babincova *et al*. conducted one of the first studies that demonstrated the synergistic effect between cisplatin and MFH.[27] Our group have shown that caco-2 cells treated by cisplatin in combination with MFH demonstrated significant cell death when compared to hot water hyperthermia under similar heat doses.[9] *Petryk, et al* demonstrated that combined treatment (cisplatin with MFH) was more effective that the treatments alone in a murine mammary adenocarcinoma model.[26]

Although there are several *in vitro* studies that have demonstrated the effectiveness of the combined treatment of cisplatin and MFH, only a few *in vivo* studies have been conducted. In this study we have evaluated the enhanced cytotoxicity of cisplatin by MFH in an ovarian model. We hypothesized that MFH will enhance the *in vivo* therapeutic effect of cisplatin. To test this hypothesis a preliminary study in nude mouse treated by cisplatin with or without MFH was performed. Results indicated that MFH improved the therapeutic effect of cisplatin inducing an intermediate effect.

5.2. Materials and methods

5.2.1. Drug and nanoparticles

The total dose of cisplatin was chosen taking into account the maximum tolerated dose (MTD) in mice which is based on body weight.[28, 29] Cisplatin (Sigma, St. Louis, MO) was dissolved in saline solution (0.9%) and then, a total dose of 7mg/kg was administrated per mouse according to the following order: a dose of 2 mg/kg in a volume dose of 20 µl was injected directly in the tumor with or without 50 mg/kg of nanoparticles. An additional dose of 5mg/kg of cisplatin in a dose volume of 100µl was injected intraperitonealy after hyperthermic treatment. The synthesis and characterization of the magnetic nanoparticles are established in the materials and methods section of the chapter 3 of this dissertation. Nanoparticles were injected directly in the tumor in a dose volume of 20 µl at 50mg Fe/kg with or without cisplatin as established before.

5.2.2. Cell culture and subcutaneous tumors

A2780/CP20 cells were donated by Dr. Edna Mora from the UPR Comprehensive Cancer Center. They were cultured in RPMI (Sigma, St. Louis, MO) with 15% fetal bovine serum and 0.1% gentamycin (Sigma, St. Louis, MO) at 37°C under 5% CO2. To form tumors, A2780/CP20 cells ($8X10^5$) in a total volume of 100 µl were injected subcutaneously in the back of nude mice. Then, mice were left to recover for three weeks until tumors were measurable. All the protocols that were used to carry out this experiment were approved by the *Institutional Animal Care and Use Committee (*IACUC) of medical sciences, university of Puerto Rico at Rio Piedras.

5.2.3. Cisplatin in combination with MFH

Mice were randomly divided in four groups as follows: group 1 (control group) which was injected with 100 µl of saline solution intraperitoneally and 20 µl directly in the tumor; group 2: formed by mice treated with cisplatin as follows: a dose of 2mg/Kg in a total volume of 20 µl was injected in the tumor and a dose of 5mg/kg in 100 µl was injected intraperitoneally; group 3: mice injected with 50mg Fe/Kg directly in the tumor in a dose volume of 20 µl and group 4: mice injected directly in the tumor with 20 µl of a solution containing a dose of 2mg/Kg of cisplatin and 50mg Fe/Kg. Groups injected with nanoparticles with or without cisplatin (group 3 and 4) were allowed to recover for 30 minutes to promote distribution of nanoparticules in the tumor. After this period of time, mice were anesthetized and type T thermocouples (Omega Engineering, Stamford, CT) were introduced into the tumor using a 20G syringe (Figure 1). Additional thermocouples were located in the wall of the mouse holder tube, and in the anus. Mice were then placed in the induction heating equipment and a magnetic field of 29.39 kA/m was applied (Figure 1). The tumor temperature was held for 30 minutes at the maximum temperature reached in the tumor, which varied between 38ºC to 43 ºC. After hyperthermic treatment, 100 µl of saline solution was injected intraperitoneally to those mice treated by MFH alone and an additional dose of 5mg/kg of cisplatin in a dose volume of 100 µl was injected intraperitoneally in mice treated by MFH with cisplatin. Our previous work demonstrated that MFH produces significant membrane fluidity, which induces higher intracellular accumulation of cisplatin.[30] For that reason, we chose this injection sequence for cisplatin in combination with magnetic nanoparticles. After treatment, mice were allowed to recover for 1 week and the size of the tumor was measured. Having completed the final period of experimentation, the mice were sacrificed according to protocol established by IACUC.

Tumor volume was determined using the following formula[31-33]:

V (mm^3) = $\frac{a^2Xb}{2}$; where a is the shortest diameter and b the largest diameter.[34]

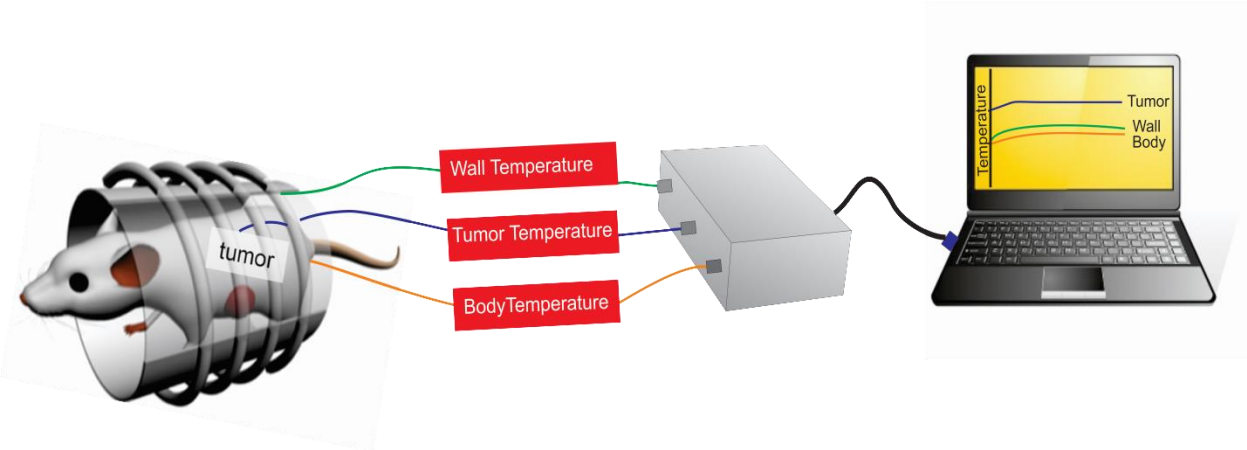

Figure 5. 1. Experimental set up for in vivo experiments (the mouse was adapted from Lee *et al.*).[35]

5.2.4. Assessing antitumor activity

There are several statistics and analysis methods to evaluate the effectiveness of combined treatments in solid tumor xenograft models.[36, 37] However, tumor volume curve as function of time is required for the application of most of these methods. In this preliminary study the tumor volume for all groups was measured only after 8 days of treatment; for that reason, the method chosen to analyze this data was the end point analysis method tumor volume (T/C) value which has been used for the determination of antitumor activity.[34, 36, 37] T/C is defined as: $\mathbf{100X}\frac{\mathbf{RTV\ treatment}}{\mathbf{RTV\ control}}$ (RTV is calculated for each mouse and is defined as: $\frac{\mathbf{final\ volume}}{\mathbf{initial\ volume}}$). Agents producing a T/C of ≤15% are considered highly active, those with a T/C of ≤ 45% but>15% are considered to have intermediate activity, and those with mean T/C values > 45% are considered to have low levels of activity.[36, 38]

5.3. Results and discussion

Hyperthermia has been used as an adjutant to enhance the cytotoxicity of anticancer drugs.[15, 21] However, side effects induced by conventional hyperthermic methods have limited his clinical application. Application of hyperthermia via magnetic nanoparticles is an attractive and novel method.[15] Several studies have demonstrated that magnetic fluid hyperthermia enhances the *in vitro* therapeutic effect of cisplatin.[9, 15] However, there are a few *in vivo* studies of this combined treatment reported. To evaluate the enhanced cytotoxicity of cisplatin using MFH in animal models, magnetic nanoparticles with or without cisplatin were directly injected in the tumor of nude mice. Particles were allowed to distribute and the drug to permeabilize for 30 minutes. After this period, a magnetic field of 29.39 kA/m was applied to each mouse for 30 minutes (Figure 5.1). Temperature profile results (Figure 5.2, Figure 5.3.) illustrated that the maximum temperature reached in the tumors varied from 38 ºC to 43 ºC under similar magnetic field conditions. For example, only three of the four mice treated by MFH alone were exposed to mild hyperthermia (40ºC - 43ºC). It was also observed that not all mice in the group treated by MFH in combination with cisplatin reached the same tumor temperature. Tumor temperature of mice 1, 3 and 4 reached mild MFH, however the tumor temperature of mouse 2 only reached 39ºC. This difference in temperature among tumors can be due to several aspects such as, the location of the thermocouple and distribution of nanoparticles inside the tumor.[39, 40] Tumors are complex, for that reason the distribution of magnetic nanoparticles within them depends on many factors such as heterogeneity, size, pH and blood flow of the tumor. The injection rate and dose of the magnetic fluid also plays an important role in nanoparticle distribution.[40] Additional studies about how to inject magnetic nanoparticles into the tumor must be done, in order to obtain homogenous magnetic fluid and temperature.

Additional challenges were found while this experiment was performed. For example, the discontinuity observed in the temperature profile of the tumors (Figure 5.2, 5.3.) was because the mice sometimes awakened in the middle of treatment, and it was necessary to take out the mouse and give him an additional infusion of anesthesia. There were also problems with the thermocouple placed in the anus; it could not remain into de anus of the animal for a long time. For that reason, body temperature was always lower than 37 ºC. For future studies it is necessary to explore other techniques of anesthesia to maintain the mice asleep for a longer time.

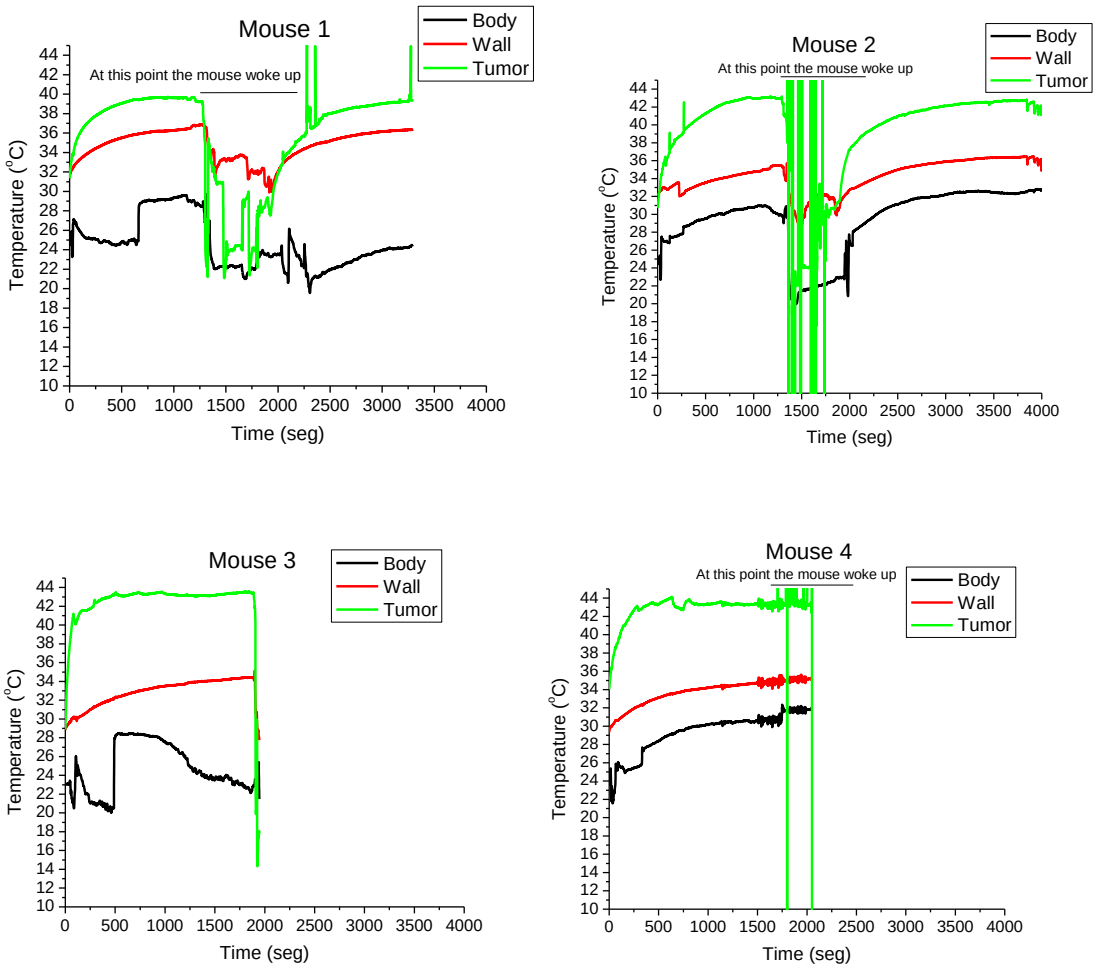

Figure 5. 2. Tumor temperature profile for mice treated with MFH for 30 minutes at a magnetic field of 39.29 KA/m.

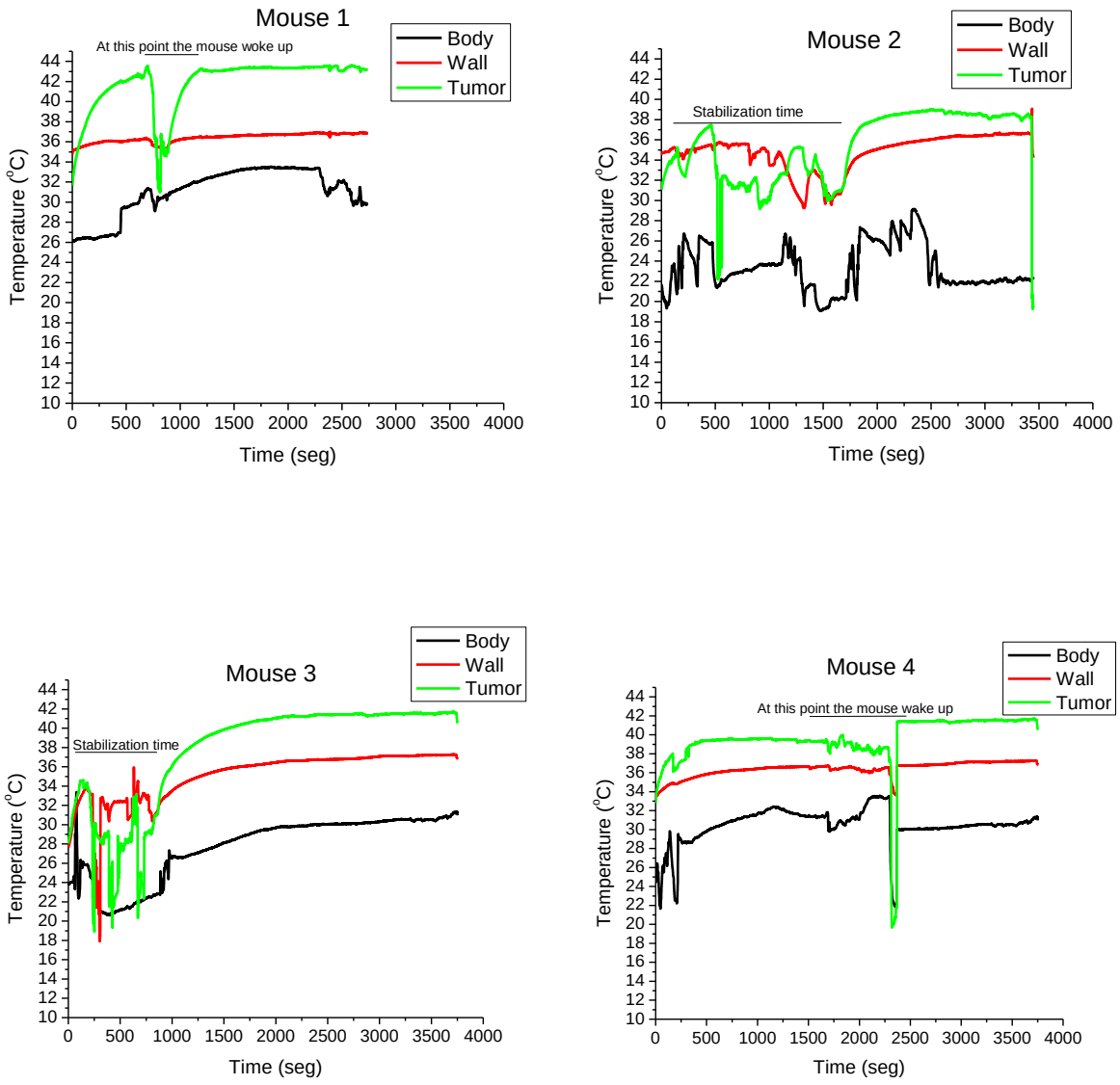

Figure 5. 3. Temperature profile of the tumors for mice treated by cisplatin in combination with MFH for 30 minutes at a magnetic field of 39.29 KA/m.

After heat treatment mice were injected intraperitoneally with an additional dose of cisplatin of 5mg/Kg or saline solution and allowed to recover for 8 days. At the end of this period of time, the tumor size was measured for each group and tumor volume values (T/C) were

determined to evaluate the effectiveness of treatments. T/C for control group was 100% as expected; tumors grew as a function of time (Table 5.1). Cisplatin as a single agent had low activity showing a T/C value of 61%. This result is consistent, because A2780/CP20 cells are resistant to cisplatin.[41, 42] We also observed that MFH did not show any activity as a single treatment (table 5.1). Nevertheless, the combination of MFH and cisplatin induced intermediate activity (table 5.1), indicating that MFH enhances the cytotoxicity of the anticancer drug cisplatin. However, this is a preliminary result because we only used an endpoint analysis method (T/C). For futures experiments tumor volume must be determined at least every two days to make a complete analysis using statistic and analysis methods.

Table 5. 1. Therapeutic response of mice treated with MFH with or without cisplatin.

Group	RTV ratio	T/C (%)	Response
Control	15	100	-
cDDP	9	61	Low activity
MFH	12	81	Low activity
cDDP+MFH	6.7	45	Intermediate activity

5.4. Conclusion

This preliminary work provides evidence of the potentiation of cisplatin using magnetic fluid hyperthermia in animal models. MFH or cisplatin alone did not show therapeutic activity as single treatments under the described doses. However, the combination treatment demostrated intermediate activity. Although these results are promising, there are challenges that need to be addressed such as, the way to accumulate and distribute magnetic nanoparticles into the tumor.

5.5. References

1. Gneveckow U, Jordan A, Scholz R, Bruss V, Waldofner N, Ricke J, et al. Description and Characterization of the Novel Hyperthermia- and Thermoablation-System Mfh 300f for Clinical Magnetic Fluid Hyperthermia. *Med Phys*. **2004**; 31: 1444-1451.

2. Laurent S, Dutz S, Hafeli UO, Mahmoudi M. Magnetic Fluid Hyperthermia: Focus on Superparamagnetic Iron Oxide Nanoparticles. *Adv Colloid Interface Sci*. **2011**; 166: 8-23.

3. Latorre M, Rinaldi C. Applications of Magnetic Nanoparticles in Medicine: Magnetic Fluid Hyperthermia. *P R Health Sci J*. **2009**; 28: 227-238.

4. Dennis CL, Ivkov R. Physics of Heat Generation Using Magnetic Nanoparticles for Hyperthermia. *Int J Hyperthermia*. 29: 715-729.

5. Dennis CL, Jackson AJ, Borchers JA, Hoopes PJ, Strawbridge R, Foreman AR, et al. Nearly Complete Regression of Tumors Via Collective Behavior of Magnetic Nanoparticles in Hyperthermia. *Nanotechnology*. **2009**; 20: 395103.

6. Johannsen M, Thiesen B, Jordan A, Taymoorian K, Gneveckow U, Waldofner N, et al. Magnetic Fluid Hyperthermia (Mfh)Reduces Prostate Cancer Growth in the Orthotopic Dunning R3327 Rat Model. *Prostate*. **2005**; 64: 283-292.

7. Jordan A, Scholz R, Wust P, Fahling H, Krause J, Wlodarczyk W, et al. Effects of Magnetic Fluid Hyperthermia (Mfh) on C3h Mammary Carcinoma in Vivo. *Int J Hyperthermia*. **1997**; 13: 587-605.

8. Alvarez-Berrios MP, Castillo A, Rinaldi C, Torres-Lugo M. Magnetic Fluid Hyperthermia Enhances Cytotoxicity of Bortezomib in Sensitive and Resistant Cancer Cell Lines. *Int J Nanomedicine*. **2013**; 9: 145-153.

9. Lee JS, Rodriguez-Luccioni HL, Mendez J, Sood AK, Lpez-Berestein G, Rinaldi C, et al. Hyperthermia Induced by Magnetic Nanoparticles Improves the Effectiveness of the Anticancer Drug Cis-Diamminedichloroplatinum. *J Nanosci Nanotechnol*. **2011**; 11: 4153-4157.

10. Rodriguez-Luccioni HL, Latorre-Esteves M, Mendez-Vega J, Soto O, Rodriguez AR, Rinaldi C, et al. Enhanced Reduction in Cell Viability by Hyperthermia Induced by Magnetic Nanoparticles. *Int J Nanomedicine*. 6: 373-380.

11. Creixell M, Bohorquez AC, Torres-Lugo M, Rinaldi C. Egfr-Targeted Magnetic Nanoparticle Heaters Kill Cancer Cells without a Perceptible Temperature Rise. *ACS Nano*. **2012**; 5: 7124-7129.

12. Jordan A, Scholz R, Koch M, Lein M, Deger S, Roigas J, et al. Evaluation of Magnetic Fluid Hyperthermia in a Standard Rat Model of Prostate Cancer. *J Endourol*. **2004**; 18: 495-500.

13. Hilger I, Hiergeist R, Hergt R, Winnefeld K, Schubert H, Kaiser WA. Thermal Ablation of Tumors Using Magnetic Nanoparticles: An in Vivo Feasibility Study. *Invest Radiol*. **2002**; 37: 580-586.

14. Wang G, Xu D, Chai Q, Tan X, Zhang Y, Gu N, et al. Magnetic Fluid Hyperthermia Inhibits the Growth of Breast Carcinoma and Downregulates Vascular Endothelial Growth Factor Expression. *Oncology Letters*. **2014**; 7: 1370-1374.

15. Torres-Lugo M, Rinaldi C. Thermal Potentiation of Chemotherapy by Magnetic Nanoparticles. *Nanomedicine (Lond)*. **2013**; 8: 1689-1707.

16. Dhar S, Kolishetti N, Lippard SJ, Farokhzad OC. Targeted Delivery of a Cisplatin Prodrug for Safer and More Effective Prostate Cancer Therapy in Vivo. *Proceedings of the National Academy of Sciences*. **2011**; 108: 1850-1855.

17. Cvitkovic E. Cumulative Toxicities from Cisplatin Therapy and Current Cytoprotective Measures. *Cancer Treat Rev*. **1998**; 24: 265-281.

18. Reedijk J. Why Does Cisplatin Reach Guanine-N7 with Competing S-Donor Ligands Available in the Cell? *Chem Rev*. **1999**; 99: 2499-2510.

19. Giaccone G. Clinical Perspectives on Platinum Resistance. *Drugs*. **2000**; 59 Suppl 4: 9-17; discussion 37-18.

20. Ohno S, Siddik ZH, Baba H, Stephens LC, Strebel FR, Wondergem J, et al. Effect of Carboplatin Combined with Whole Body Hyperthermia on Normal Tissue and Tumor in Rats. *Cancer Res*. **1991**; 51: 2994-3000.

21. Helm CW, Randall-Whitis L, Martin RS, 3rd, Metzinger DS, Gordinier ME, Parker LP, et al. Hyperthermic Intraperitoneal Chemotherapy in Conjunction with Surgery for the Treatment of Recurrent Ovarian Carcinoma. *Gynecol Oncol*. **2007**; 105: 90-96.

22. Zakris EL, Dewhirst MW, Riviere JE, Hoopes PJ, Page RL, Oleson JR. Pharmacokinetics and Toxicity of Intraperitoneal Cisplatin Combined with Regional Hyperthermia. *J Clin Oncol*. **1987**; 5: 1613-1620.

23. Li FR, Yan WH, Guo YH, Qi H, Zhou HX. Preparation of Carboplatin-Fe@C-Loaded Chitosan Nanoparticles and Study on Hyperthermia Combined with Pharmacotherapy for Liver Cancer. *Int J Hyperthermia*. **2009**; 25: 383-391.

24. Ito A, Saito H, Mitobe K, Minamiya Y, Takahashi N, Maruyama K, et al. Inhibition of Heat Shock Protein 90 Sensitizes Melanoma Cells to Thermosensitive Ferromagnetic Particle-Mediated Hyperthermia with Low Curie Temperature. *Cancer Sci*. **2009**; 100: 558-564.

25. Wagstaff AJ, Brown SD, Holden MR, Craig GE, Plumb JA, Brown RE, et al. Cisplatin Drug Delivery Using Gold-Coated Iron Oxide Nanoparticles for Enhanced Tumour Targeting with External Magnetic Fields. *Inorganica Chimica Acta*. **2012**; 393: 328-333.

26. Petryk AA, Giustini AJ, Gottesman RE, Kaufman PA, Hoopes PJ. Magnetic Nanoparticle Hyperthermia Enhancement of Cisplatin Chemotherapy Cancer Treatment. *Int J Hyperthermia*. **2013**; 29: 845-851.

27. Babincov M, Altanerov V, Altaner C, Bergemann C, Babinec P. In Vitro Analysis of Cisplatin Functionalized Magnetic Nanoparticles in Combined Cancer Chemotherapy and Electromagnetic Hyperthermia. *IEEE Trans Nanobioscience*. **2008**; 7: 15-19.

28. Leite EA, Lana ÃnMQ, Carvalho Junior ÃlD, Coelho LGV, De Oliveira MnC. Acute Toxicity Study of Cisplatin Loaded Long-Circulating and Ph-Sensitive Liposomes Administered in Mice. *Journal of Biomedical Nanotechnology*. **2012**; 8: 229-239.

29. Boven E, van der Vijgh WJ, Nauta MM, Schluper HM, Pinedo HM. Comparative Activity and Distribution Studies of Five Platinum Analogues in Nude Mice Bearing Human Ovarian Carcinoma Xenografts. *Cancer Res*. **1985**; 45: 86-90.

30. Alvarez-Berrios MP, Castillo A, Mendez J, Soto O, Rinaldi C, Torres-Lugo M. Hyperthermic Potentiation of Cisplatin by Magnetic Nanoparticle Heaters Is Correlated with an Increase in Cell Membrane Fluidity. *Int J Nanomedicine*. **2013**; 8: 1003-1013.

31. Jensen MM, Jorgensen JT, Binderup T, Kjaer A. Tumor Volume in Subcutaneous Mouse Xenografts Measured by Microct Is More Accurate and Reproducible Than Determined by 18f-Fdg-Micropet or External Caliper. *BMC Med Imaging*. **2008**; 8: 16.

32. Euhus DM, Hudd C, LaRegina MC, Johnson FE. Tumor Measurement in the Nude Mouse. *J Surg Oncol*. **1986**; 31: 229-234.

33. Tomayko MM, Reynolds CP. Determination of Subcutaneous Tumor Size in Athymic (Nude) Mice. *Cancer Chemother Pharmacol*. **1989**; 24: 148-154.

34. LoRusso PM, Aukerman SL, Polin L, Redman BG, Valdivieso M, Biernat L, et al. Antitumor Efficacy of Interleukin-2 Alone and in Combination with Adriamycin and Dacarbazine in Murine Solid Tumor Systems. *Cancer Res*. **1990**; 50: 5876-5882.

35. Lee JH, Jang JT, Choi JS, Moon SH, Noh SH, Kim JW, et al. Exchange-Coupled Magnetic Nanoparticles for Efficient Heat Induction. *Nat Nanotechnol*. **2011**; 6: 418-422.

36. Fang H, Harned TM, Kalous O, Maldonado V, DeClerck YA, Reynolds CP. Synergistic Activity of Fenretinide and the Bcl-2 Family Protein Inhibitor Abt-737 against Human Neuroblastoma. *Clin Cancer Res*. **2011**; 17: 7093-7104.

37. Carol H, Morton CL, Gorlick R, Kolb EA, Keir ST, Reynolds CP, et al. Initial Testing (Stage 1) of the Akt Inhibitor Gsk690693 by the Pediatric Preclinical Testing Program. *Pediatr Blood Cancer*. **2011**; 55: 1329-1337.

38. Carol H, Morton CL, Gorlick R, Kolb EA, Keir ST, Reynolds CP, et al. Initial Testing (Stage 1) of the Akt Inhibitor Gsk690693 by the Pediatric Preclinical Testing Program. *Pediatr Blood Cancer*. **2010**; 55: 1329-1337.

39. Giustini AJ, Ivkov R, Hoopes PJ. Magnetic Nanoparticle Biodistribution Following Intratumoral Administration. *Nanotechnology*. **2011**; 22: 345101.

40. Gooneratne CP, Kurnicki A, Yamada S, Mukhopadhyay SC, Kosel Jr. Analysis of the Distribution of Magnetic Fluid inside Tumors by a Giant Magnetoresistance Probe. *PLoS ONE*. **2013**; 8: e81227.

41. Chappell NP, Teng PN, Hood BL, Wang G, Darcy KM, Hamilton CA, et al. Mitochondrial Proteomic Analysis of Cisplatin Resistance in Ovarian Cancer. *J Proteome Res*. **2012**; 11: 4605-4614.

42. Godwin AK, Meister A, O'Dwyer PJ, Huang CS, Hamilton TC, Anderson ME. High Resistance to Cisplatin in Human Ovarian Cancer Cell Lines Is Associated with Marked Increase of Glutathione Synthesis. *Proc Natl Acad Sci U S A*. **1992**; 89: 3070-3074.

Chapter 6

Final Remarks: Conclusions and Thesis Contributions

The aim of this dissertation was to study MFH as an adjutant to improve the cytotoxicity of anticancer drugs and the potential mechanisms by which this potentiation occurs. To accomplish this goal, two anticancer drugs which have shown limited clinical effects were chosen: bortezomib and cisplatin. Then, cellular studies were conducted for BZ in sensitive and resistant cancer cell lines, *in vitro* and *in vivo* studies were evaluated for cisplatin and finally potential *in vitro* mechanism was evaluated for both drugs. *In vitro* results were compared with an external source of heat as a control (HWH).

Results presented in this dissertation demonstrated that hyperthermia via magnetic nanoparticles enhances the therapeutic effect of bortezomib and cisplatin. MFH combined with BZ induced cell cytotoxicity in sensitive and resistant cell lines, to a higher extent than HWH at the same temperature conditions. On the other hand, combination of MFH and cisplatin proved to be most effective in reducing cell viability and clonogenicity than those cells treated by HWH. Preliminary *in vivo* studies also showed that MFH enhances cisplatin cytotoxicity.

This work also showed that MFH induces marked cellular effects which are responsible for the potentiation of these drugs. Our data provided convincing evidence that MFH-induced cell membrane permeability is significantly greater than that induced by HWH under similar temperature conditions, and it is at least one of the mechanisms responsible for MFH potentiation of cDDP in Caco-2 cells. One of the mechanisms by which MFH enhances BZ cytotoxicity in MCF-7 cells is the formation and subsequent accumulation of aggregated proteins

in the cytosol due to the interruption of their transport to the perinuclear area through microtubules.

This work demonstrated that the employment of magnetic nanoparticles to induce local hyperthermia (MFH) is a powerful tool to enhance the therapeutic effects of chemotherapeutics even when drug resistance has been developed, converting it as a potential platform for cancer treatment. The mechanisms by which MFH improves BZ or cDDP cytotoxicity proposed in this dissertation could contribute to the rescue of other anti-neoplastic drugs which have not shown activity as single agents. However, there are still some issues that need to be optimized in order to translate this platform to the clinic, such as the way to accumulate and distribute magnetic nanoparticles into the tumor.

Appendix A

Authorization for the *in vivo* experiment issued by IACUC

University of Puerto Rico
Medical Sciences Campus
Institutional Animal Care and Use Committee

September 30, 2013

Edna Mora, MD
UPRCCC Second Floor Lab. 10
Medical Center Area,
San Juan, PR 00936

0740312: Characterization of Tumor Targeting Magnetic Nanoparitcles in Vivo

Dear Dr. Mora:

The Medical Sciences Campus Institutional Animal Care and Use Committee (IACUC) evaluated your 3rd year submission for the above protocol on September 27, 2013.

This is to inform you that your protocol is **approved**. You are granted permission to continue the study as described immediately. The expiration date of the study is October 23, 2014 unless closed before that date.

This approval must be renewed annually. Be advice that any changes to the approved protocol must be submitted and approved by the IACUC before initiating any activity. If you have any questions or require additional information, you may contact Mrs. Carmen Ramos, IACUC Secretary at (787) 282-0031, or at carmen.ramos8@upr.edu before submitting the protocol.

Cordially,

Elizabeth Rivera, DVM
Chairperson

cer

C: ARC

University of Puerto Rico, Medical Sciences Campus
Institutional Animal Care and Use Committee
PO Box 365067 San Juan, PR 00936-5067
Medical Center Area, Caribbean Cardiovascular Hospital, 8th floor, Office 821, Rio Piedras, PR 00935
Tel. (787) 282-0031

ANIMAL STUDY RENEWAL FORM

A. Administrative Information		IACUC Number: 0740312
Name of Principal Investigator **Edna M. Mora**	Telephone	Extension
Title of Project **Characterization of tumor-targeting Magnetic Nanoparticles in vivo**		
E-mail address	Fax Number	
Mailing address **UPRCCC Second Floor, Lab 10, Medical Center Area, San Juan, PR 00936**		

B. Year of the Renewal Requesting *(For 4th year renewals submit the Animal Study Proposal Form)*

- ☐ 2nd year renewal
- ☐ 5th year renewal
- ☐ 8th year renewal
- ☒ 3rd year renewal
- ☐ 6th year renewal
- ☐ 9th year renewal

C. Modifications

- ☒ **No**
- ☐ **Yes** *(Include Minor Modification Request Form or the Animal Study Proposal Form if it's a major modification)*

D. Project status	E. Common and Scientific Name of animal species used *(strain if applicable)*
☒ Active ☐ Inactive (project never initiated)	**mua musculum/foxn1 (nude mice)**

F. Number of animals used (per year) *Provide the number of animals used and to be used in the following years*	Year 1 (or Year 4)	Year 2 (or Year 5)	Year 3 (or Year 6)
Number of animals	**20**	**00**	**400**
Sex	**females**	**females**	**females**
Weight (age)	**(3-5 weeks)**	**(3-5 weeks)**	**(3-5 weeks)**
TOTAL NUMBER OF ANIMALS FOR THREE YEARS OF THE STUDY			**420**

G. Mark whichever of the literature searches applies to your study

- ☒ Procedure does not unnecessarily duplicate previous experiments. *(Provide two current literature searches to demonstrate that the study is not duplicative. Include results of current literature search, description of search engines and keywords used.)*
- ☒ Category D or E *(Provide two current literature searches on alternative methods and procedures to minimize pain and discomfort. Describe search engines, results and keywords used.)*

I certify that all information provided is true and correct:

Signature Edna M. Mora Date Sept 18, EM 2013

Submit original and 12 copies of this form and the attachments (letter, searches, certificates, etc).

IACUC APPROVED
University of Puerto Rico, Medical Sciences Campus
FROM 9 27 13 TO 10 13 14
IACUC CHAIRPERSON